Chemical sensors (Chemosensors)

"A chemosensor is molecule of abiotic origin that signals the presence of matter or energy"

(A. W. Czarnick)

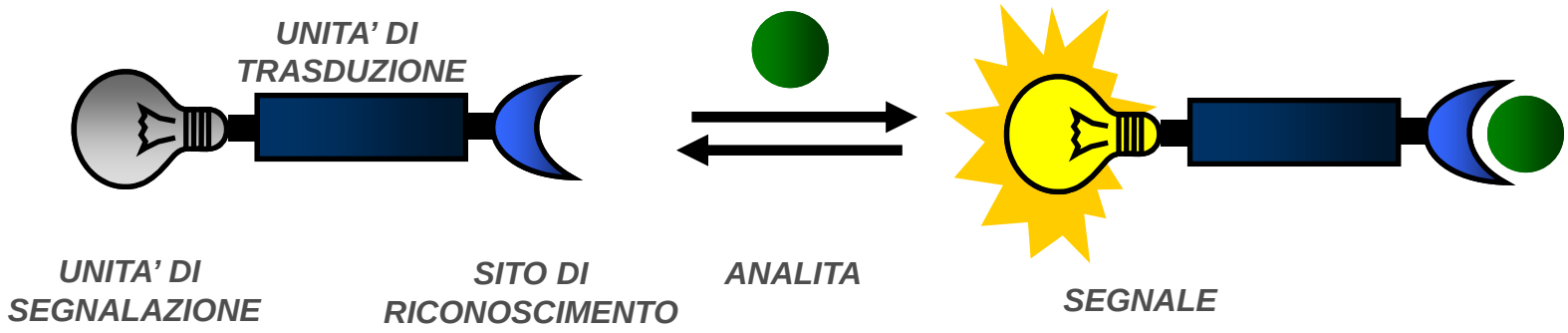

Working mode

- A receptor capable to selectively bind the analyte
- A site with some tunable moelcular property
- A transduction mechanism that converts the recongintion into a modification of the tunable property $\Rightarrow$ **signal**

In principle, any measurable molecular property can be used

Chemical sensors (Chemosensors)

Sensor: device that interacts reversibly with an analyte with measurable signal generation

A chemosensor is not a sensor, strictly speaking, as it is not a device, but it can be the active part of the device.

Most used:

- Redox potential
- Absorbance (color)
- Luminescence (fluorescence)
- NMR relaxation times (recent)

Fluorescent chemosensor

It is a chemosensor that generate a fluorescence signal

Why fluorescence?

✓ Sensitivity (even single molecule detection is possible)
✓ High spatial and temporal resolution
✓ Low cost and easily performed instrumentations

Photoluminescence

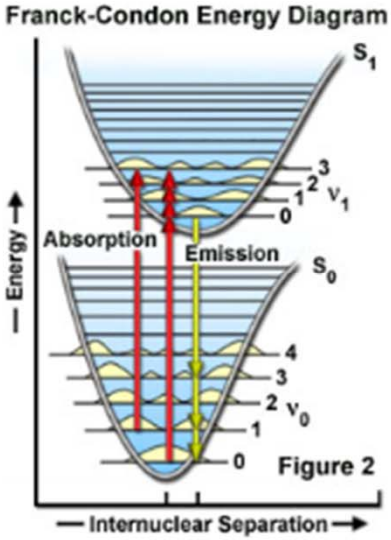

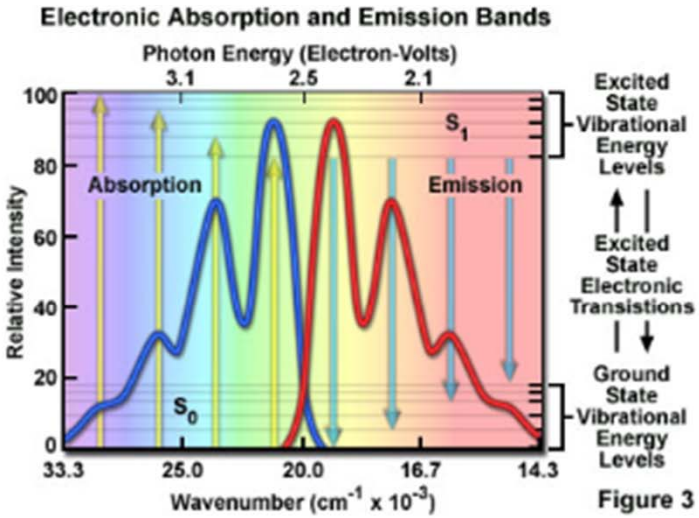

Emission of photons by molecules as a consequence of electronic transitions

Which signal do we measure with fluorescent chemosensors?

- ✓ Fluorescence quenching (ON-OFF)
- ✓ Fluorescence increase (OFF-ON)
- ✓ Emission spectrum shape modification (ratiometric)
- ✓ Life-time
- ✓ Emission anisotropy

STRATEGIE PER LA PROGETTAZIONE DI UN SENSORE SUPRAMOLECOLARE

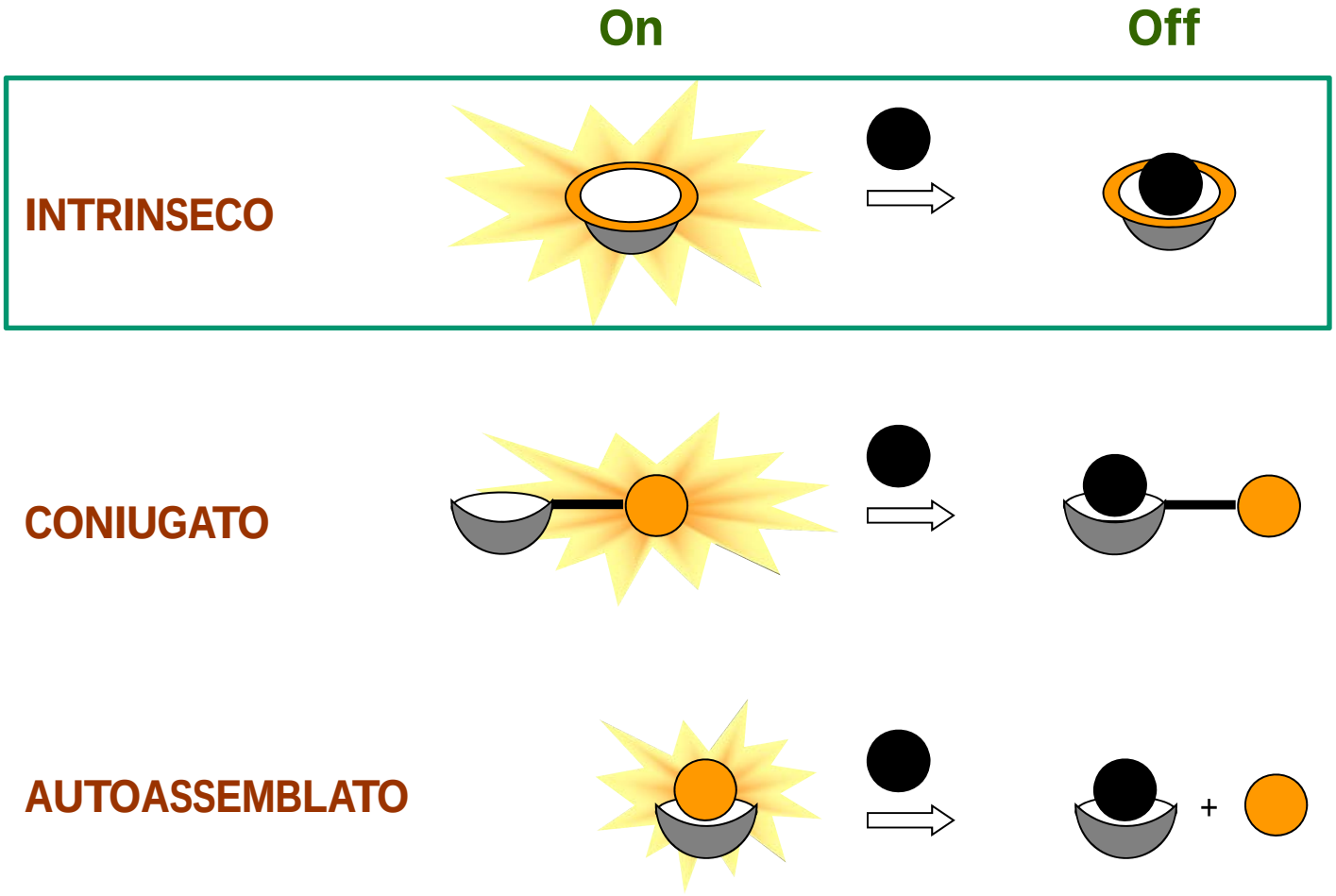

Esempi di sensori intrinseci

Ca^{2+}

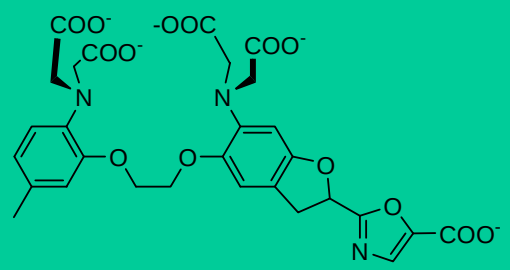

FURA-2
(Tsien 1980)

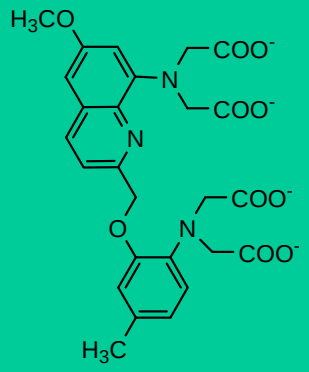

Quin-2
(Tsien 1985)

Mg^{2+}

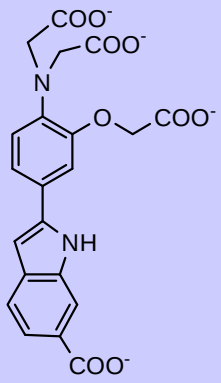

Mag-Indo-1
(London 1989)

Na^{+}

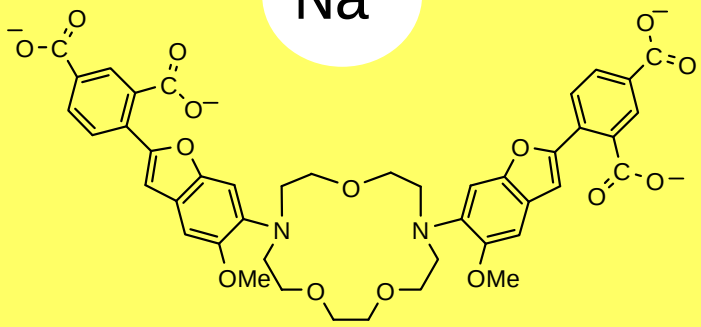

(Tsien 1989)

Fura-2

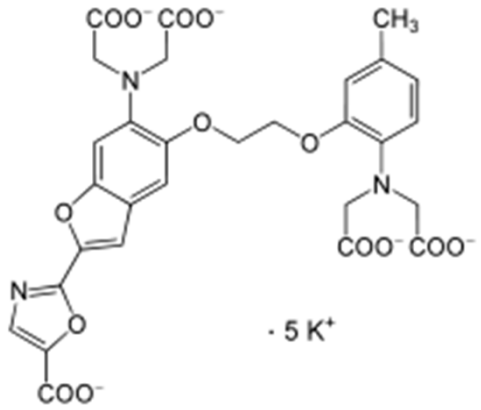

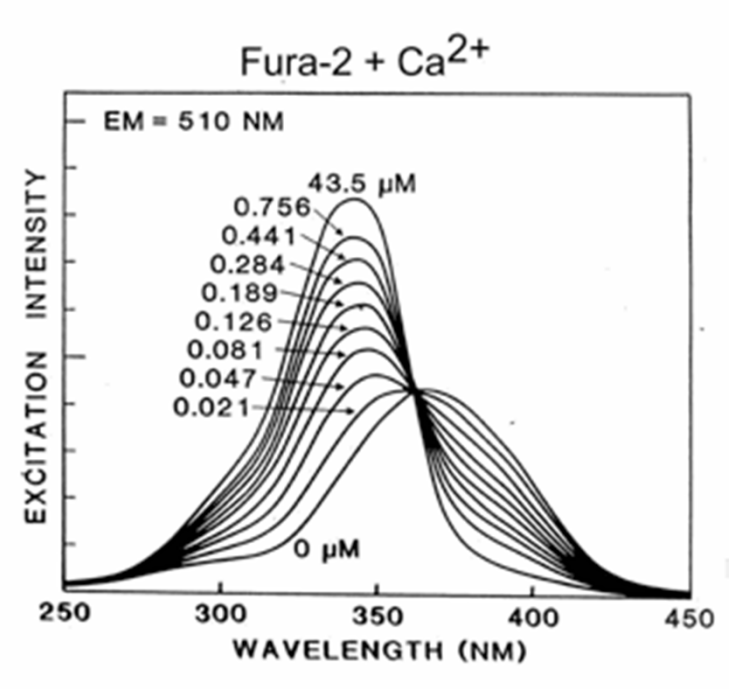

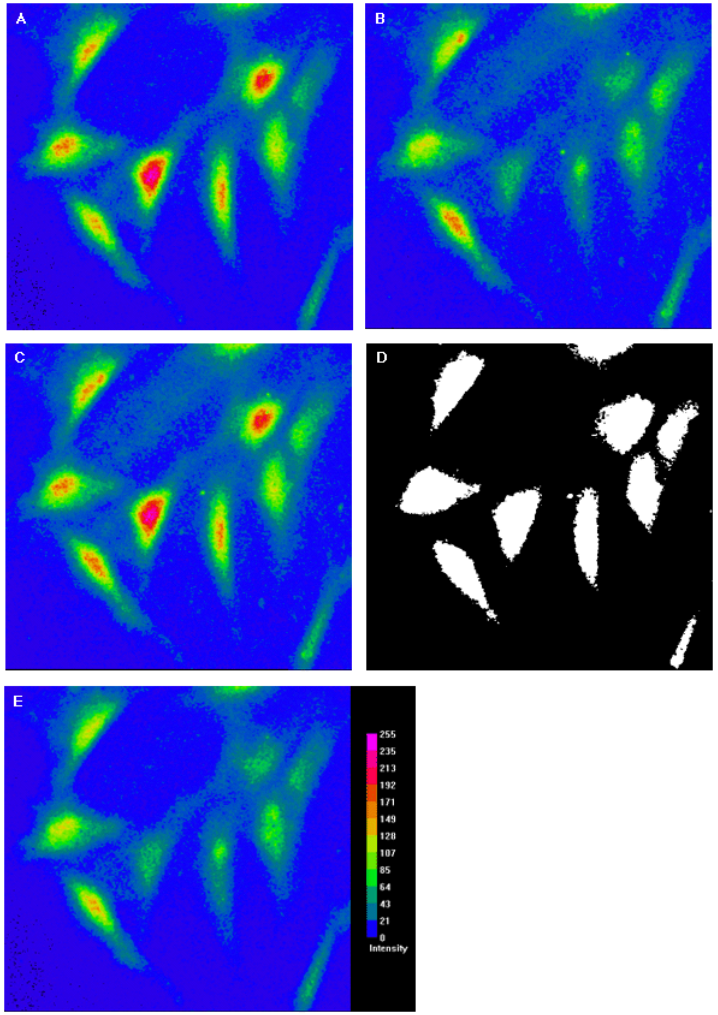

R. Y. Tsien, *J. Biol. Chem.* **1985**, *6*, 3440

Internal charge transfer (ICT)

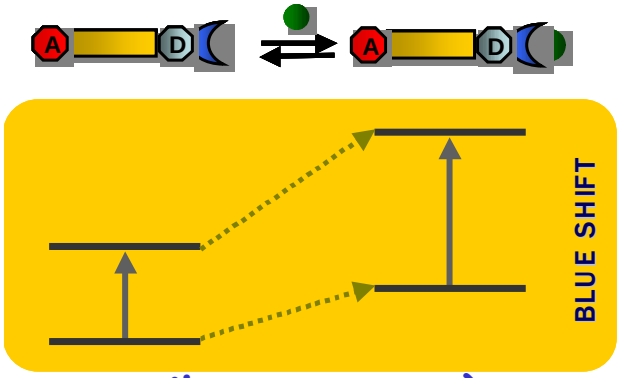

se il recettore è legato al gruppo elettron donatore

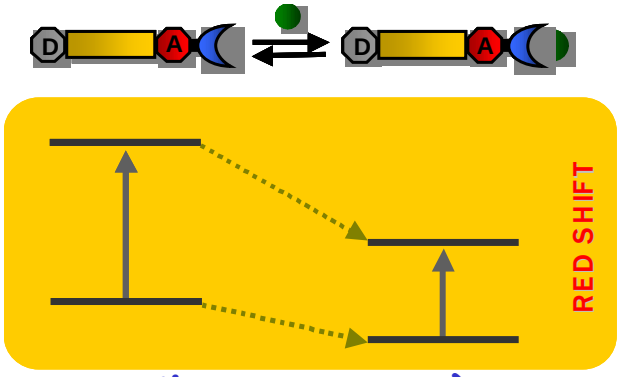

se il recettore è legato al gruppo elettron attrattore

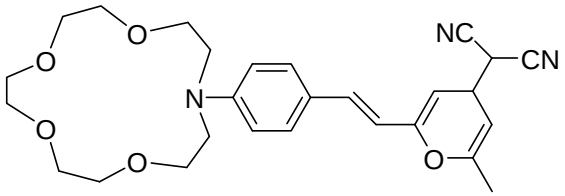

DCM-Crown

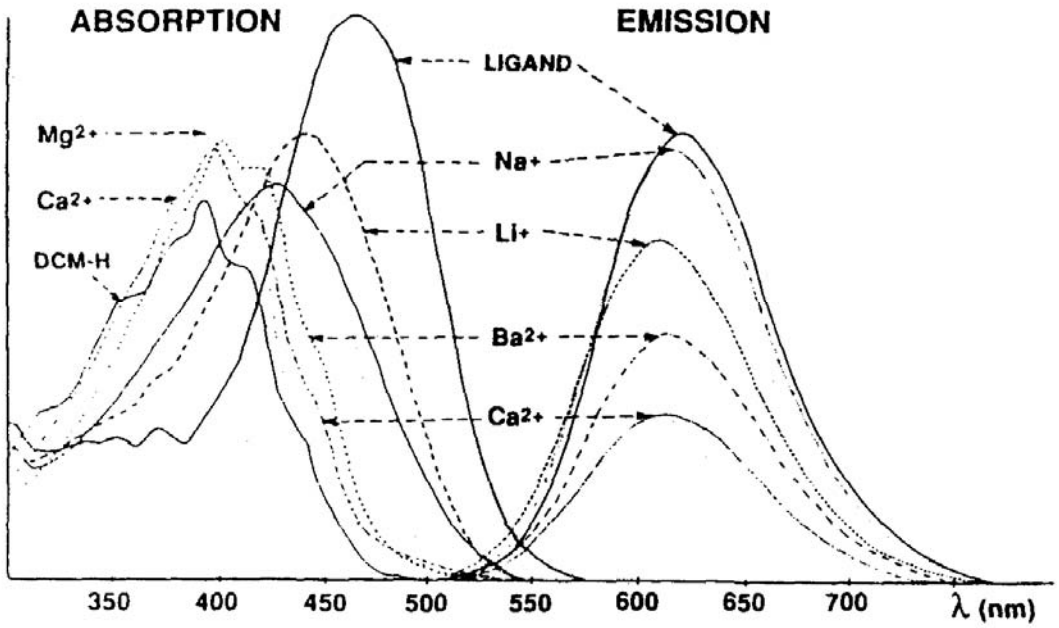

Valeur et al. *J. Phys. Chem.* **1989**, *93*, 3871

Intrinsic chemosensor

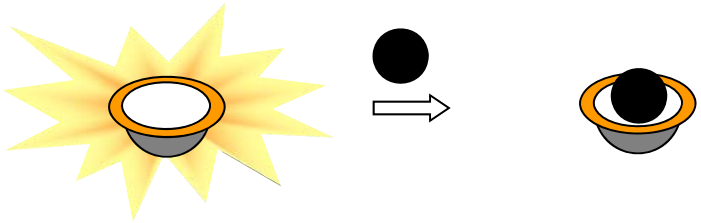

Design: **the donor atoms for the complexation of the substrate are part of the fluorophore π system, therefore the analyte binds to a receptor subsite which is an integrated part of the fluorophore aromatic system.**

Advantage: **the direct interaction between the bound substrate and the fluorophore automatically leads to the modification of the emission properties. The transduction mechanism is somehow intrinsic to the chemosensor structure.**

Weakness: **rigidity of the design. They have to be designed around the substrate and any modification of the binding site may results in a change of the emission properties of the dye and** ***vice versa*****.**

STRATEGIE PER LA PROGETTAZIONE DI UN SENSORE SUPRAMOLECOLARE

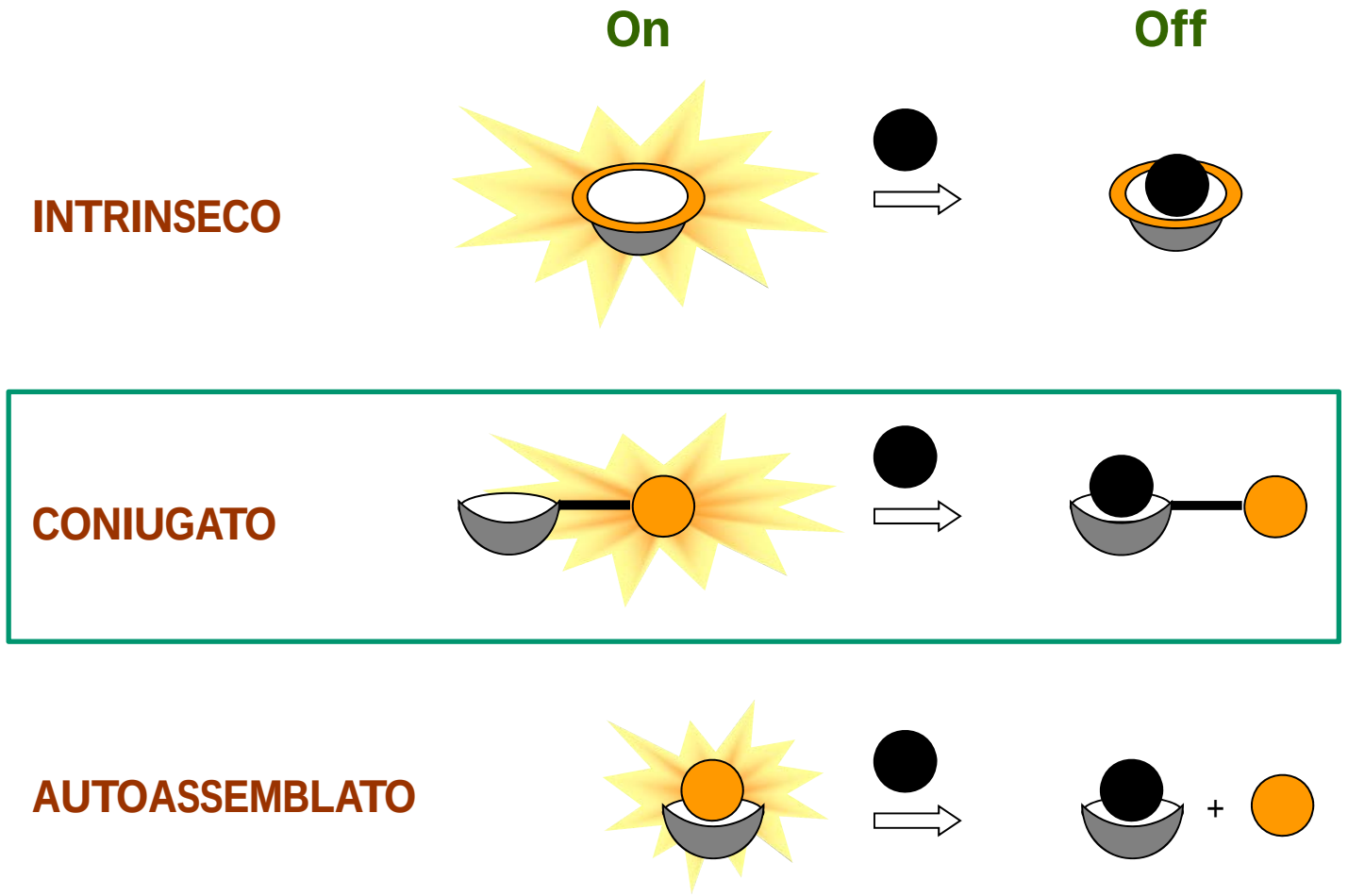

Photoinduced electron transfer (PET)

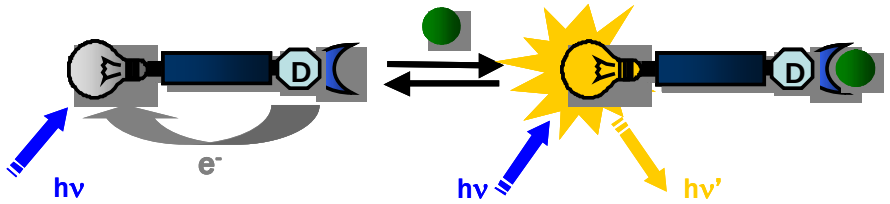

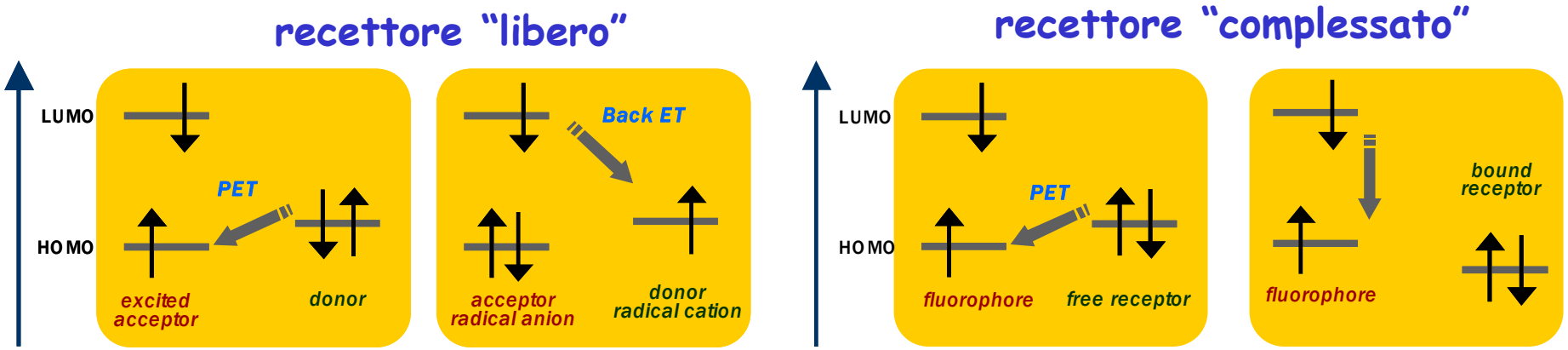

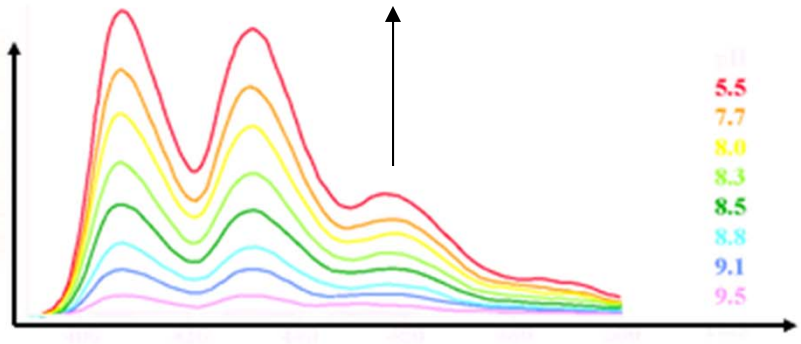

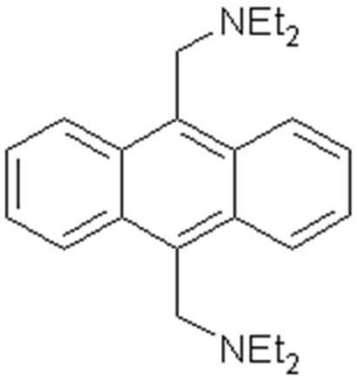

Conjugate chemosensors: ET and PET

Active substrates

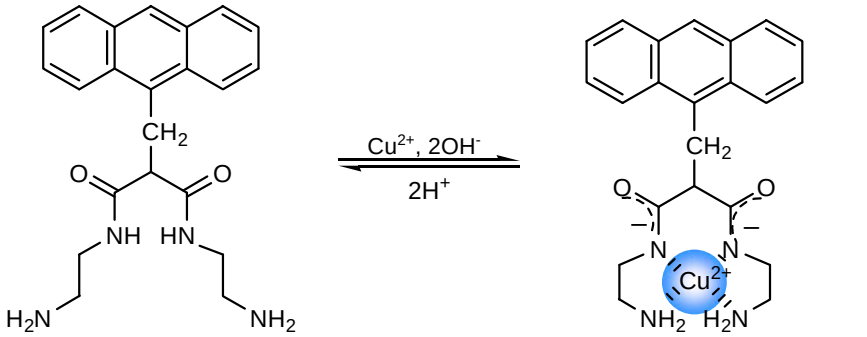

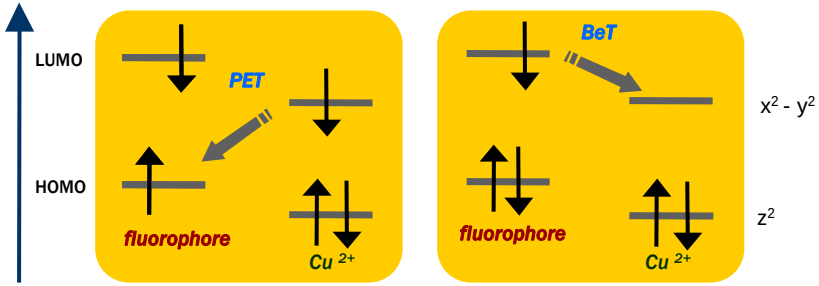

Fabbrizzi et al. *Chem Eur. J.* **1996**, *2*, 75.

Silent substrates

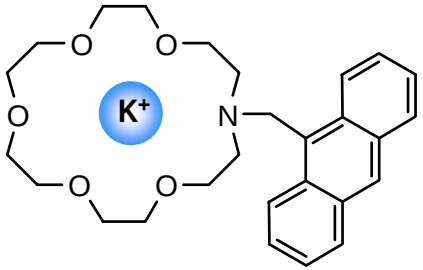

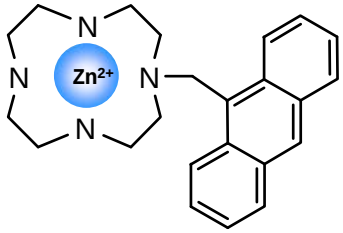

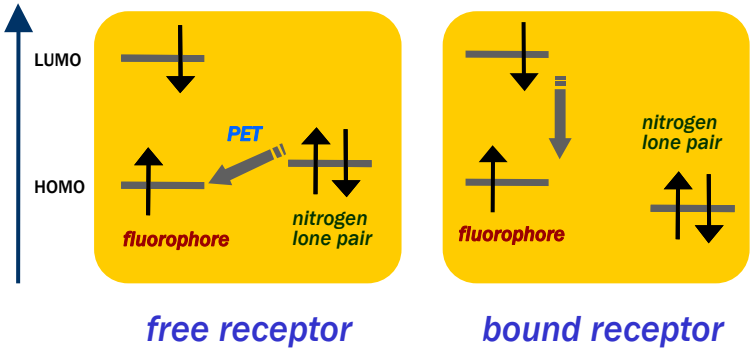

free receptor *bound receptor*

De Silva, **1986**

Czarnik *Acc. Chem. Res.*, **1994**, *27*, 302-308

Conjugate chemosensors: ATMCA (pH)

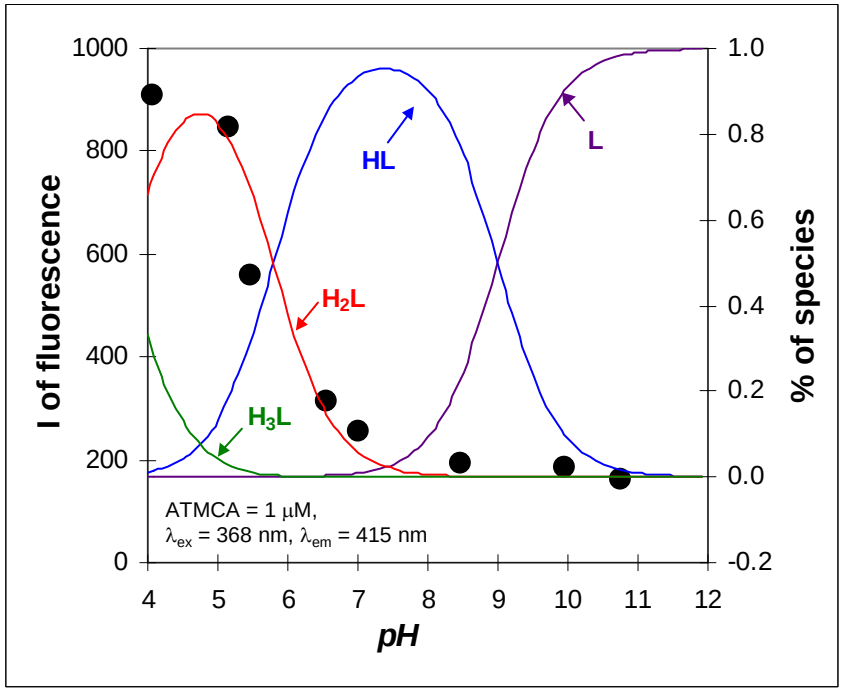

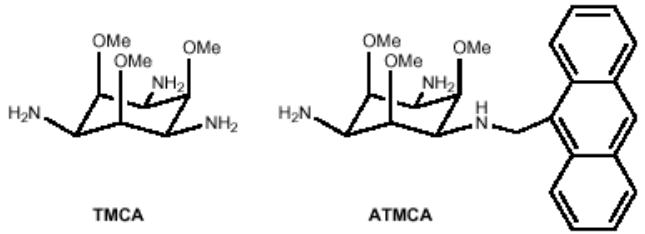

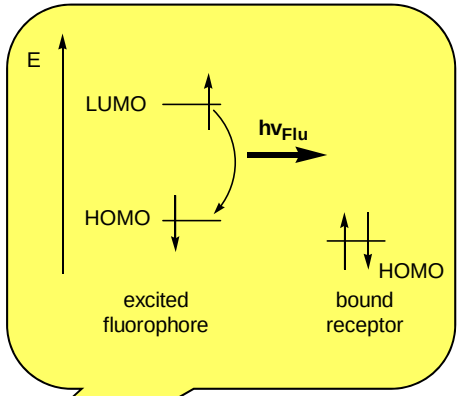

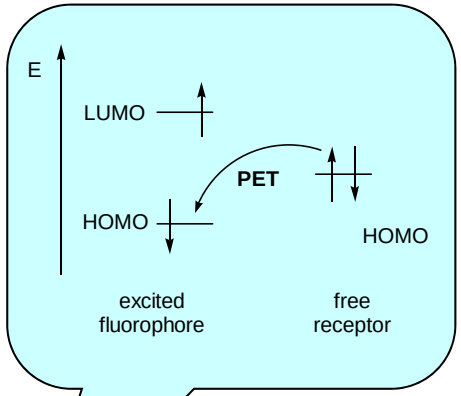

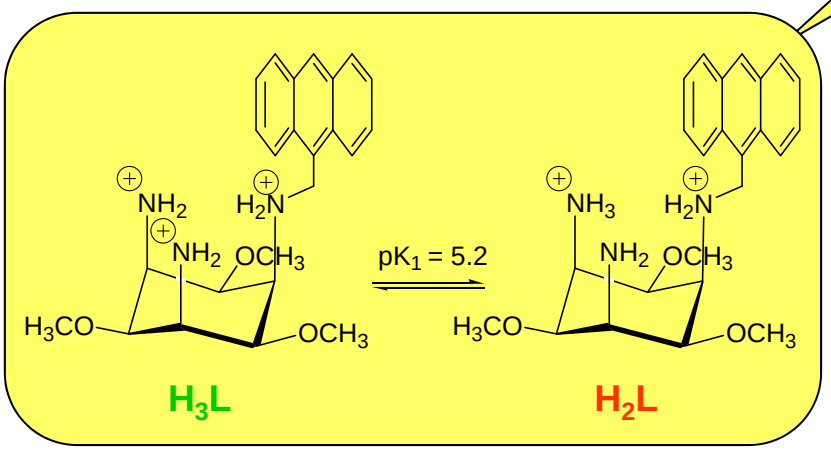

pK2 = 6.9

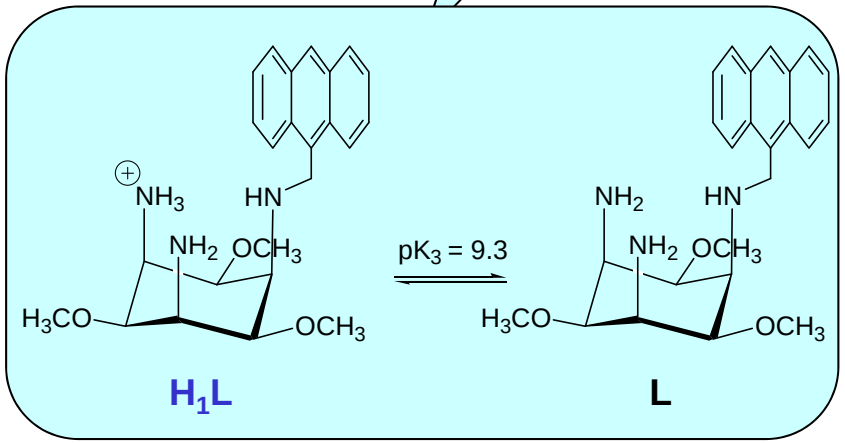

Conjugate chemosensors: ATMCA (Cu^{2+})

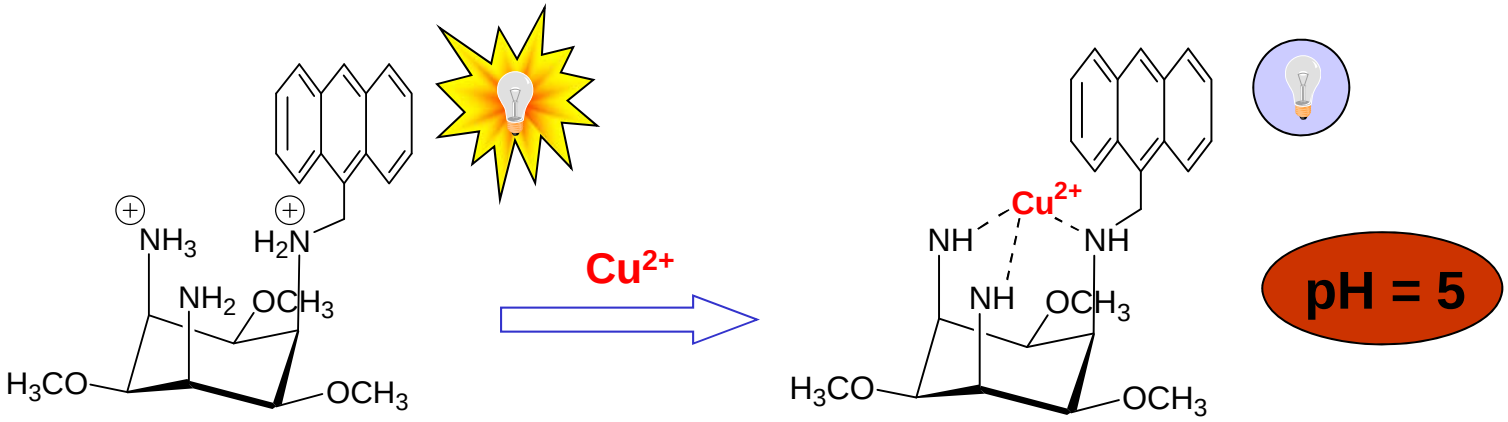

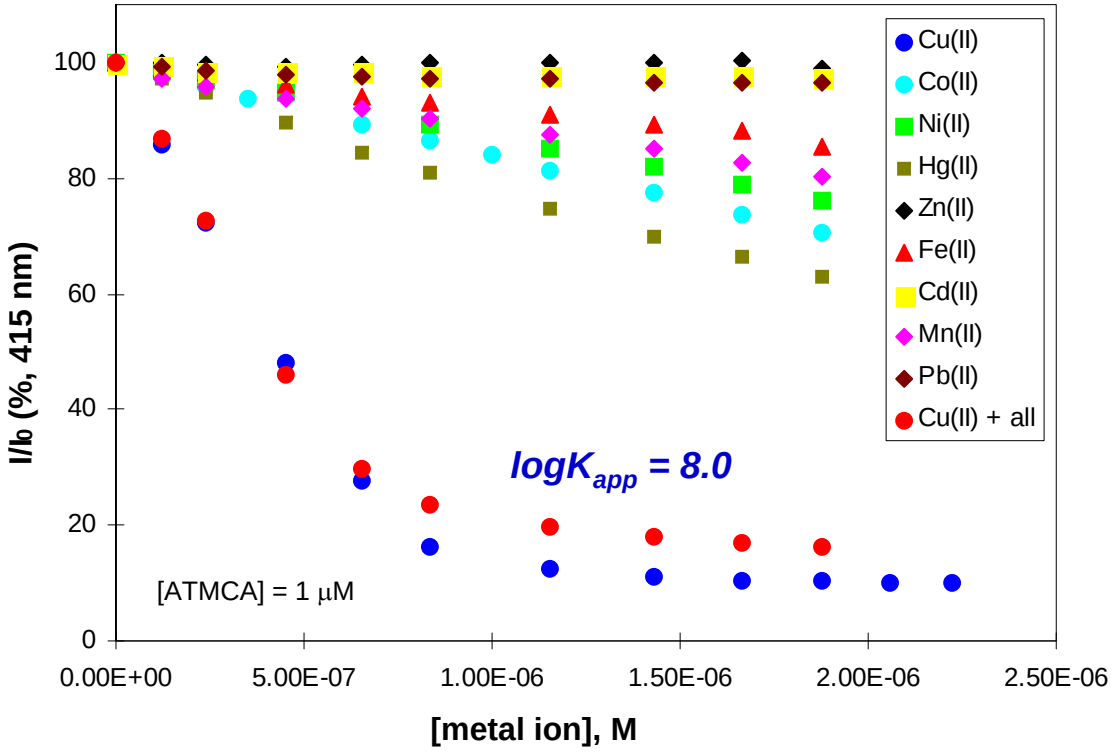

Conjugate chemosensors: ATMCA (Zn^{2+})

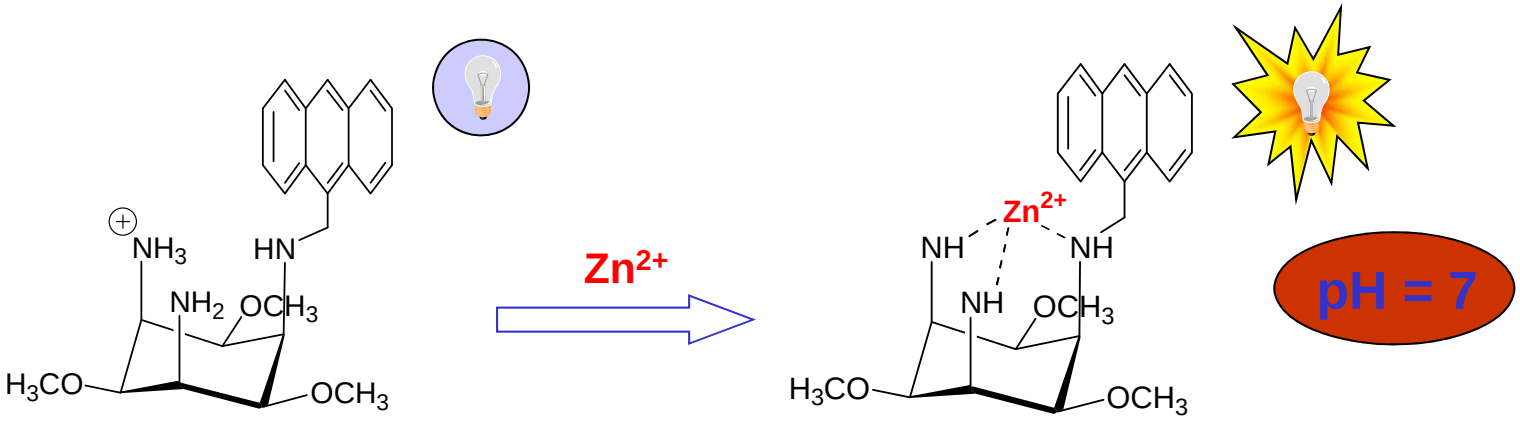

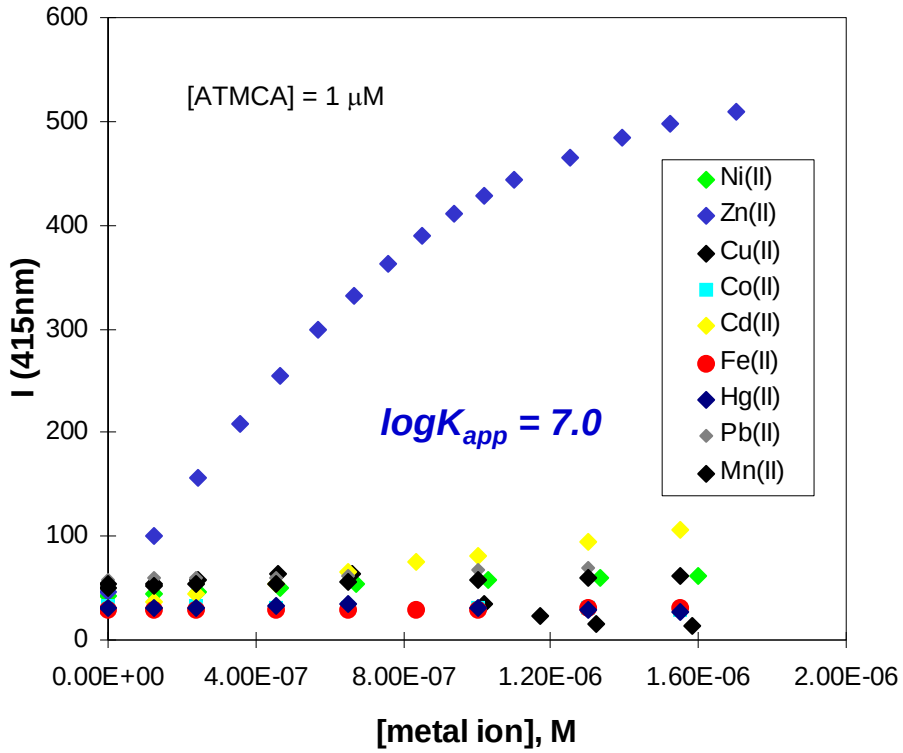

Conjugate chemosensors: ATMCA (Zn^{2+})

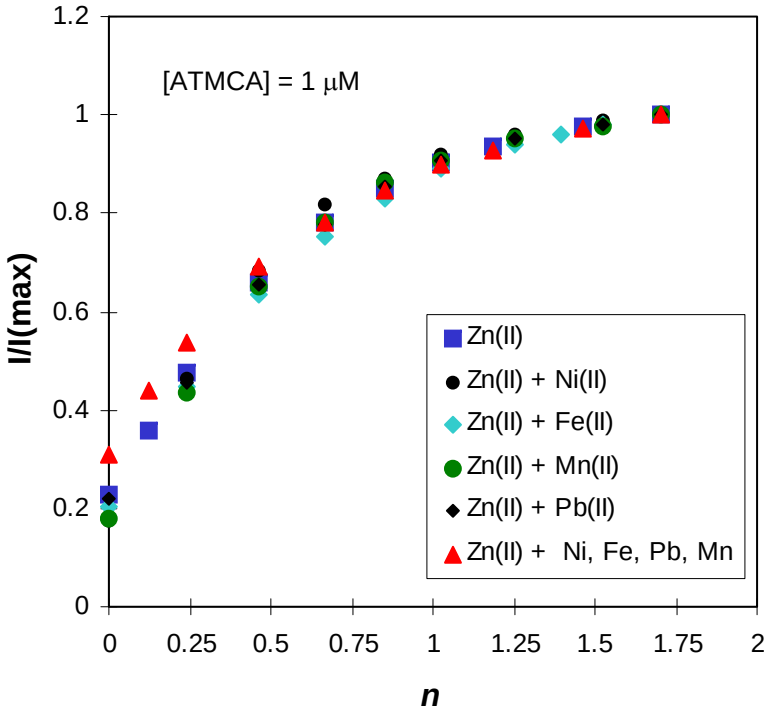

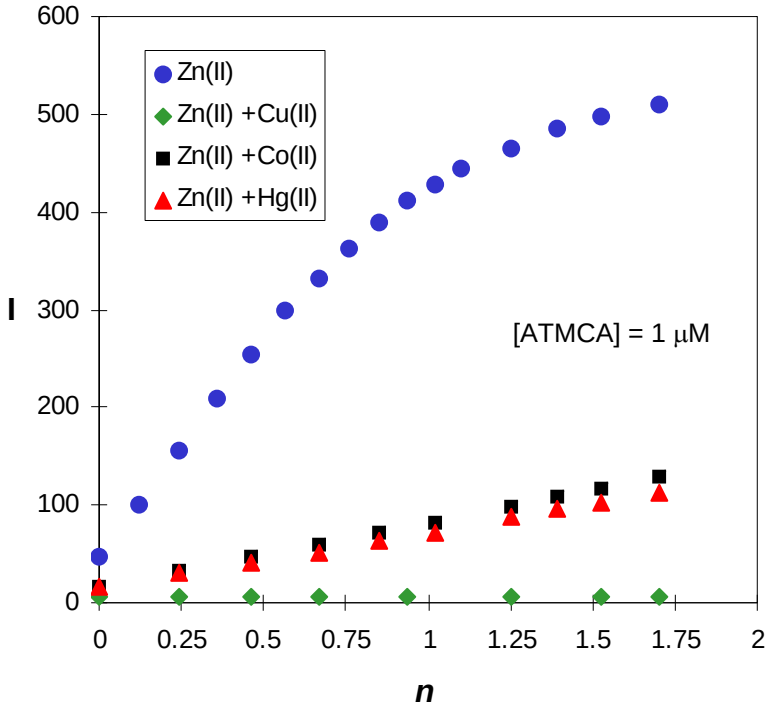

Applicazione biomedica di sensori intrinseci

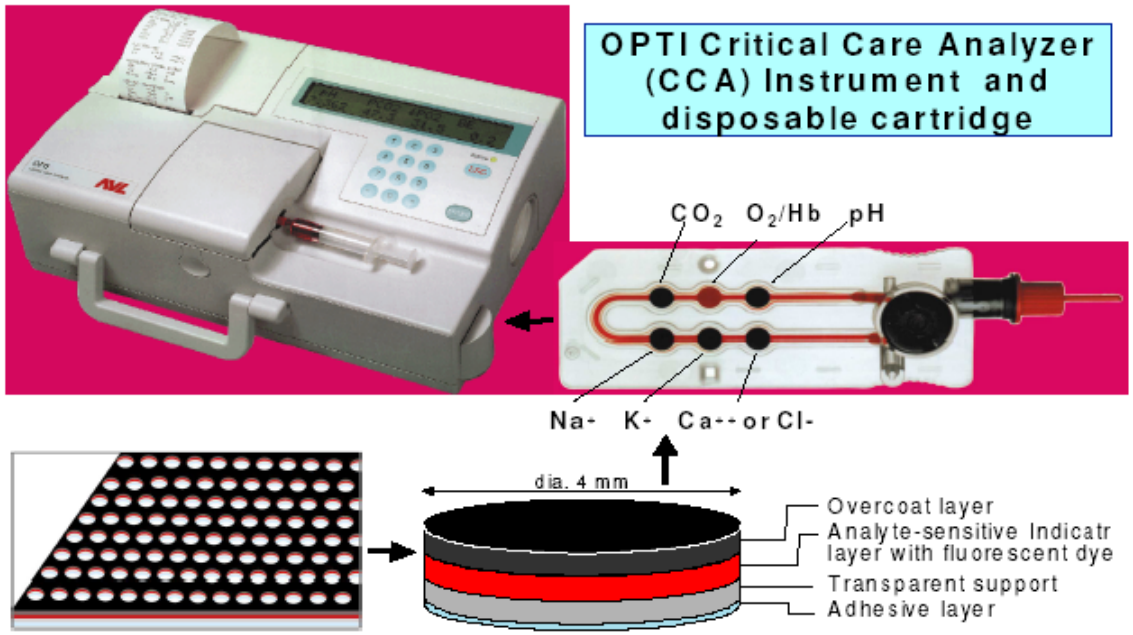

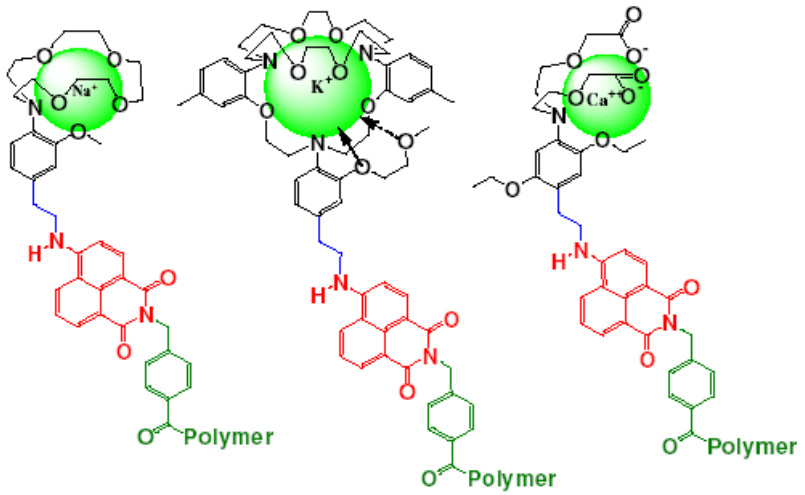

J.K. Tusa, H. He, JACS,

Formazione di eccimeri

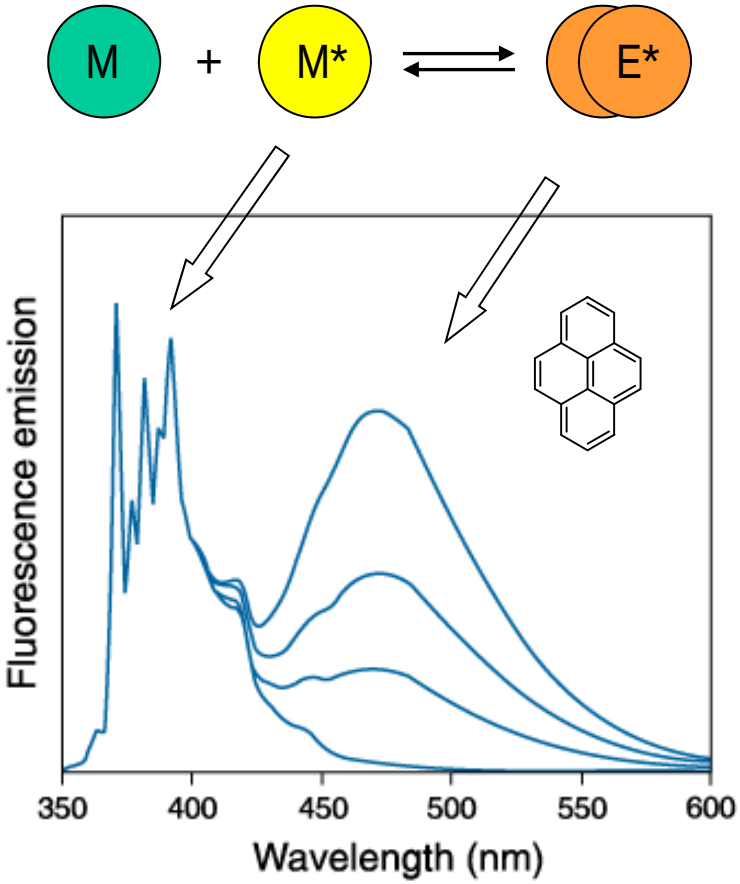

La complessazione del catione provoca una variazione conformazionale

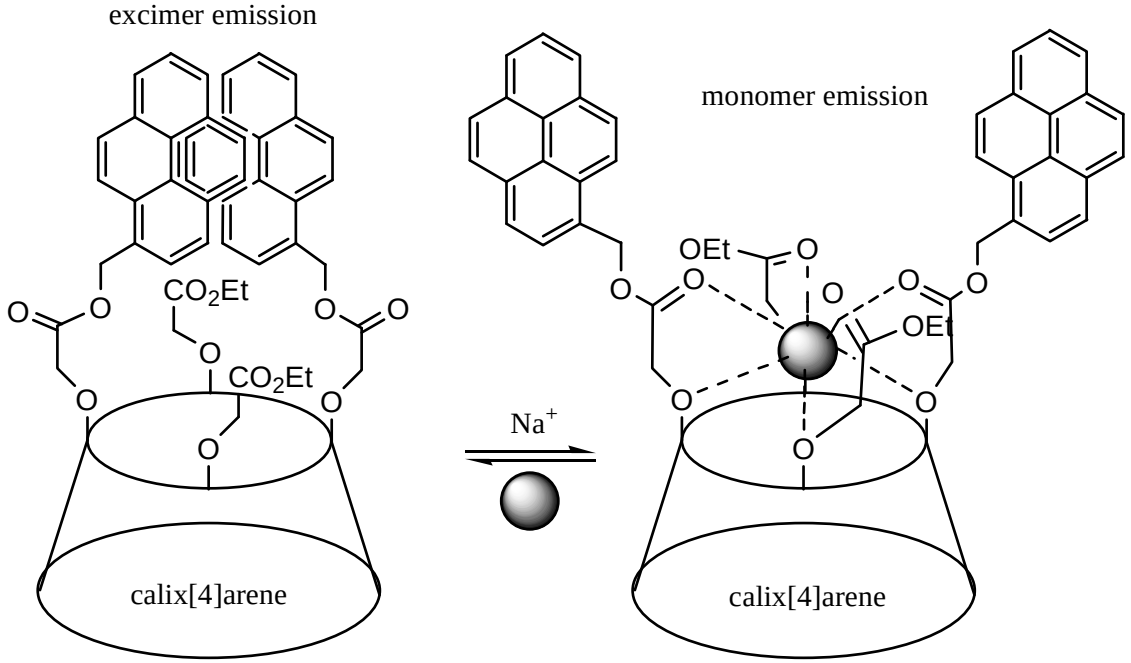

Jin et al. *J. Chem. Soc., Chem. Commun.*, **1992**, 499.

Altri effetti dovuti alla variazione della conformazione

planarizzazione del diarile

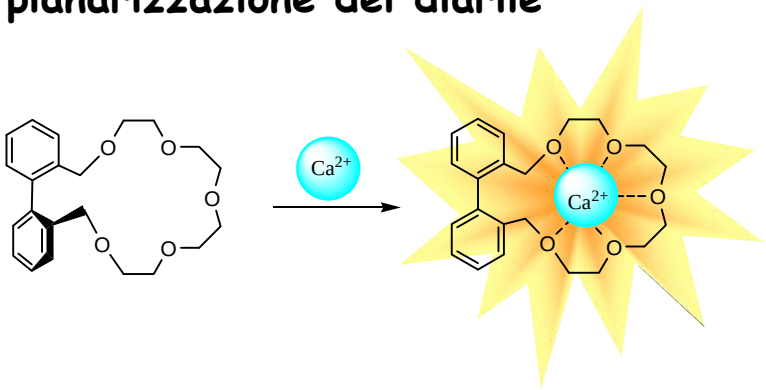

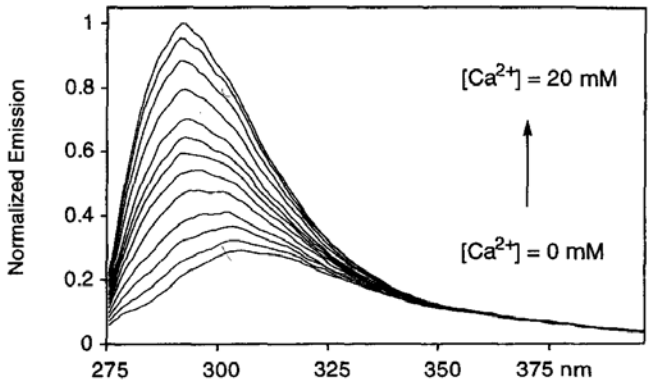

Finney et al. *J. Am. Chem. Soc.* **2001**, *123*, 1260.

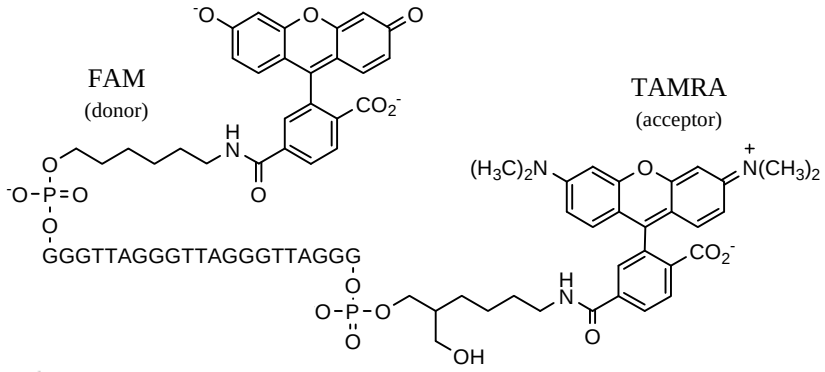

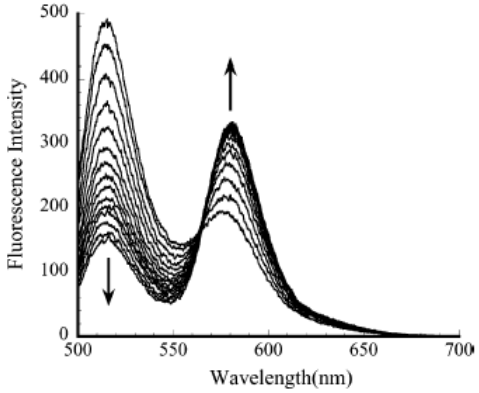

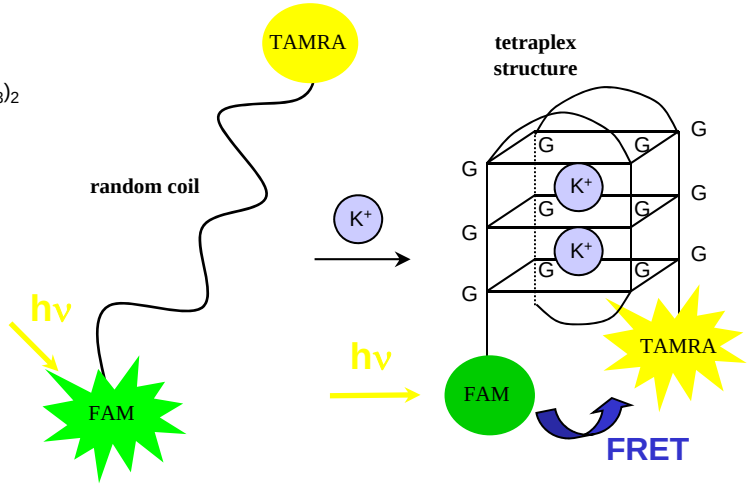

Takenaka et al. *J. Am. Chem. Soc.* **2002**, *124*, 14286.

Conjugate chemosensors

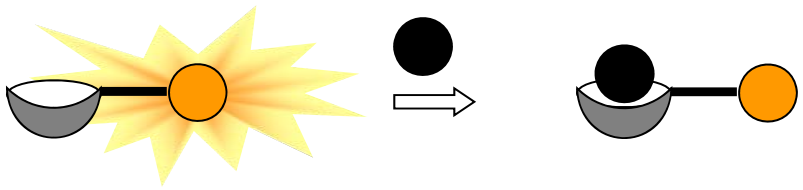

Design: the receptor is electronically insulated from the π-system of the fluorophore by a spacer.

Advantage: modularity. The two subunits (receptor and fluorophore) can be designed and optimized separately and then eventually connected.

Weakness: the overall design of the system must foresee the presence of some transduction mechanism, since the analyte and the signaling unit are no more in a direct contact. Moreover, the synthesis if often demanding

STRATEGIE PER LA PROGETTAZIONE DI UN SENSORE SUPRAMOLECOLARE

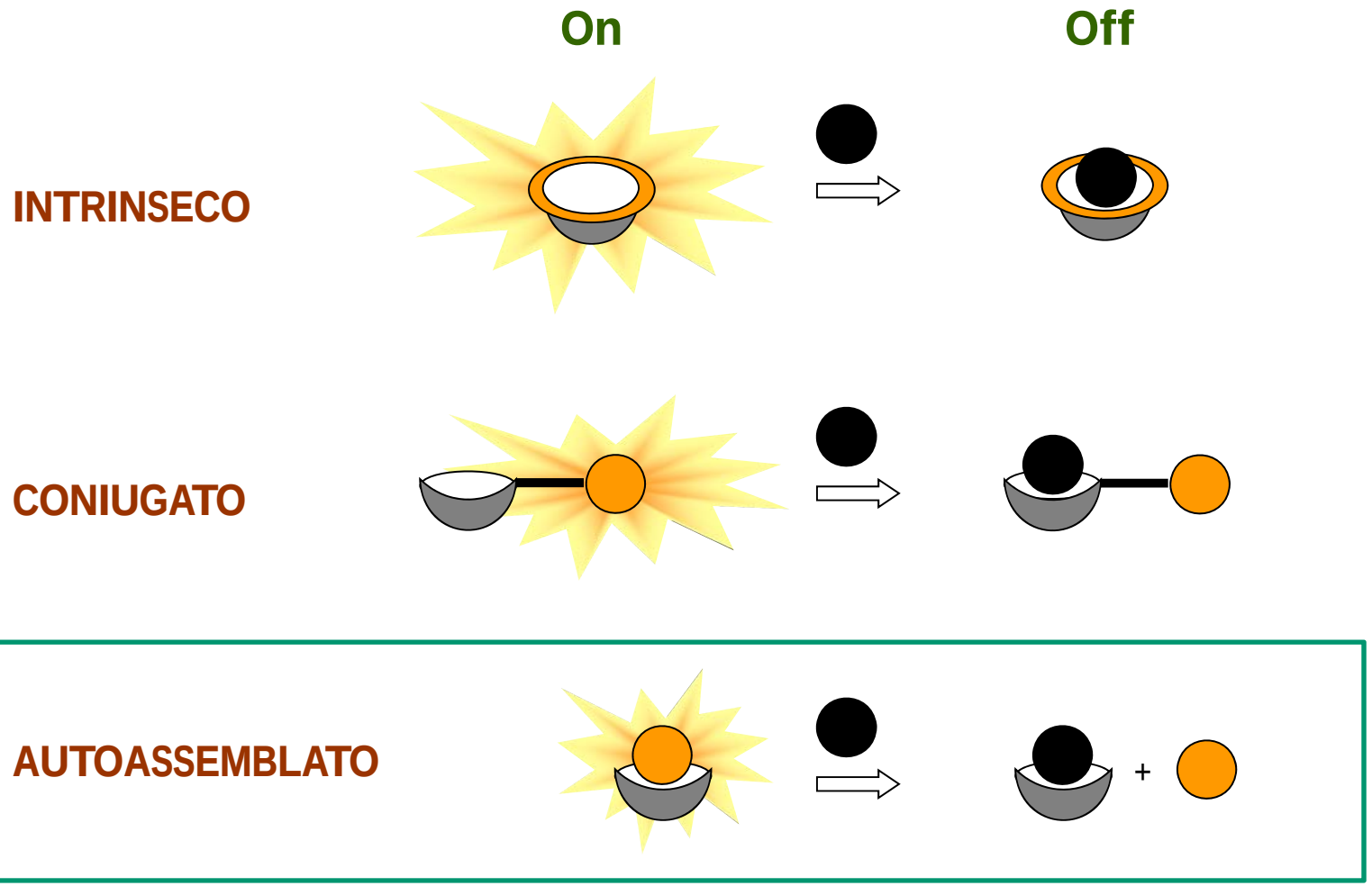

SELF-ASSEMBLED chemosensors: ATMCA·Zn(II) (organic anions)

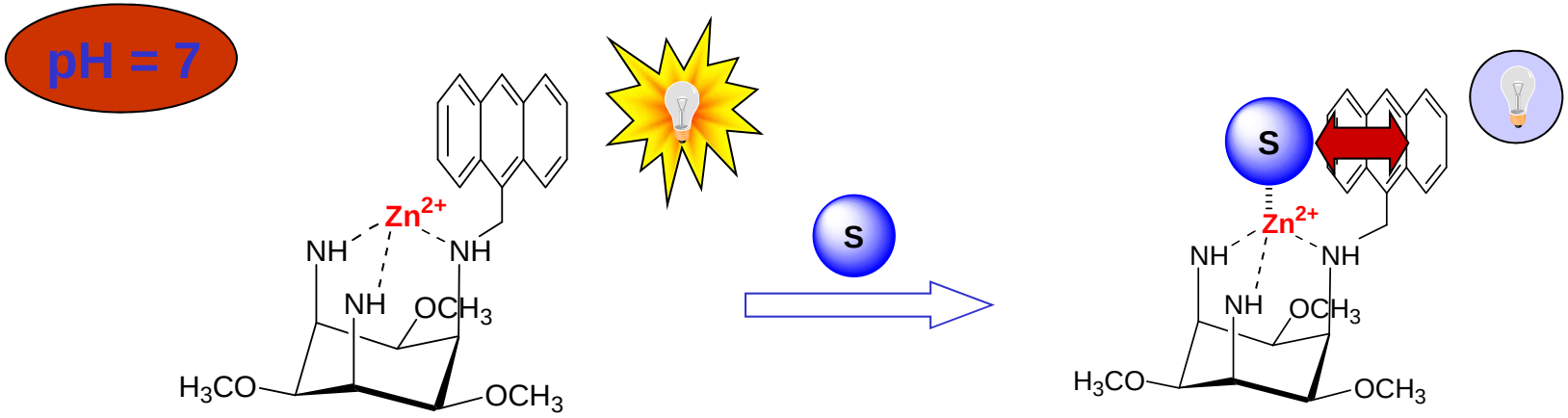

A organic substrate (anions) may bind to the Zn(II) ions forming a ternary complex. If the substrate is able to interact with the fluorophore this may result in the quenching of the fluorescence emission.

SELF-ASSEMBLED chemosensors: ATMCA·Zn(II) (nucleobases and nucleotides)

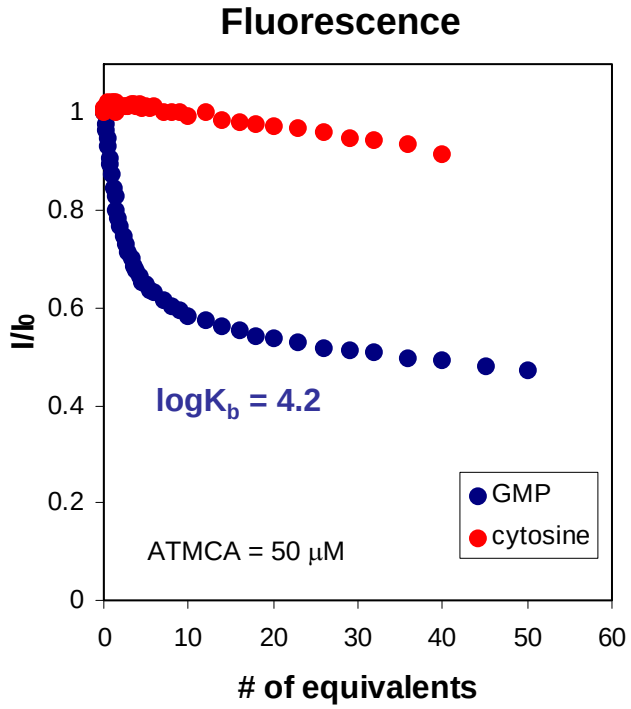

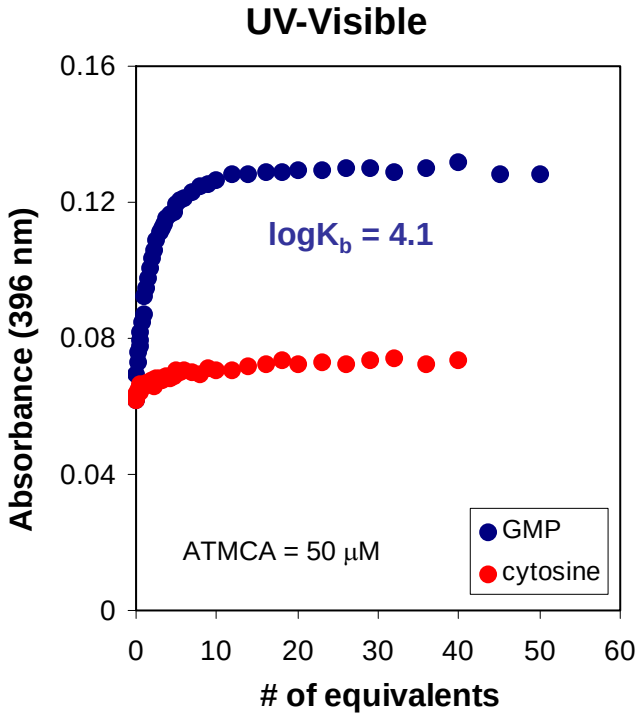

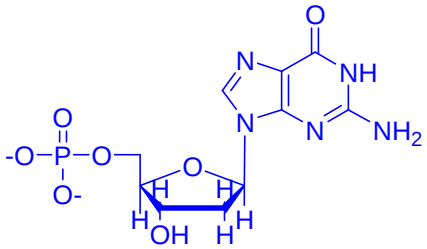

Guanosine-5'monophosphate (GMP)

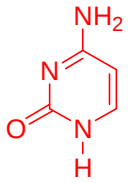

Cytosine

SELF-ASSEMBLED chemosensors: ATMCA·Zn(II) (nucleobases and nucleotides)

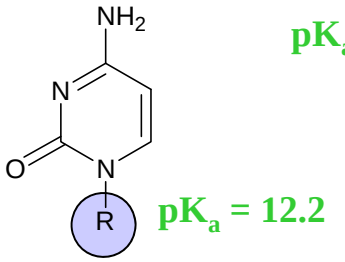

$pK_a = 12.2$

R = H: Cytosine (**no binding**)
R = A: CMP (**no binding**)

$pK_a = 9.9$

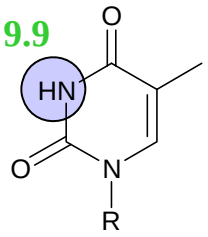

R = H: Thymine (**3.6**; **30%**)
R = A: TMP (4.5; **25%**)

$pK_a = 9.4$

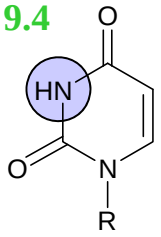

R = H: Uracyl (**3.6**; **31%**)
R = A: UMP (**4.0**; **30%**)

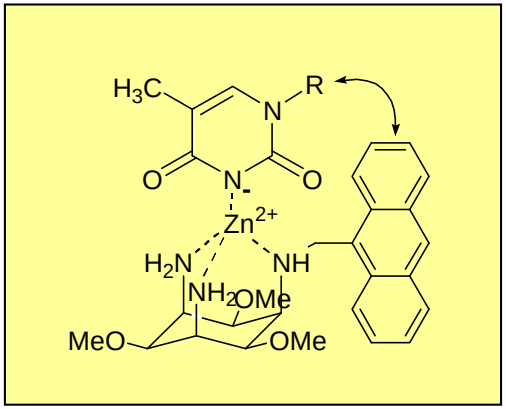

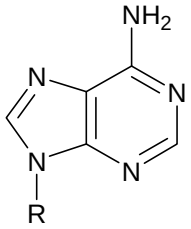

R = H: Adenine (**not soluble**)
R = A: AMP (**no binding**)

$pK_a = 9.3$

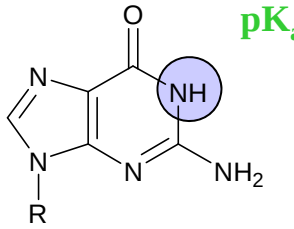

R = H:Guanine (**not soluble**)
R = A: GMP (**4.2**; **53%**)

Binding and quenching appear to be related to the presence of an **acidic amide (imide) proton** and to **stacking**

A=

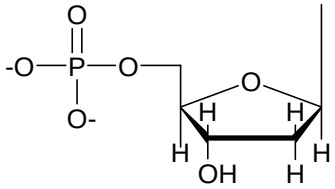

blu = $\log K_b$
red = % of quenching

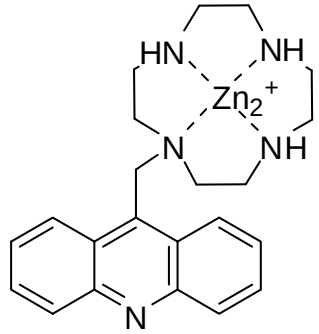

Kimura et al. *J. Am. Chem. Soc.* **1994**, *116*, 3848.

SELF-ASSEMBLED chemosensors: ATMCA·Zn(II) (carboxylic acids)

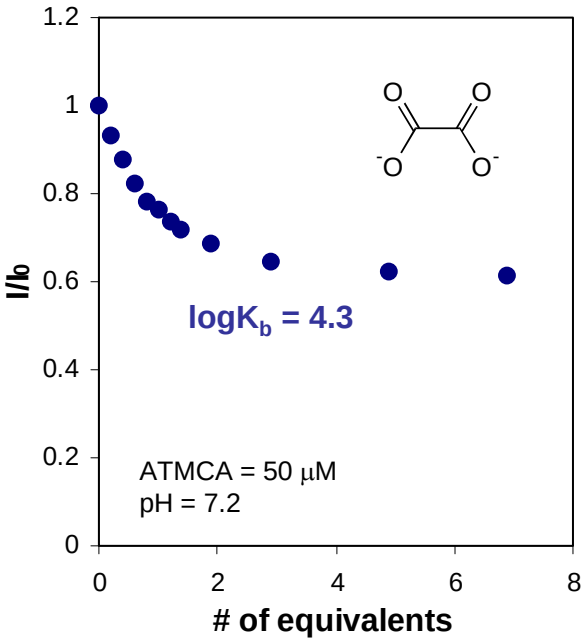

Other dicarboxylic acids (malonic, succinic), monocarboxylic acids and amino acids do not bind to ATMCA.

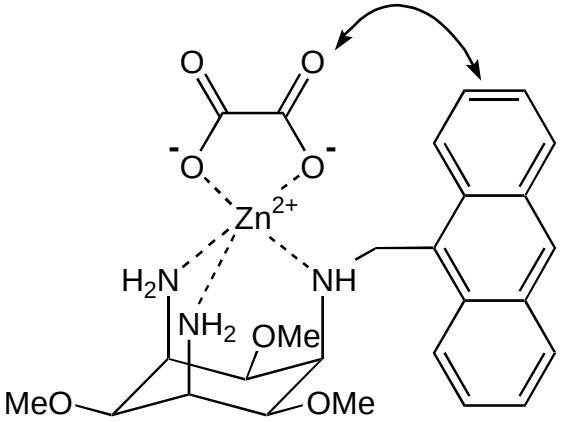

The formation of a **5 atoms chelate** appears to be crucial for binding and signalling.

SELF-ASSEMBLED chemosensors: ATMCA·Zn(II) (vitamin B13)

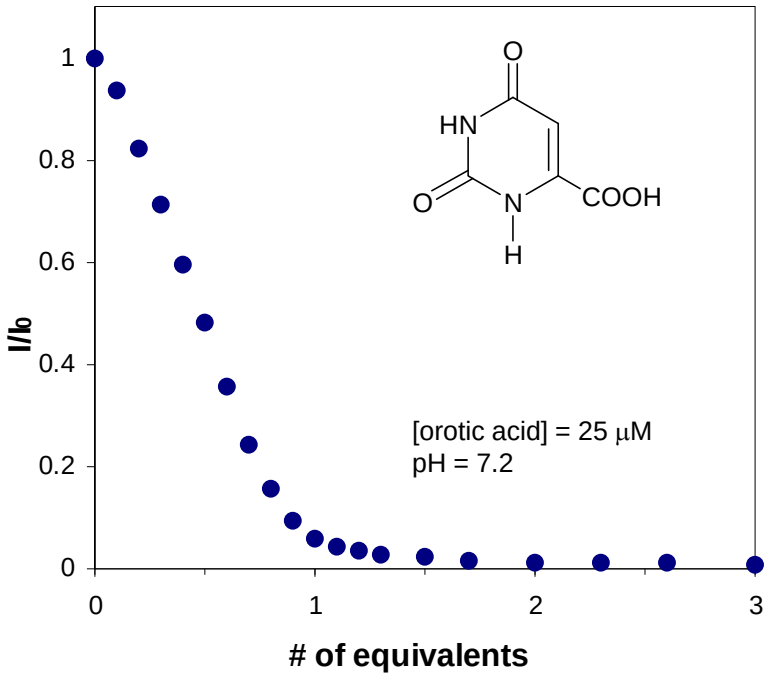

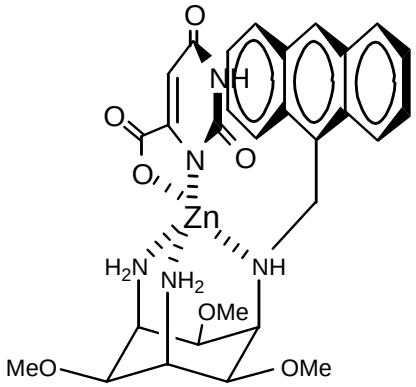

Orotic acid conjugates an **acidic amide proton** with the formation of a **5 atoms chelate** and **stacking**.

The result is a **strong binding** (**$\log K_b$ = 6.6**) and **total quench** of the fluorescence emission.

“Chemosensing ensemble”

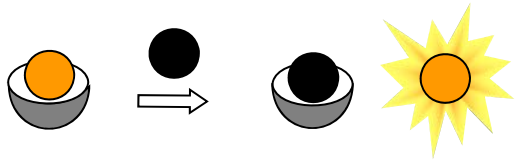

chemosensing ensemble

Sistema autoassemblato mediante interazioni ione-ione: l’analita rimpiazza il rilevatore

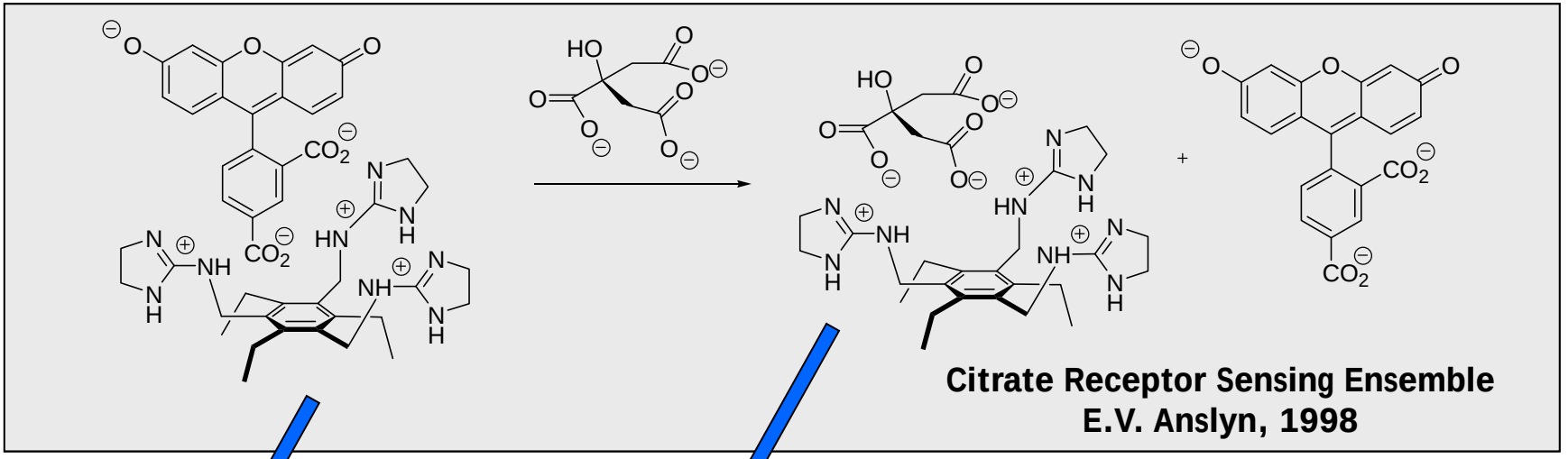

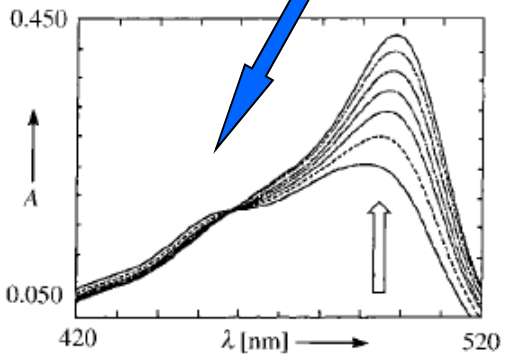

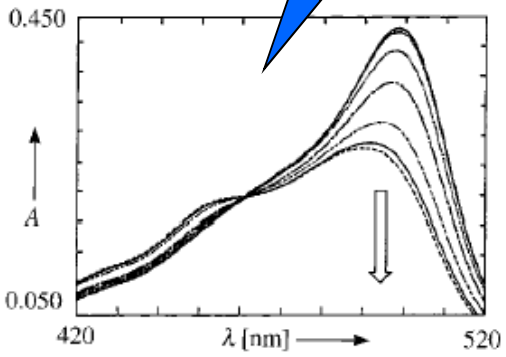

Table 1. Concentration of citrate [mM] in beverages determined by different methods.

	Gravimetric	NMR	**1**+**2**, absorption	**1**+**2**, emission
citrate model solution	30.1	–	30.3	29.9
calibration solution	1.33	–	1.205	1.39
orange juice	–	43.1	44.1	44.7
Gatorade	–	15.95	15.05	15.1
Powerade	–	12.4	11.1	11.3
All Sport	–	7.4	7.1	8.1
Mountain Dew	–	7.95	5.5	5.4
tonic water	–	21.0	21.15	20.8
Coca Cola	–	0	0	<0.5
Diet Coke	–	<0.2	<0.4	<0.7

Sistema autoassemblato mediante interazioni ione-metallo: stesso principio del "chemosensing ensemble"

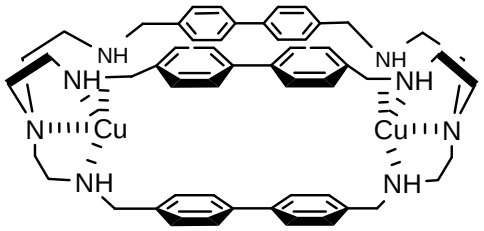

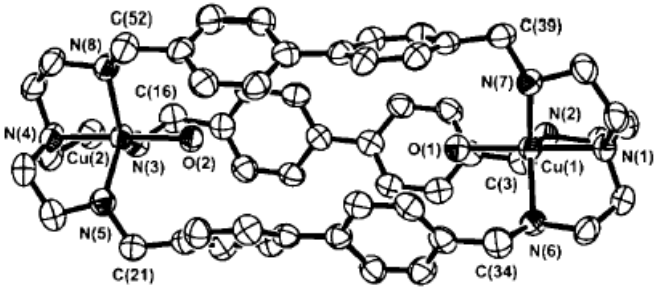

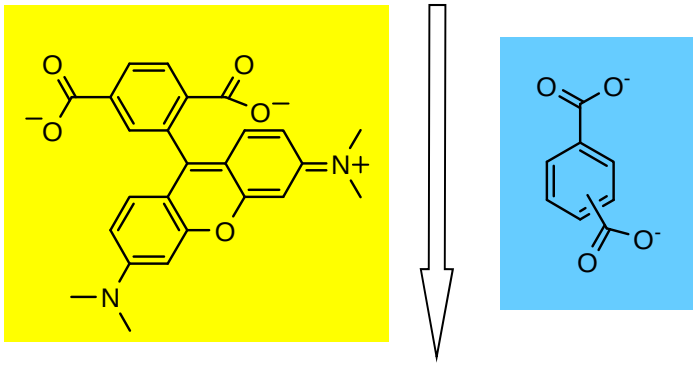

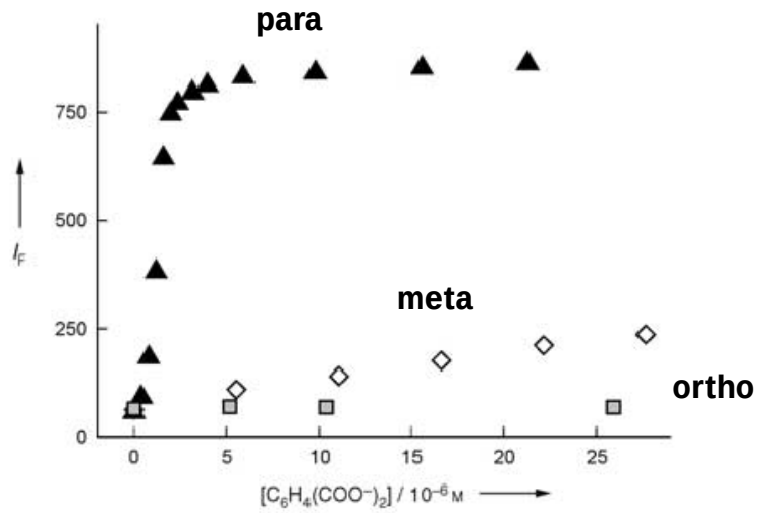

Fabbrizzi et al. *Angew. Chem.* **2004**, *43*, 3847.

The approach is general and it has been applied to the detection of several substrates (tartrate, gallic acid, heparin, phosphates, carbonate, amino acids and short peptides).

Pattern-Based Discrimination of Enantiomeric and Structurally Similar Amino Acids

I complessi con Cu(II) dei leganti chirali 1-3 con i cromofori interagiscono con ammino acidi (L e D) dando gradi diversi di sostituzione e variazioni di colore caratteristiche per ciascun sistema

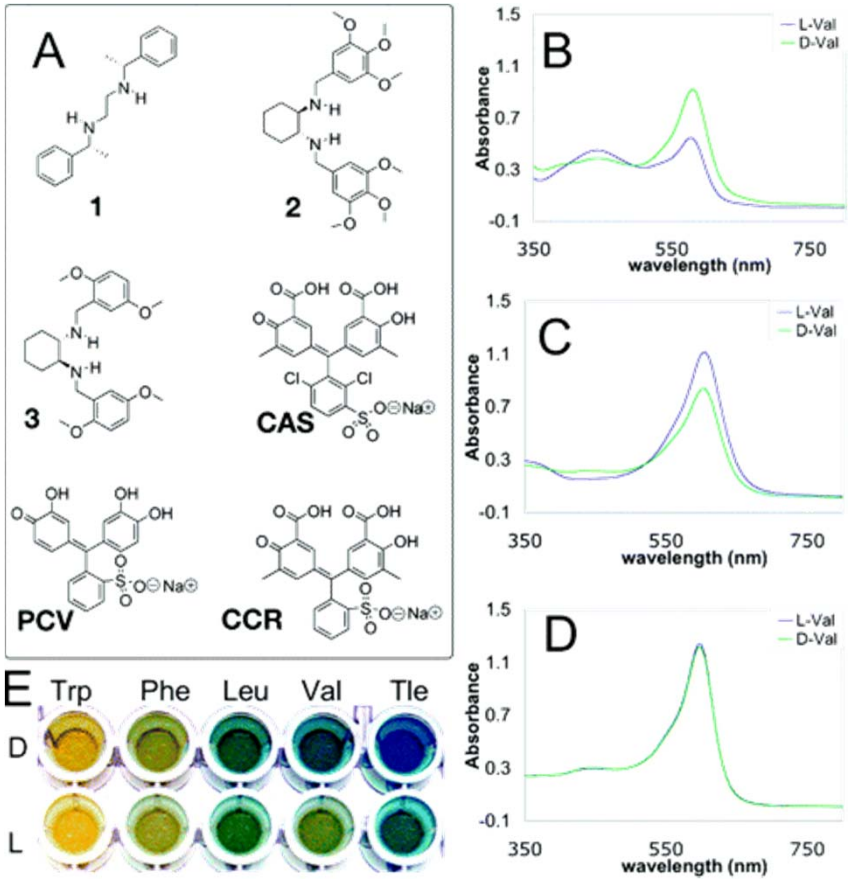

Figure 1 (A) Ligands and indicators used to construct sensor array. Absorbance spectra for (B) **1** [35 mM], $Cu(OTf)_2$ [157 μM], **CCR** [75 μM], and Val [200 μM]; (C) **3** [1.2 mM], $Cu(OTf)_2$ [393 μM], **CAS** [36 μM], and Val [2.5 mM]; (D) *N*,*N*'-tetramethylethylenediamine [4.5 mM], $Cu(OTf)_2$ [200 μM], **CAS** [55 μM], and Val [200 μM]. (E) Colorimetric output for **1** [35 mM], $Cu(OTf)_2$ [235 M], **CAS** [35 M], and amino acid [200 μM]. All studies carried out in 1:1 MeOH:H_2O, 50 mM HEPES buffer, pH = 7.8.

Pattern-Based Discrimination of Enantiomeric and Structurally Similar Amino Acids

Taking different combinations of the ligands and indicators with $Cu(OTf)_2$ (OTf = trifluoromethanesulfonate) and varying the concentrations of the species, we created a library of IDAs (Indicator Displacement Assay). Both enantiomers of the naturally occurring amino acids Leu, Val, Trp, and Phe, as well as the unnatural amino acid tert-leucine (Tle), were examined, giving a total of 10 analytes. For each analyte, absorbance spectra were recorded under a set of 21 different conditions.

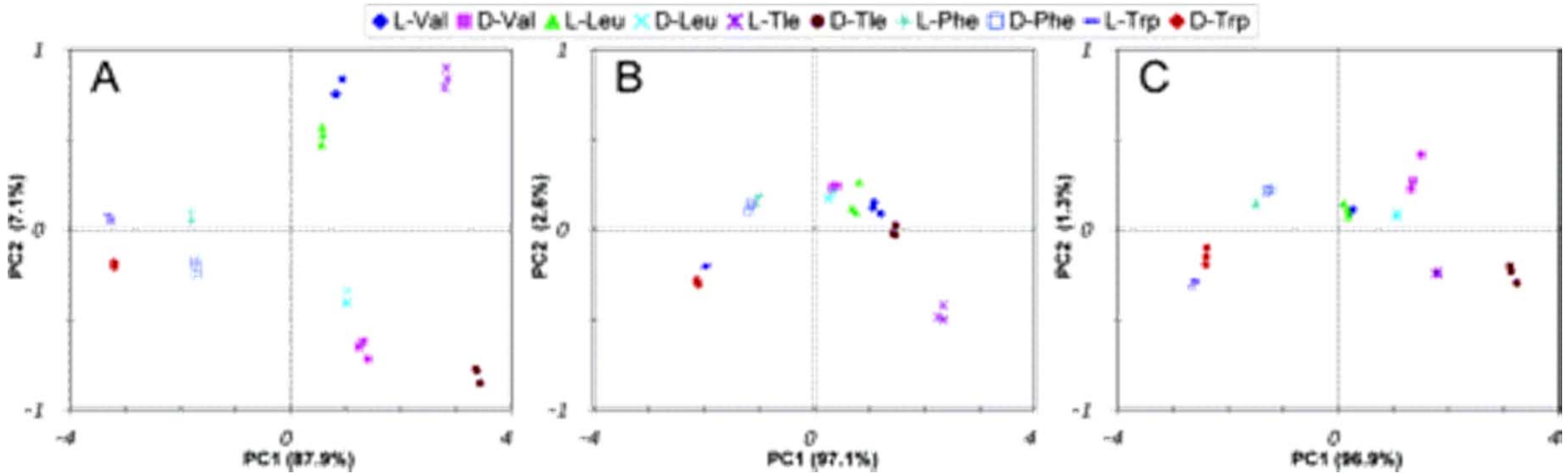

Two-dimensional PCA (principal component analysis) plots for D and L amino acids prepared (A) from data for all 21 enantioselective indicator displacement assays (IDAs), (B) from data for 8 IDAs selective for D amino acids, and (C) from data for 13 IDAs selective for L configuration.

Self-organized chemosensors: quantum dots

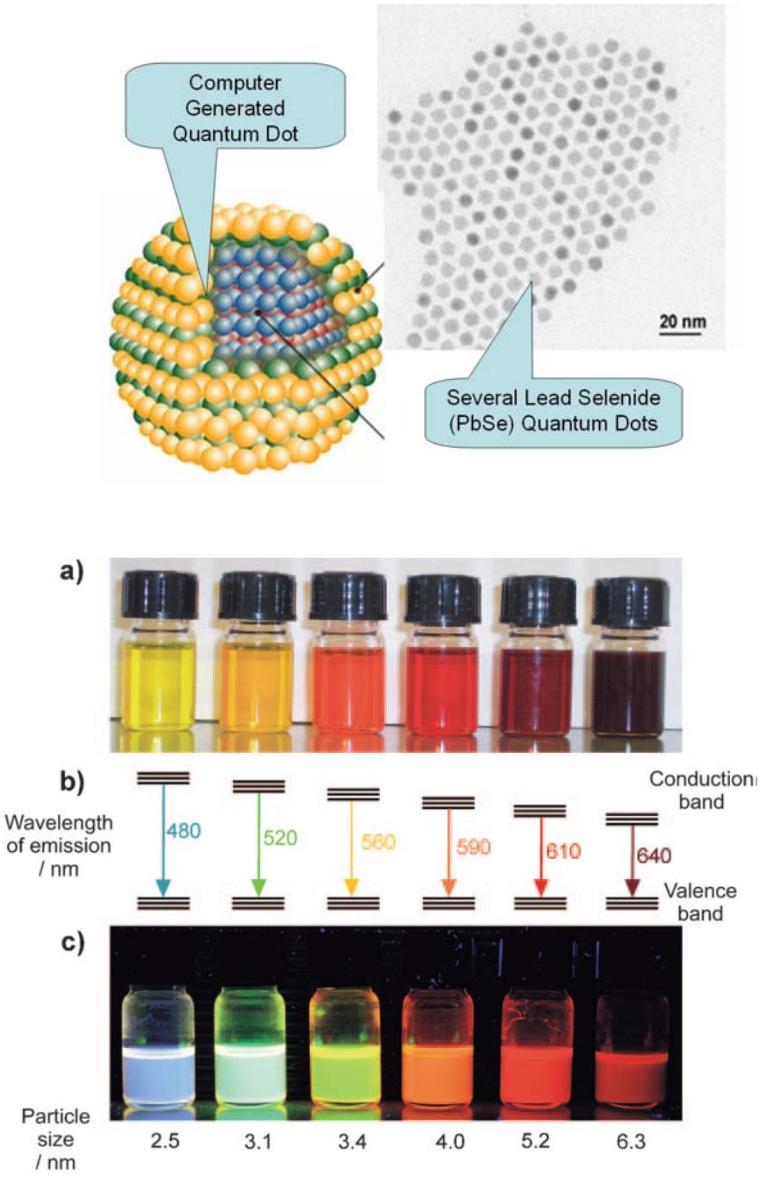

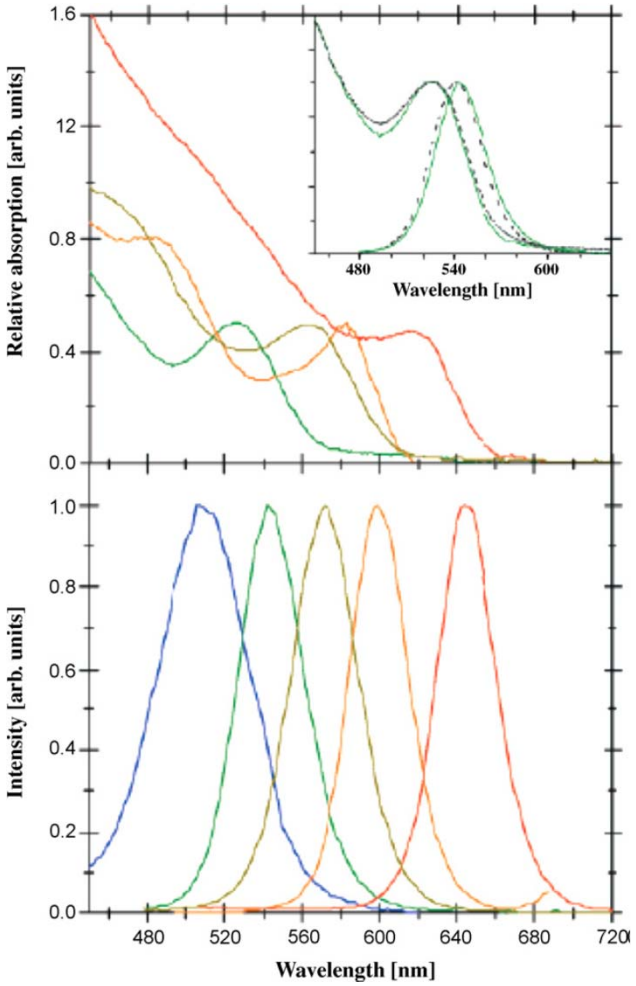

Self-organized chemosensors: quantum dots

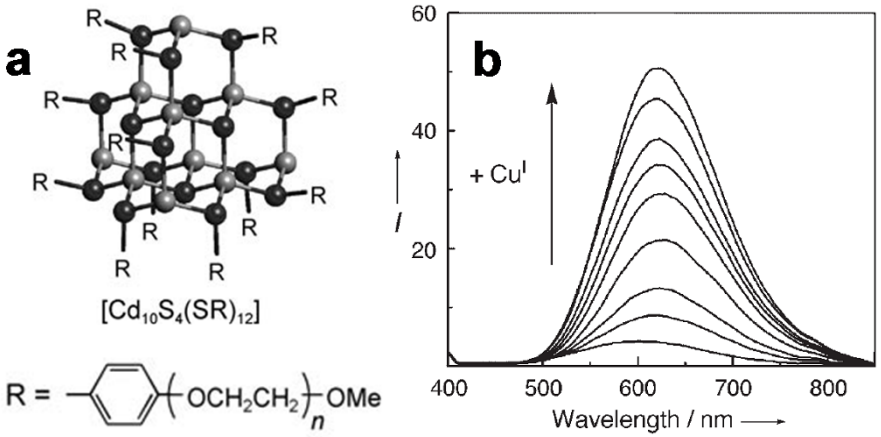

Analyte induced modulation of surface excitons recombination

K. Konishi and T. Hiratani, *Angew. Chem. Int. Ed.*, 2006, **45**, 5191-5194

Self-organization of binding sites

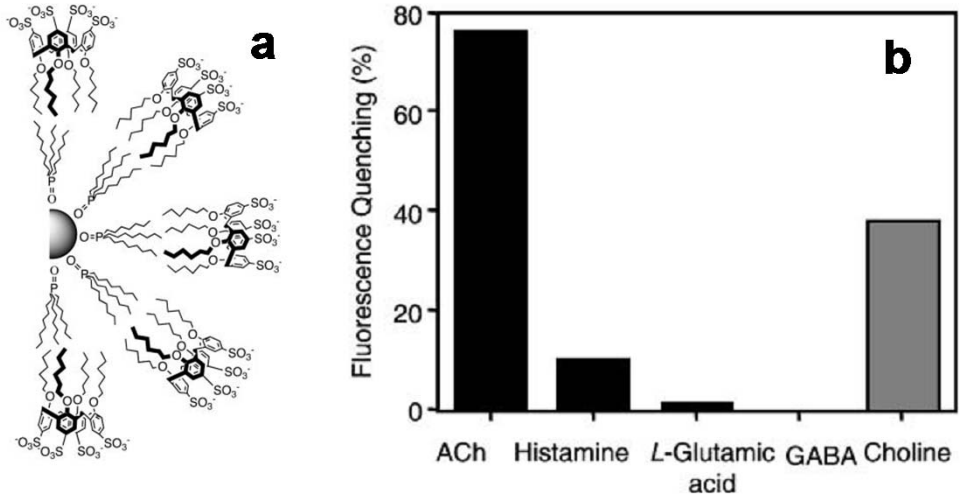

T. Jin, F. Fujii, H. Sakata, M. Tamura, and M. Kinjo, *Chem. Commun.*, 2005, 4300-4302

Self-organized chemosensors: quantum dots

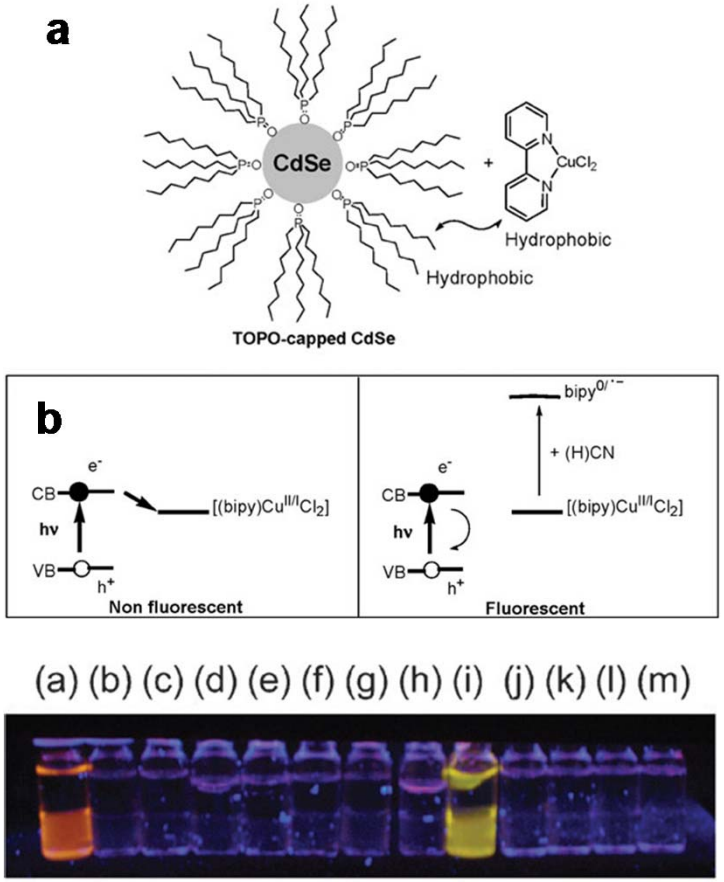

Cyanide sensing by ET interruption

A. Touceda-Varela, E. I. Stevenson, J. A. Galve-Gasion, D. T. F. Dryden, and J. C. Mareque-Rivas, *Chem. Commun.*, 2008, 1998-2000

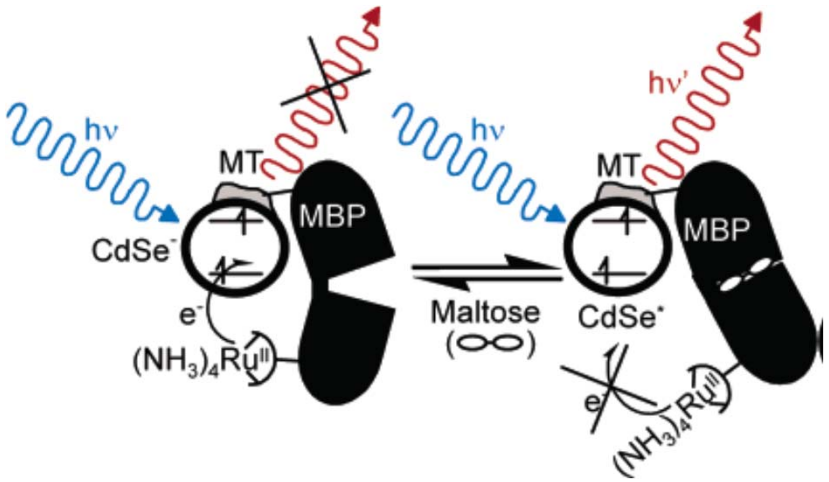

Maltose sensing by PET modulation

M. G. Sandros, D. Gao, and D. E. Benson, *J. Am. Chem. Soc.*, 2005, **127**, 12198-12199

Self-organized chemosensors: quantum dots

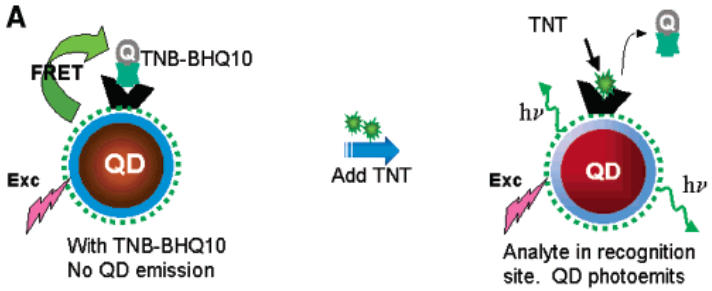

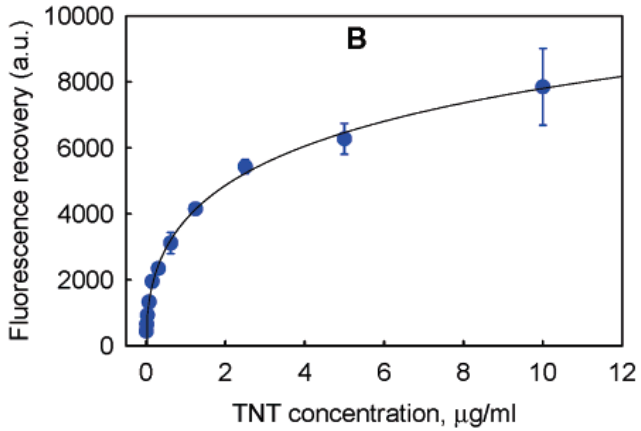

Chemosensing ensamble with a quencher, OFF-ON TNT detection

E. R. Goldman, I. L. Medintz, J. L. Whitley, A. Hayhurst, A. R. Clapp, H. T. Uyeda, J. R. Deschamps, M. E. Lassman, and H. Mattoussi, *J. Am. Chem. Soc.*, 2005, **127**, 6744-6751.

Chemosensing ensamble with a dye, FRET ratiometric sugar/dopamine detection

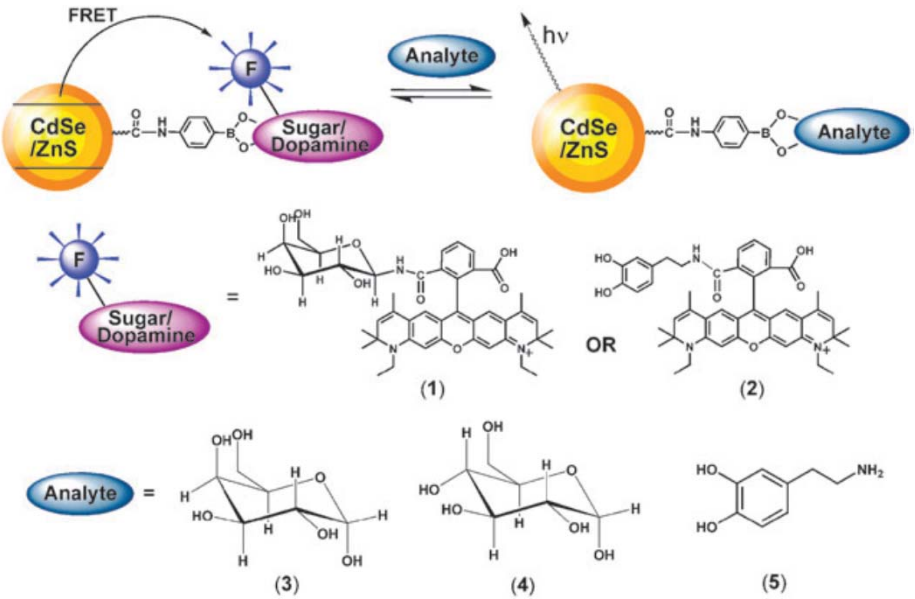

R. Freeman, L. Bahshi, T. Finder, R. Gill, and I. Willner, *Chem. Commun.*, 2009, 764-766

Sensori autoassemblati

Struttura: recettore e unità attiva non solo non sono elettronicamente isolati ma addirittura non sono legati l'uno all'altro; si devono autoassemblare in soluzione

Vantaggi: preparazione, ottimizzazione e modificazione sono relativamente semplici

Punti deboli: trovare un meccanismo di trasduzione del segnale , diffocltà di progettazione del recettore

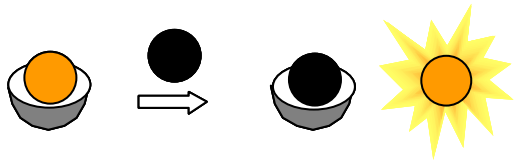

chemosensing ensemble

Sensori organizzati da un opportuno agente templante

L'approccio si basa sull'autoassemblaggio (o l'autoorganizzazione) di una molecola fluorescente e del recettore su di un opportuno agente templante così da formare un sistema organizzato. In questo sistema assemblato le due subunità non interagiscono direttamente e la comunicazione tra substrato complessato e molecola fluorescente è garantita dalla loro vicinanza spaziale.

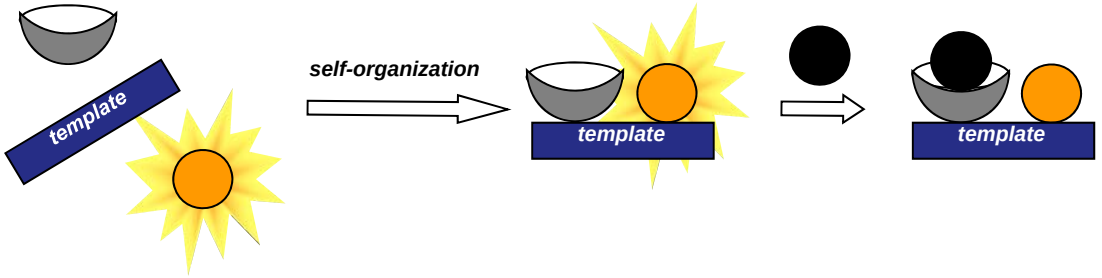

Agenti templanti:

- Aggregati di tensioattivi
- Monostrati
- Superfici di vetro
- Nanoparticelle

Self-Organized Chemosensors

In Surfactant Micellar Aggregates

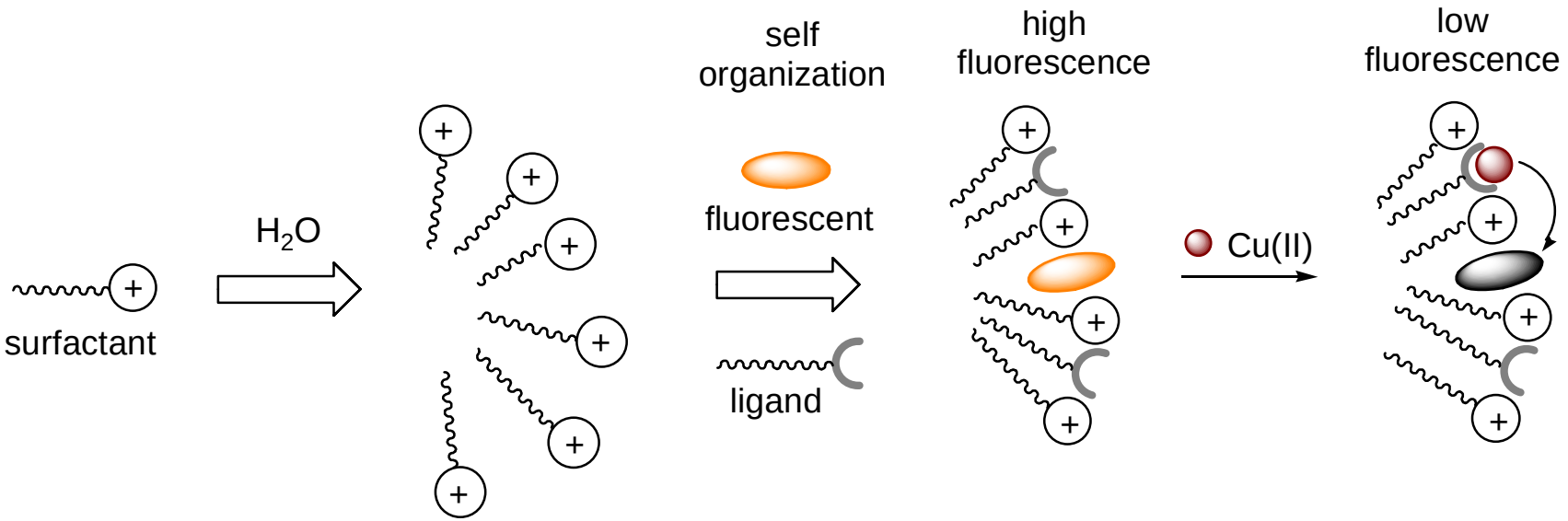

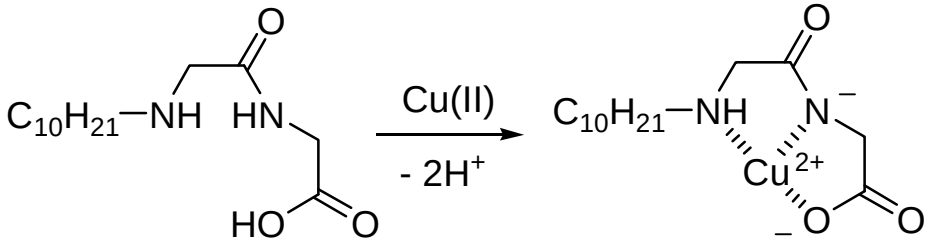

ligand = C_{10}GlyGLy

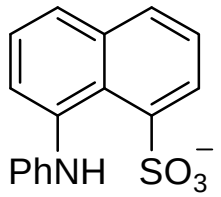

fluorescent dye = ANS

Angew. Chem. Int. Ed. **1999**, *38*, 3061-3064

Langmuir **2001**, *17*, 7521-7528.

Cu^{2+} sensing and sensitivity tuning

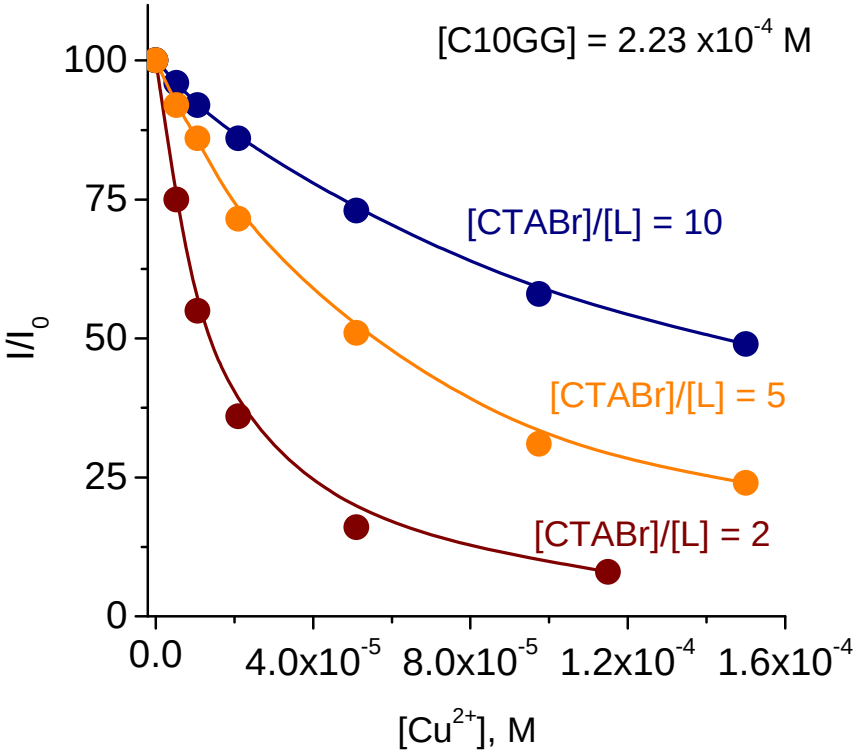

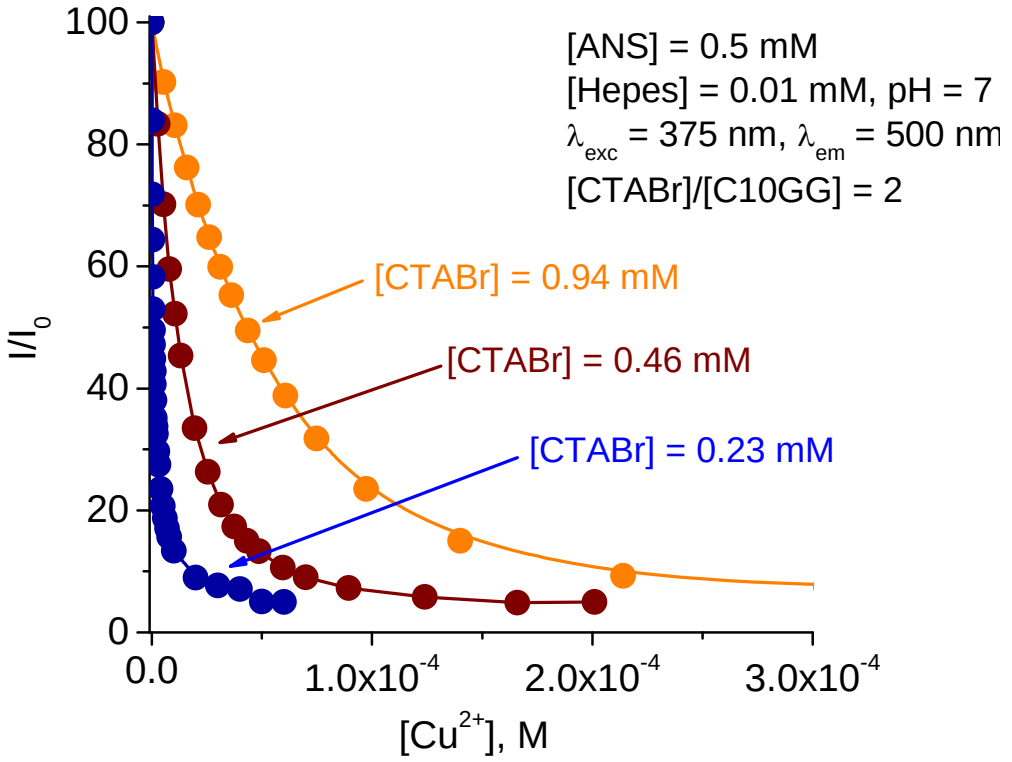

10% Emission decrease at
6.5×10^{-8} M Cu^{2+} concentration

Sensing in Micellar Aggregates: combinatorial screening

Fluorophores

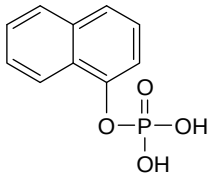

1-NAFOSF

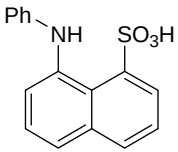

ANS

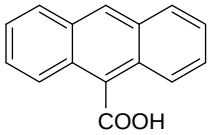

ACA

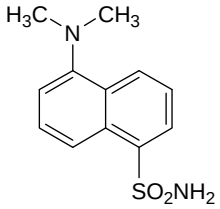

DANSA

Surfactants

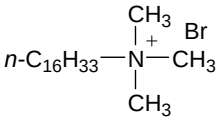

CTABr

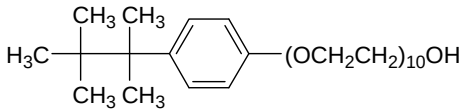

Triton X-100

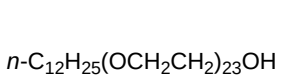

Brij 35

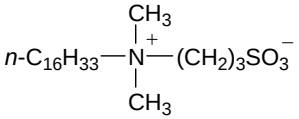

DMMAPS

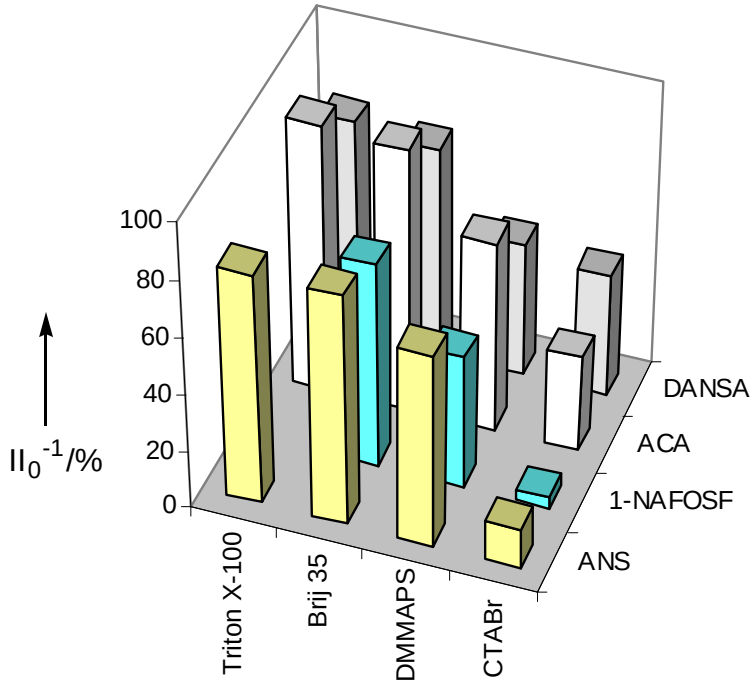

Utilizzo di monostrati come agenti templanti: sensore per Cu(II)

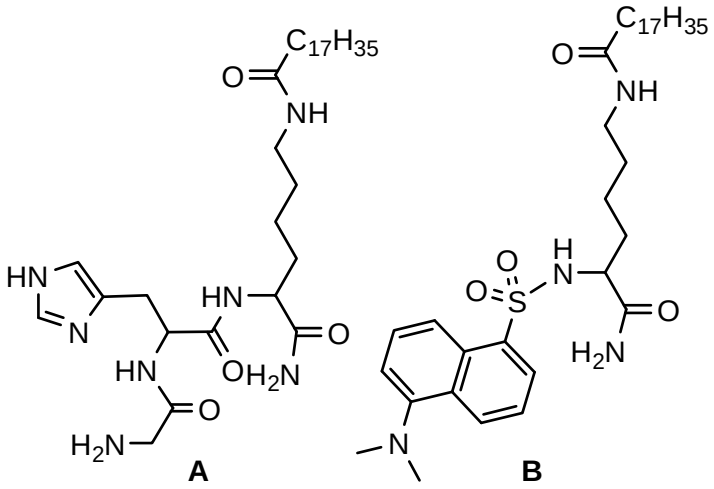

leblanc et al. *J. Am. Chem. Soc.* **2003**, *125*, 2680.

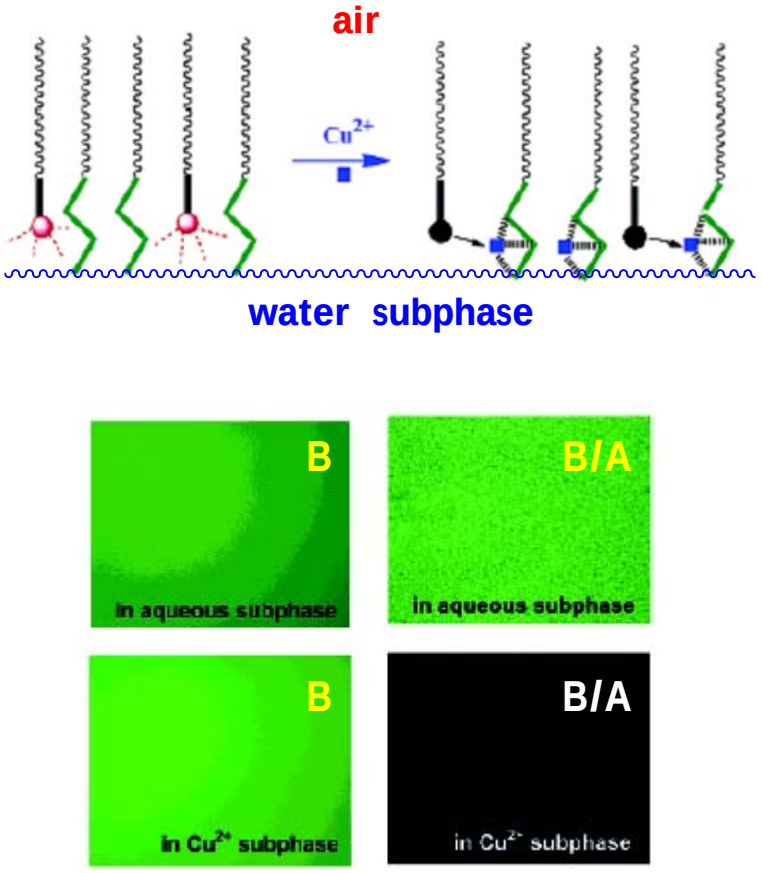

Epifluorescence images of Langmuir monolayers of lipids **B**, and **A**/**B** (90:10, molar ratio) in the absence and presence of copper ions (10^{-5} M) in the subphase

Self-Organized Chemosensors

In Surfactant Micellar Aggregates

Advantages:

- Prepared just by mixing components (no synthesis)
- Tuning of sensitivity just by variation of components ratio
- Modification of the system just by substitution of one component

Limitations:

- Sensitivity to environmental conditions (temperature, ionic strength)
- Concentration limit (c.m.c.)

Self-Organized Chemosensors on SiO_2 nanoparticles

Synthesis

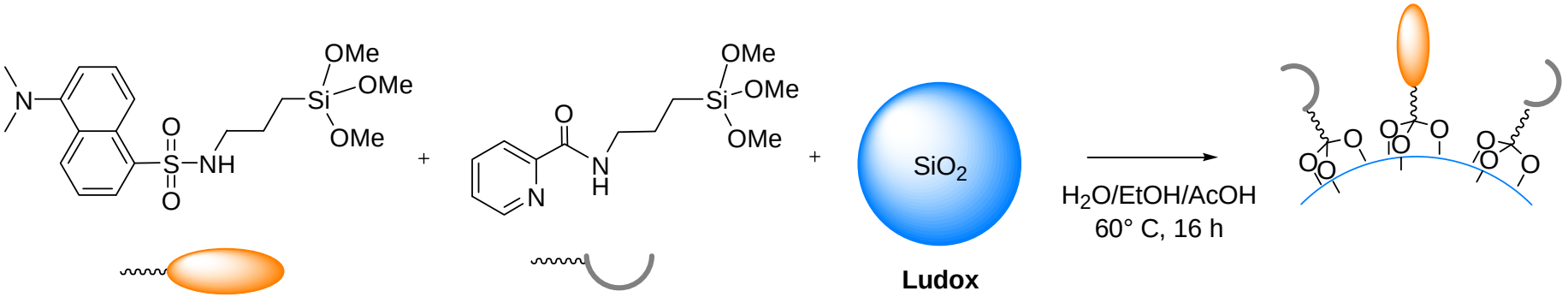

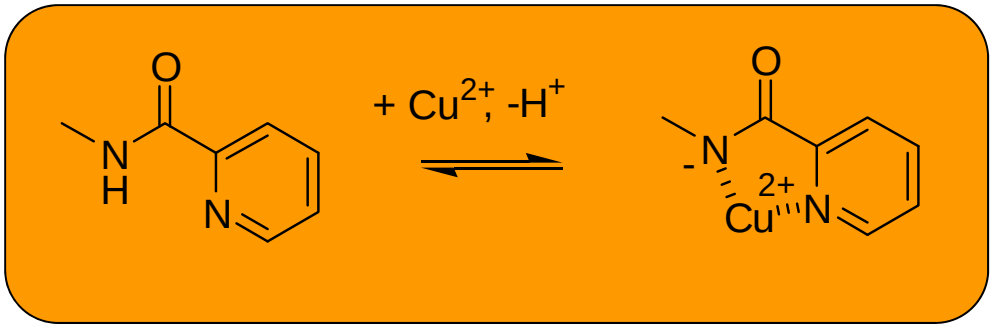

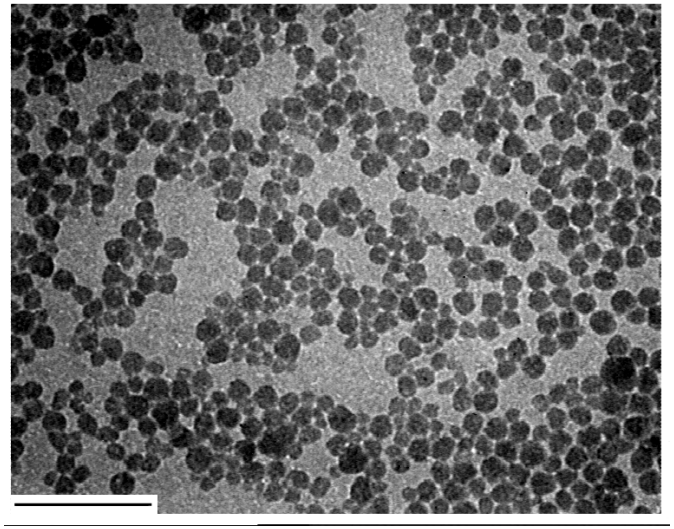

Chem. Commun. **2003,** 3026-3027

Self-Organized Chemosensors on SiO_2 nanoparticles

Cu^{2+} detection

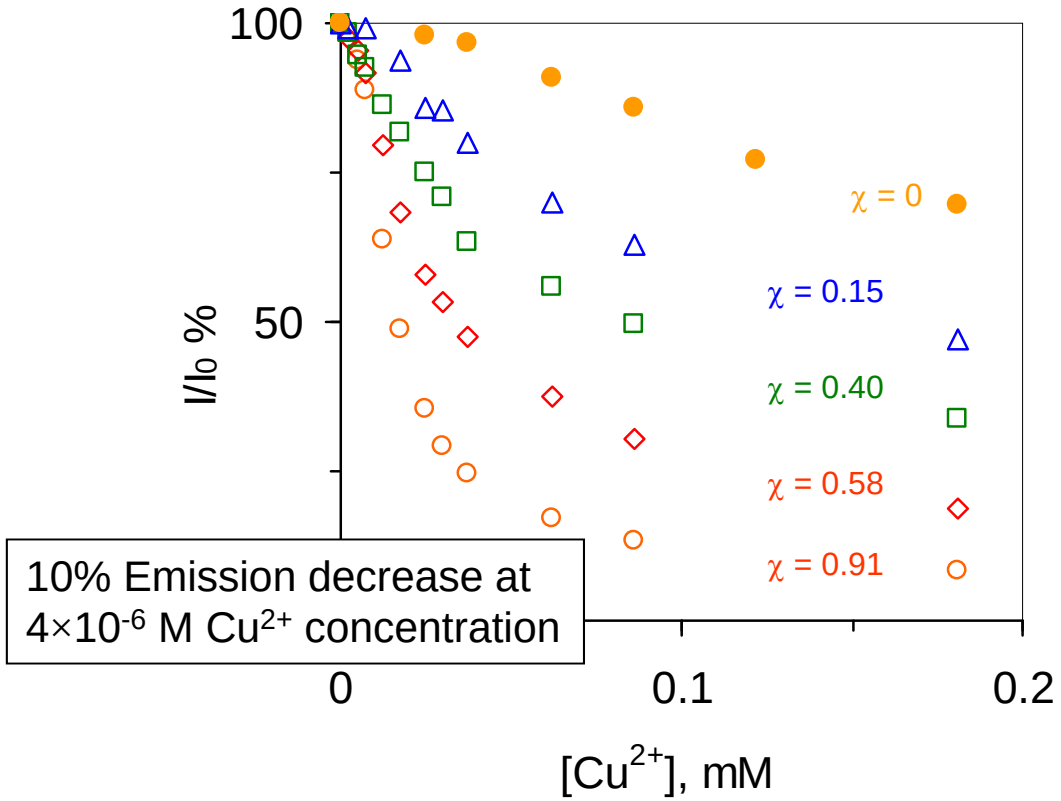

$$\chi = \frac{[L]}{[F]+[L]}$$

Spectrofluorimetric titration of CSNs (0.03 mg/ml) with $Cu(NO_3)_2$ in 10% water/DMSO, HEPES buffer 0.01 M pH 7, 25 °C.

Self-Organized Chemosensors on SiO_2 nanoparticles

Sensitivity enhancement by cooperative binding

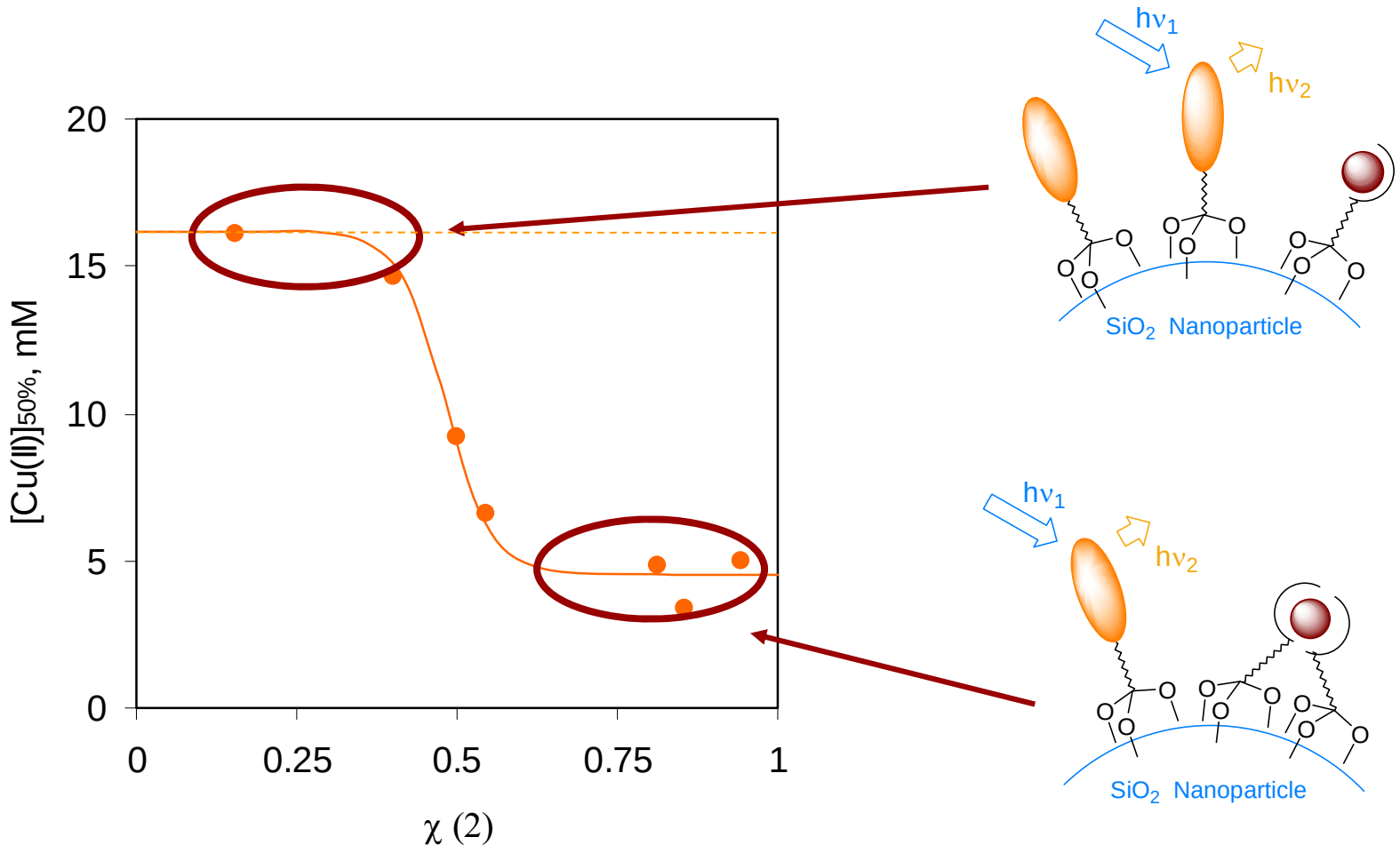

$[Cu^{2+}]_{50\%}$ as a function of **2** molar fraction on the CSNs ([**2**] = 2 μM, 10% water/DMSO, HEPES buffer 0.01 M pH 7, 25 °C

Self-Organized Chemosensors on SiO_2 nanoparticles

Components switching: signaling unit

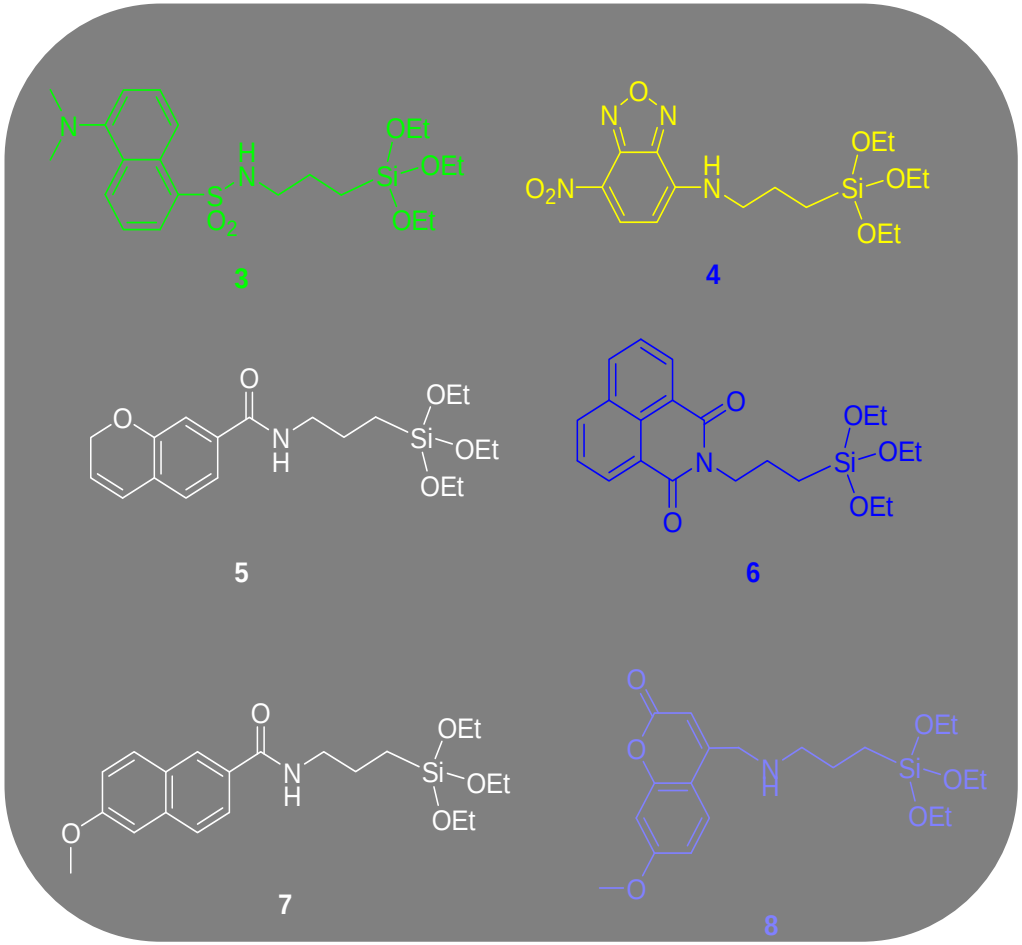

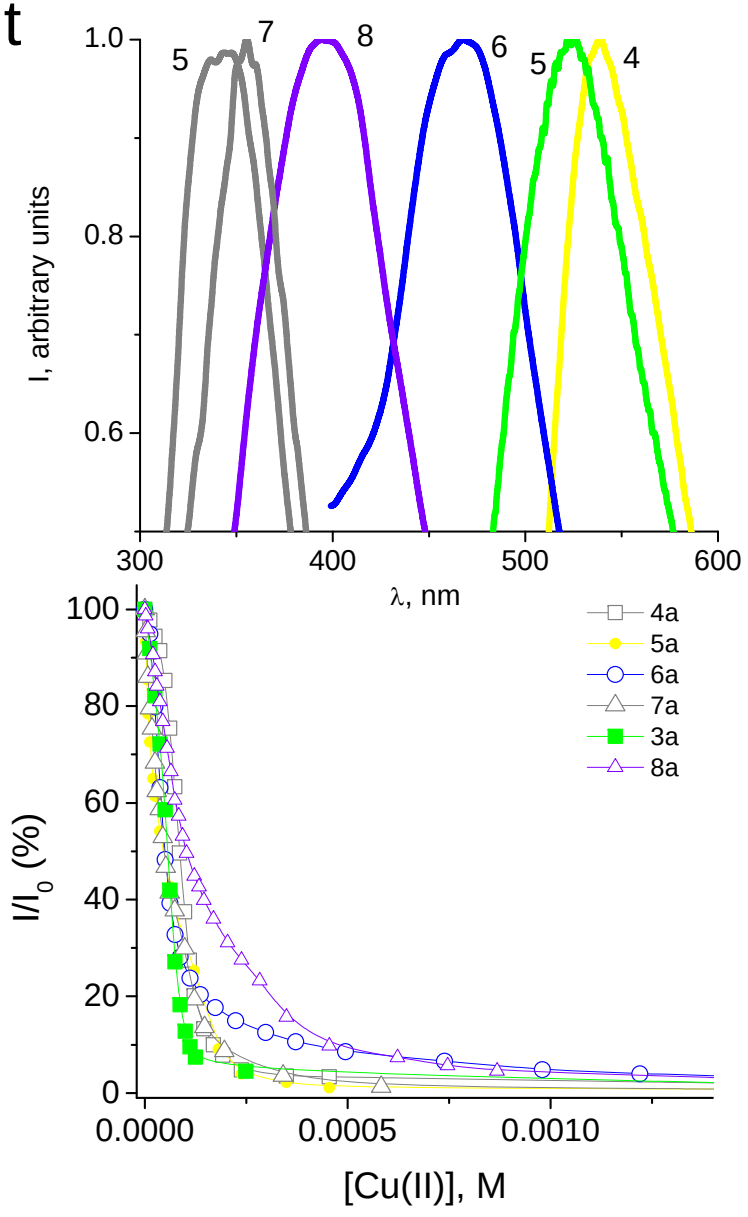

Self-Organized Chemosensors on SiO_2 nanoparticles

Components switching: binding unit

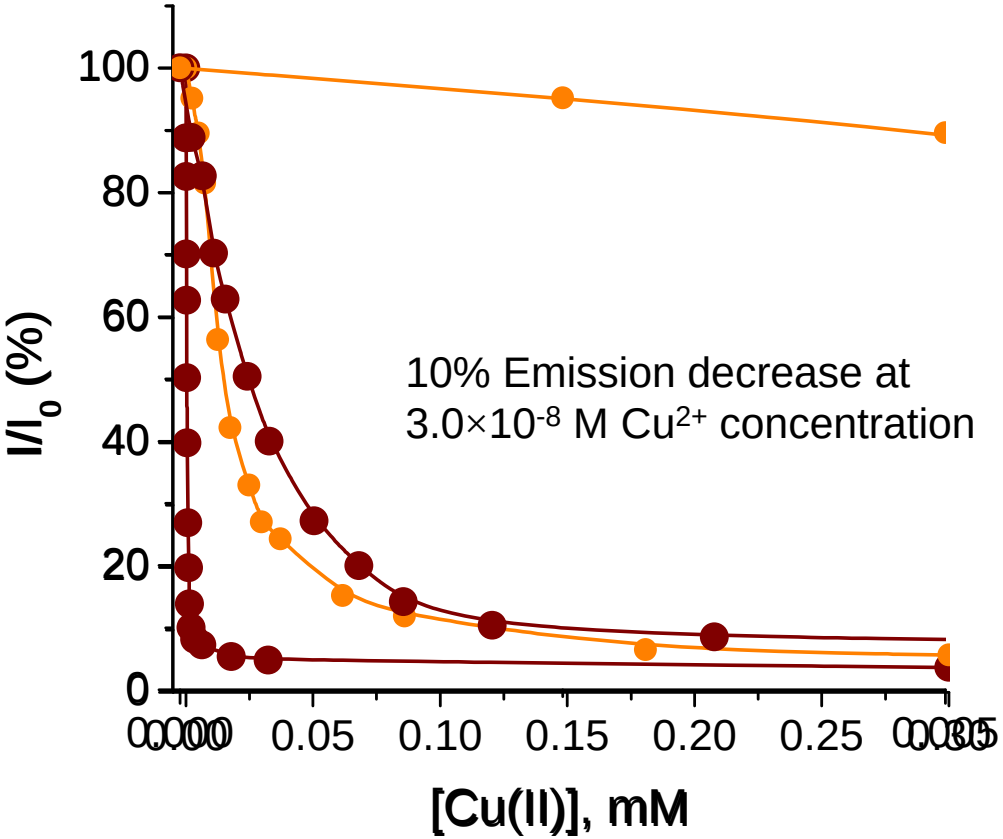

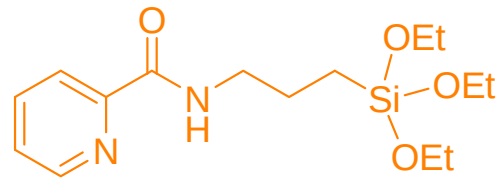

1

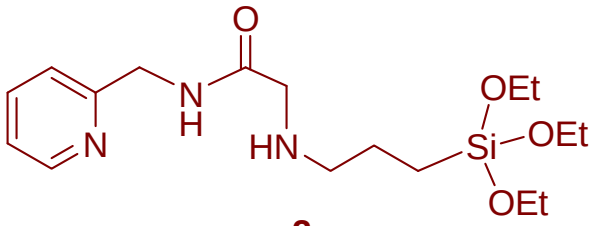

2

Conditions: DMSO/acqua 9:1, HEPES 0.01 M pH 7, 25 °C, λ_{exc}=340 nm, λ_{em}=520 nm.

J. Mat. Chem. **2004,** *15*, 2687-2696

Self-Organized Chemosensors on SiO_2 nanoparticles

Selectivity

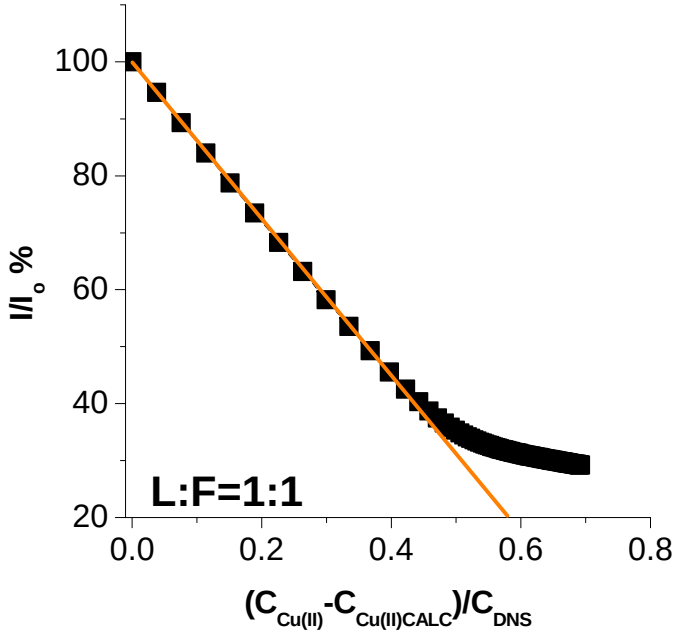

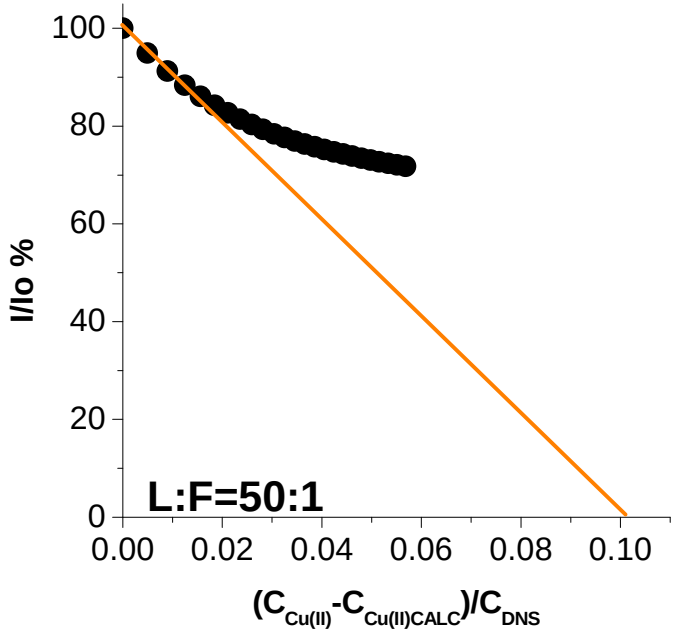

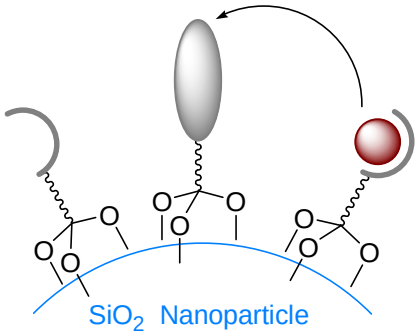

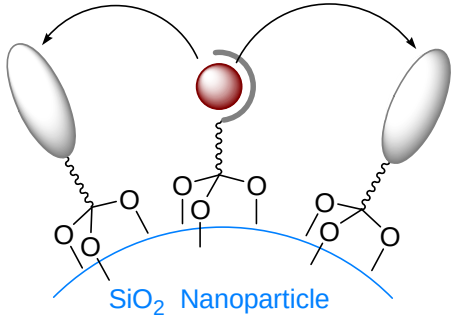

Superfici di vetro come agenti templanti: un sensore per ioni metallici

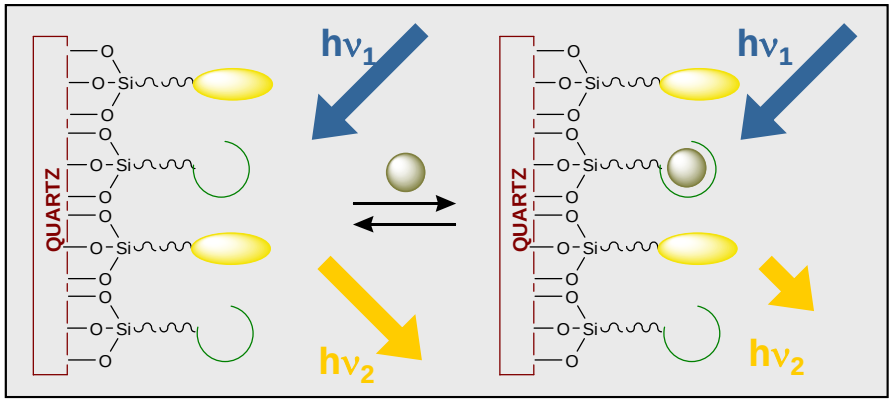

fluoroforo

ligando

ione metallico

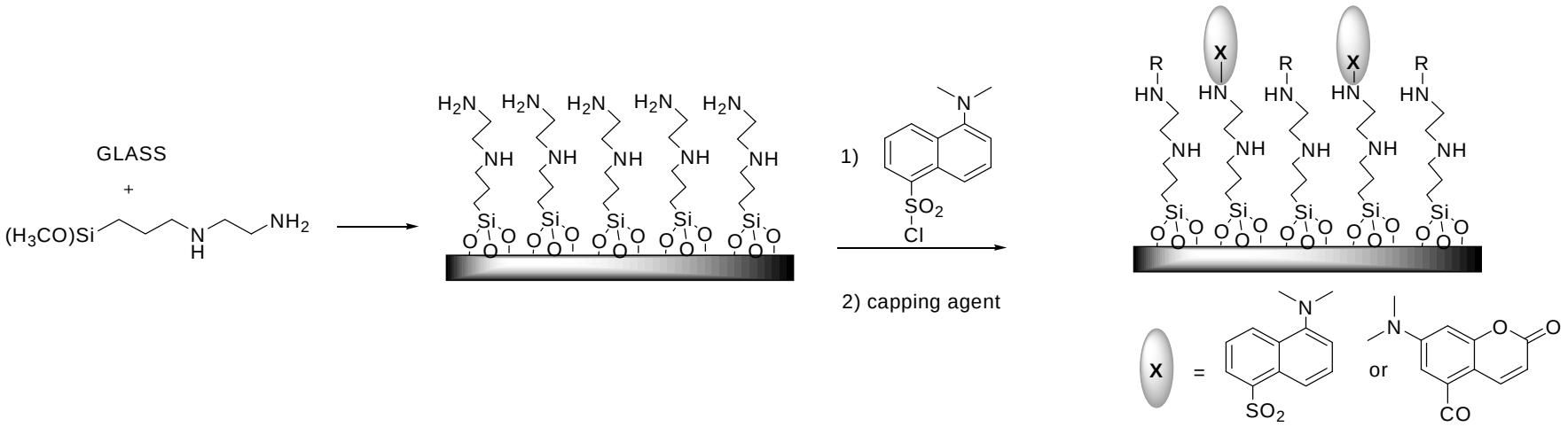

sensitivity for Pb^{2+} in the 0.1 mM range

R = H, $COCH_3$, or $CONHC_6H_{13}$

Crego-Calama and Reinhoudt *Adv. Mater.* **2001**, *13*, 1171

Superfici di vetro come agenti templanti:
selezione combinatoria del sistema migliore

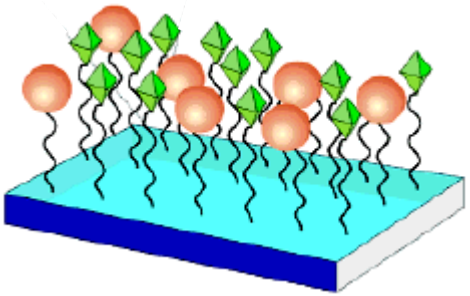

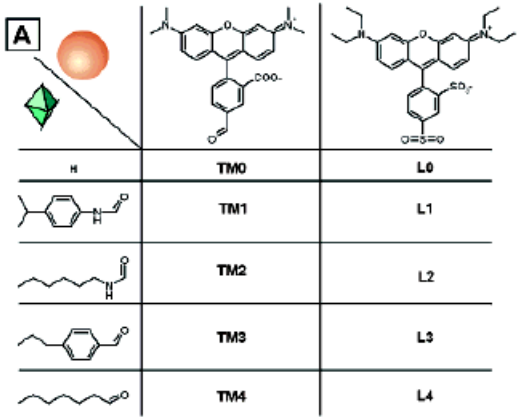

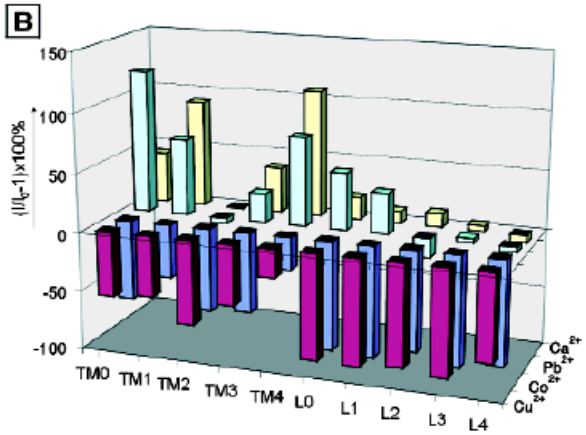

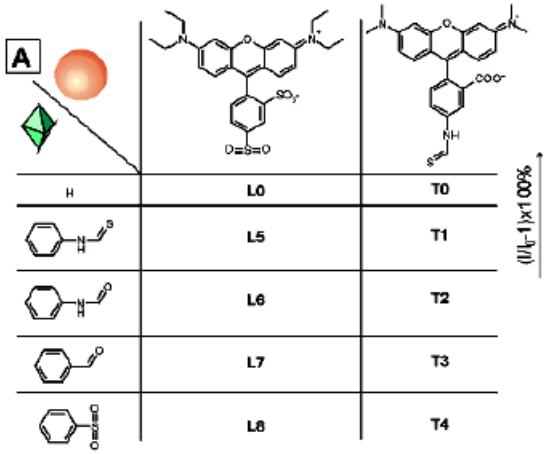

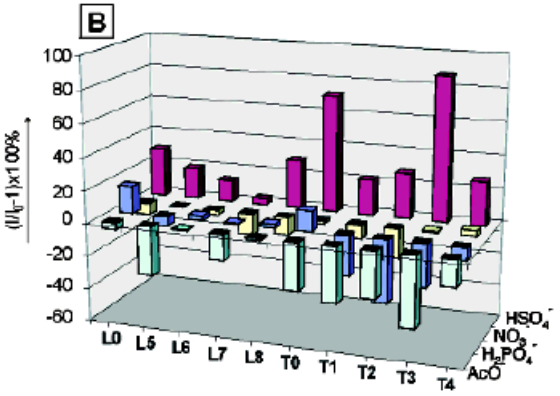

Crego-Calama, Reinhoudt and al. *J. Am. Chem. Soc.* **2004**, *126*, 7293

Sensori autorganizzati su/in nanoparticelle: PEBBLES

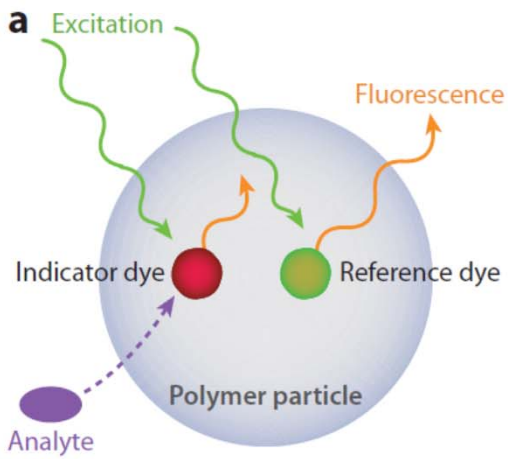

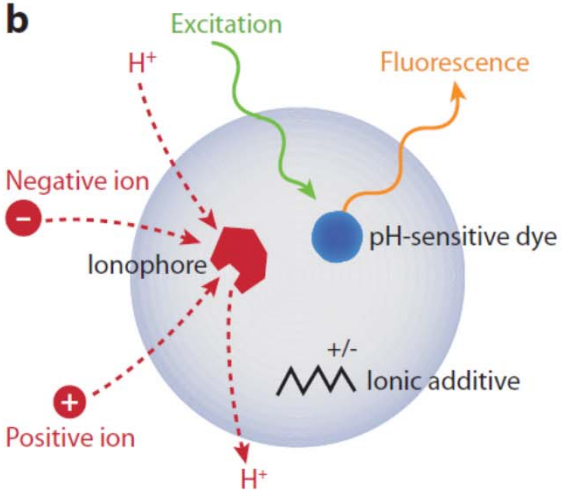

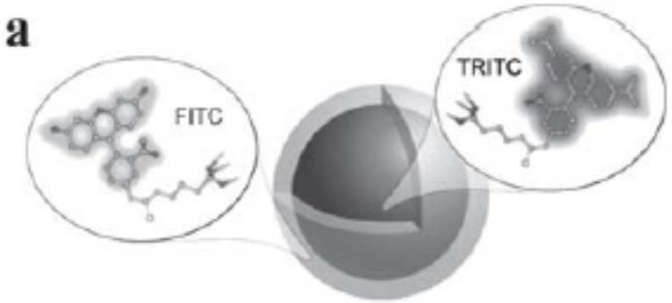

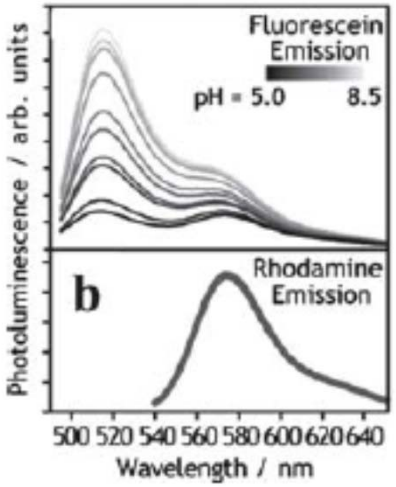

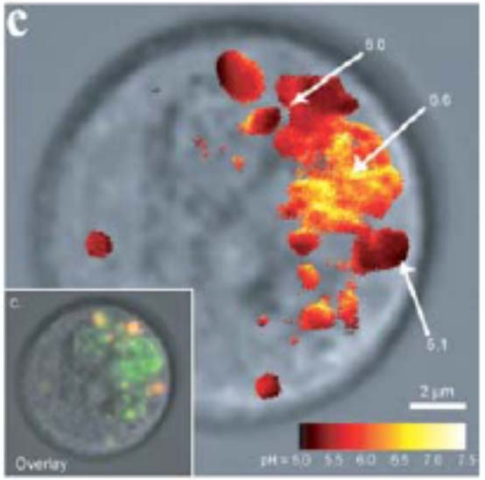

A. Burns, P. Sengupta, T. Zedayko, B. Baird, and U. Wiesner, *Small*, 2006, **2**, 723-726

Core-shell silica nanoparticles for Pb^{2+} detection

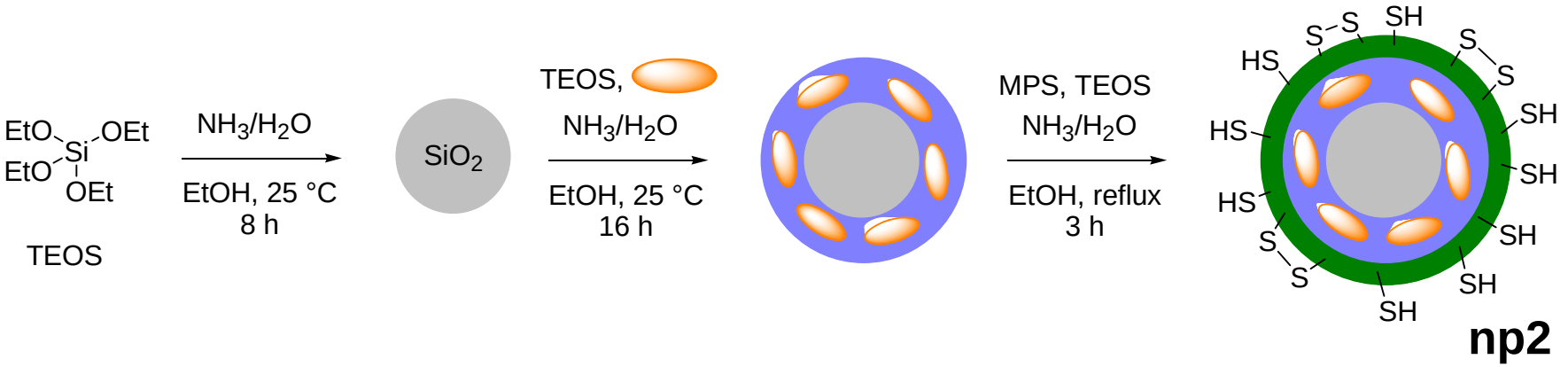

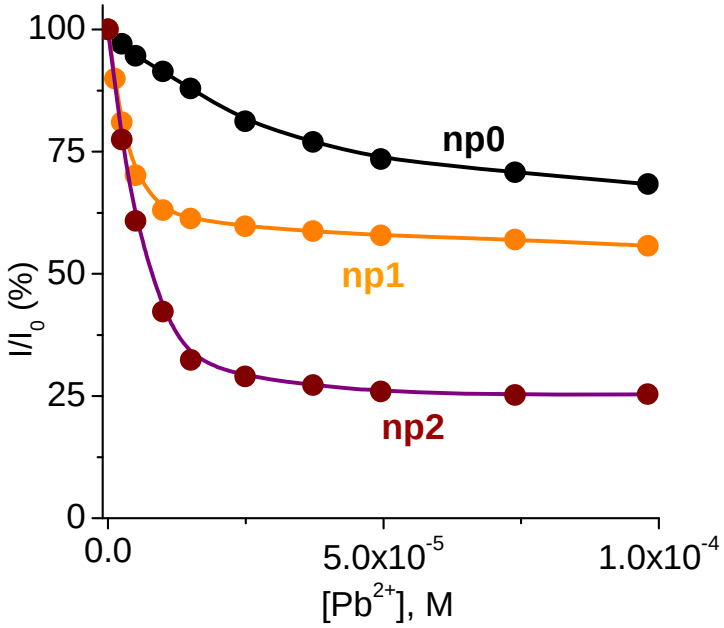

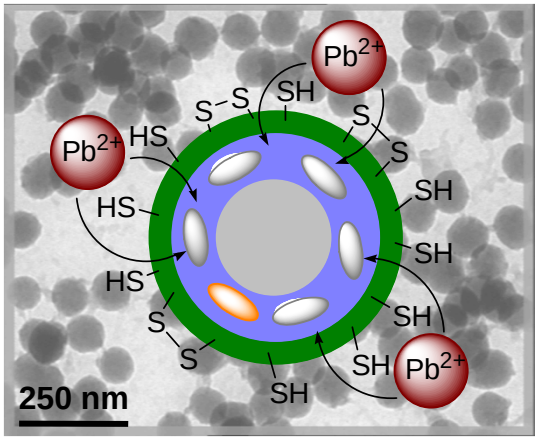

Langmuir **2007**, *23*, 8632-8636

Ratiometric sensing

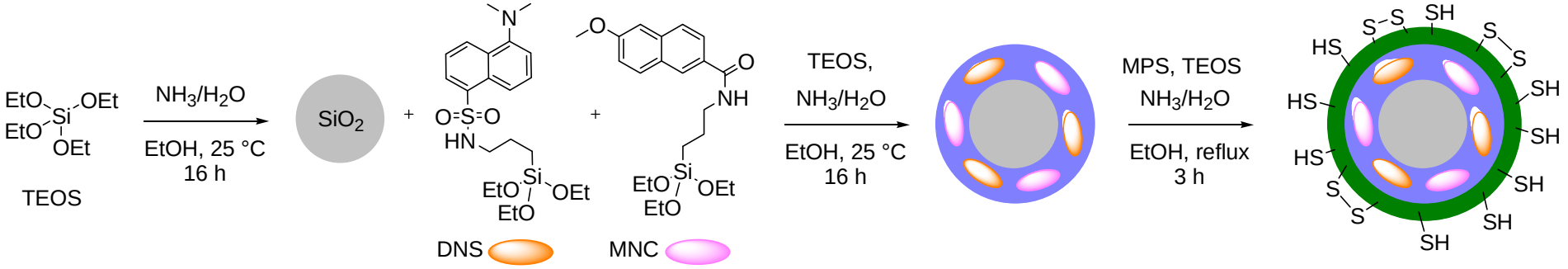

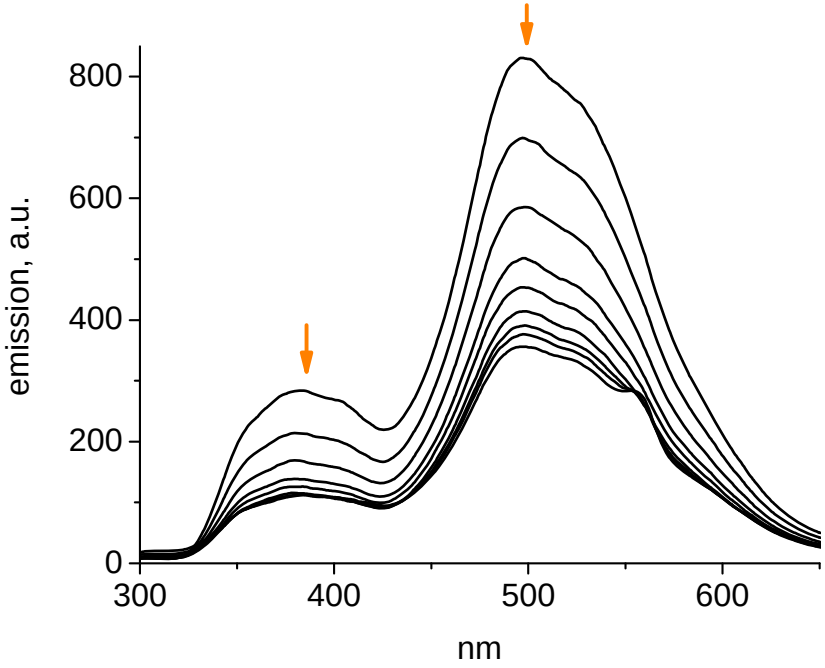

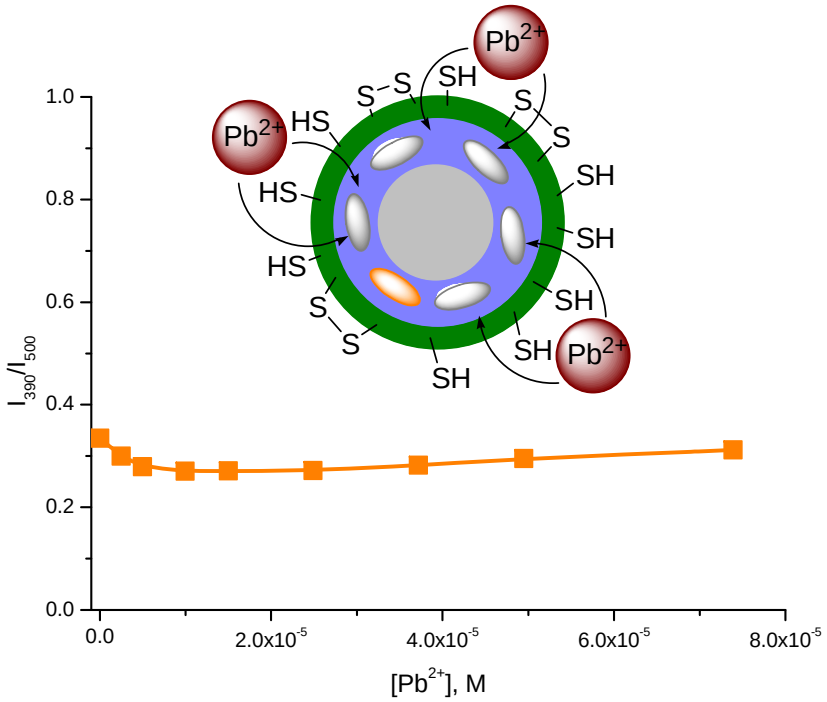

Ratiometric sensing

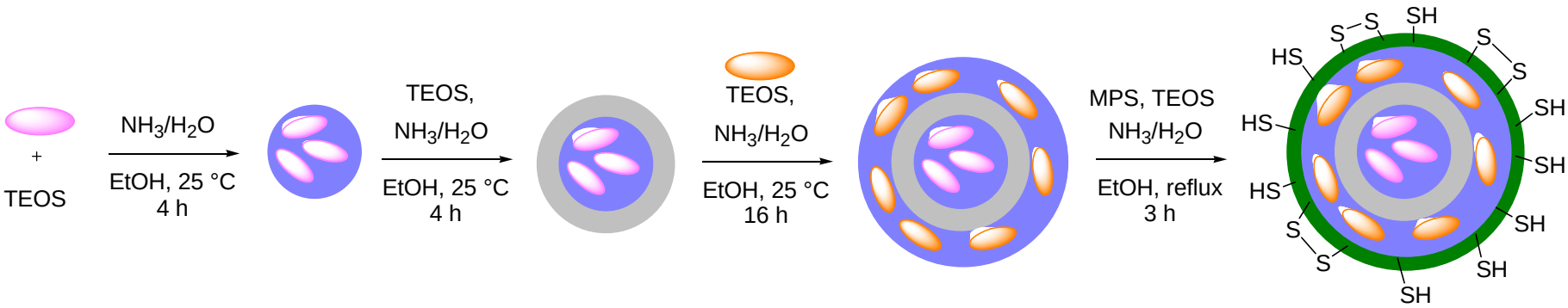

np3

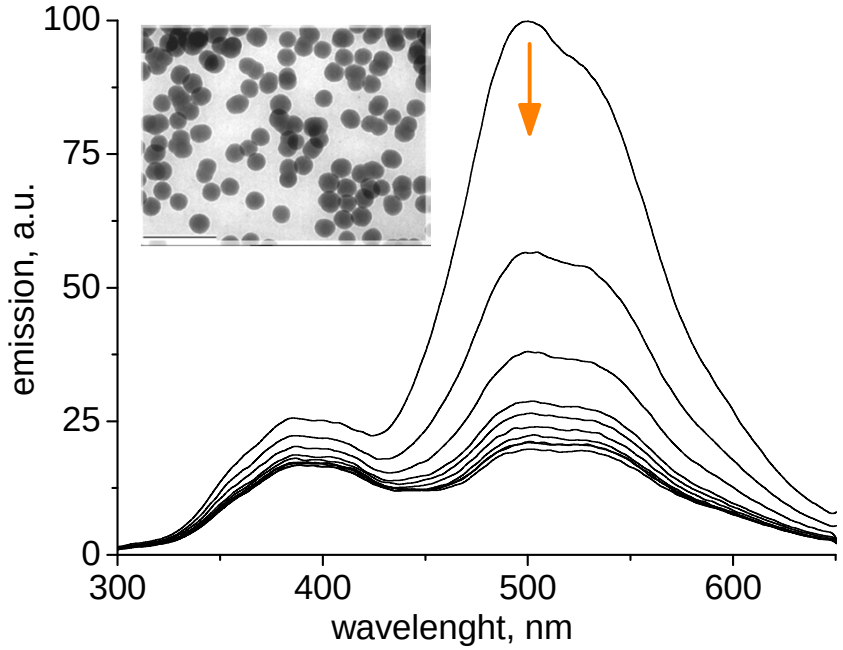

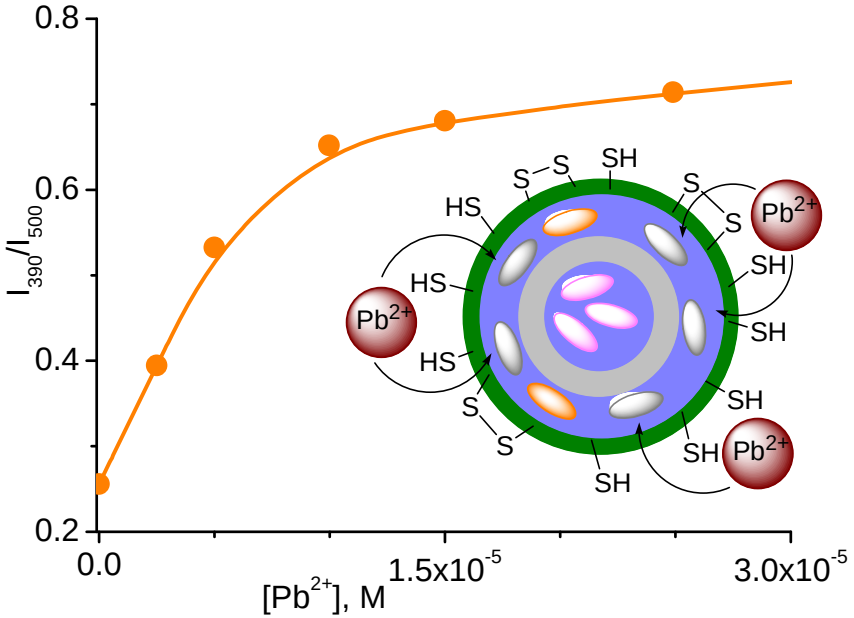

Active PEBBLES for O_2 sensing

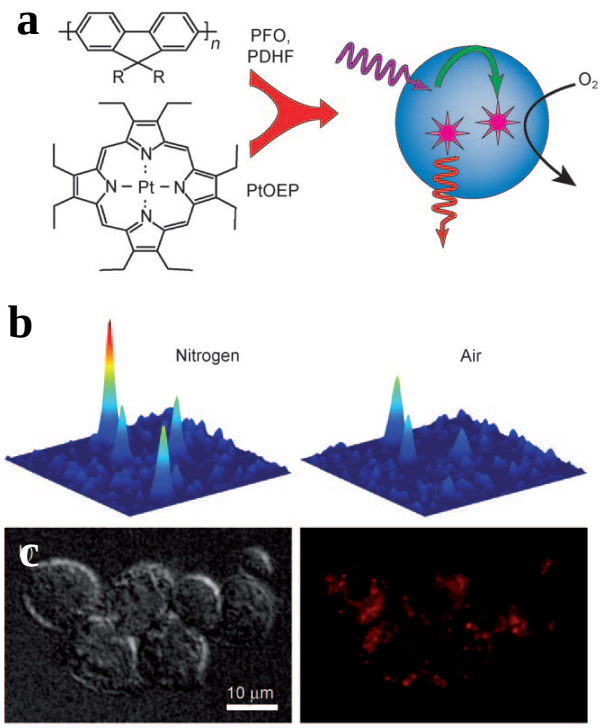

FRET QI 87%
Brightness 1000-fold

Single particle oxygen detection

C. F. Wu, B. Bull, K. Christensen, and J. McNeill, *Angew. Chem. Int. Ed.*, 2009, **48**, 2741-2745.

Other sensing schemes

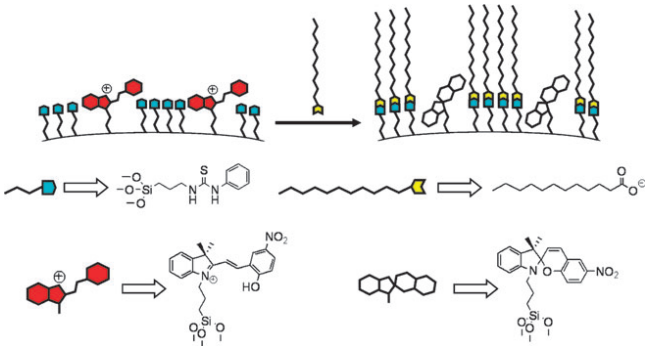

Carboxylate detection

P. Calero, E. Aznar, J. M. Lloris, M. D. Marcos, R. Martinez-Manez, J. V. Ros-Lis, J. Soto, and F. Sancenon, *Chem. Commun.*, 2008, 1668-1670.

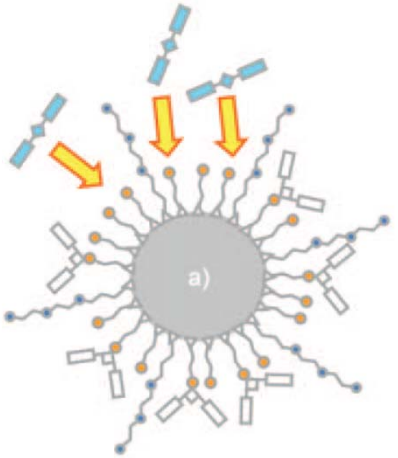

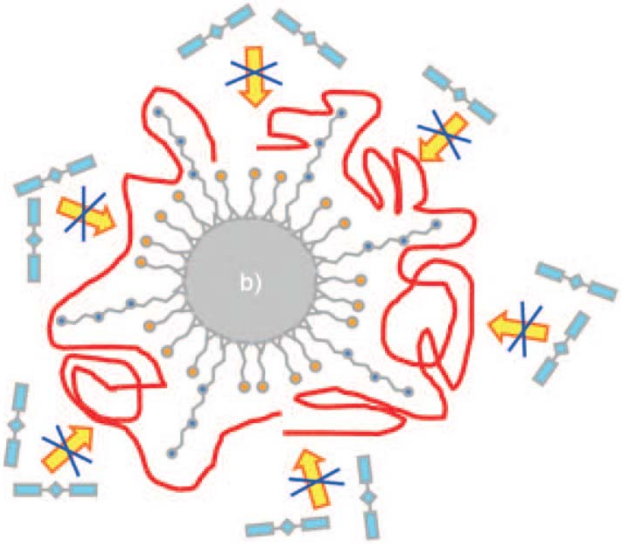

Eparin (polyanion) detection

P. Calero, E. Aznar, J. M. Lloris, M. D. Marcos, R. Martinez-Manez, J. V. Ros-Lis, J. Soto, and F. Sancenon, *Chem. Commun.*, 2008, 1668-1670.

NANO-HPLC

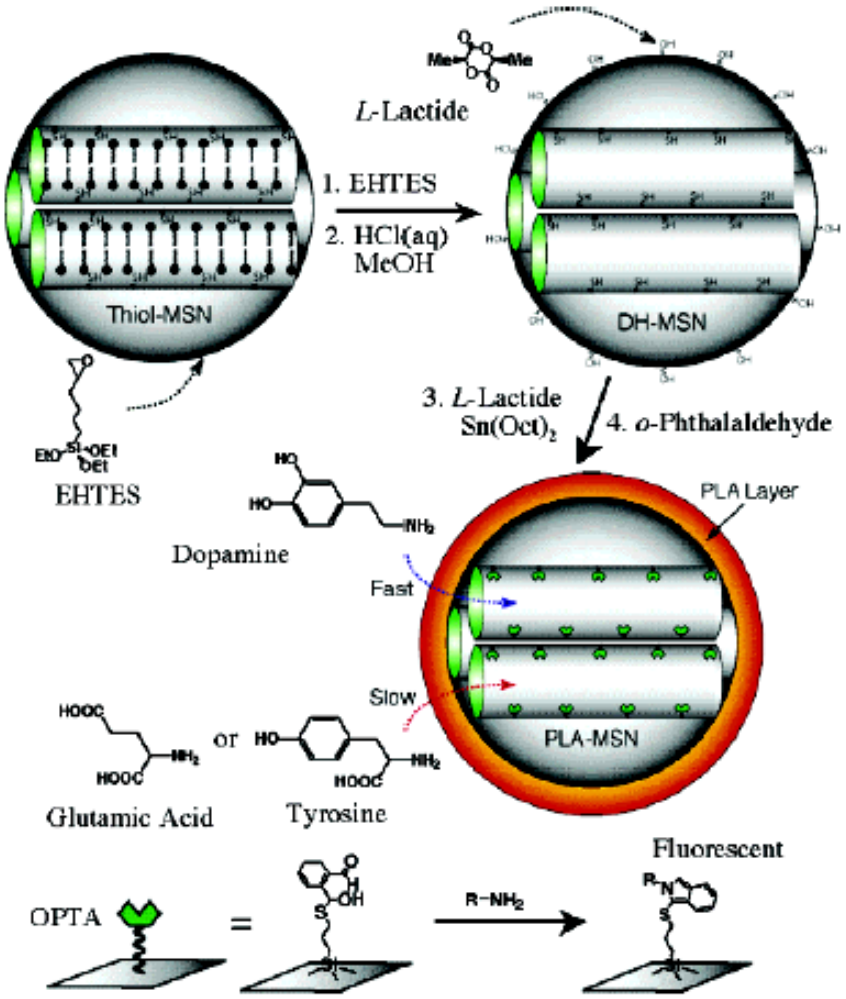

Figure 1. Schematic representation of the synthesis of PLA-coated MSN-based fluorescence sensor system for detection of amine-containing neurotransmitters, i.e., dopamine, glutamic acid, and tyrosine (R-NH_2). (5,6-epoxyhexyltriethoxysilane = EHTES, cetyltrimethylammonium bromide (CTAB) surfactant = ●∼∼∼∼).

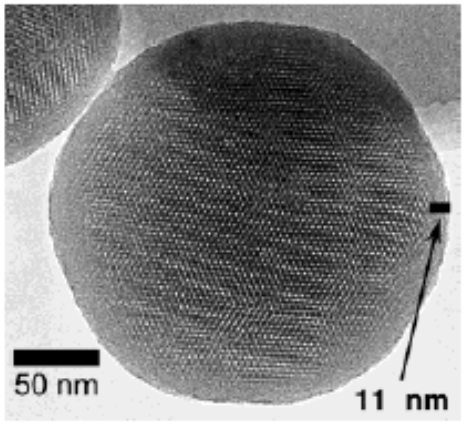

TEM micrograph of PLA-coated mesoporous MSN nanoparticles

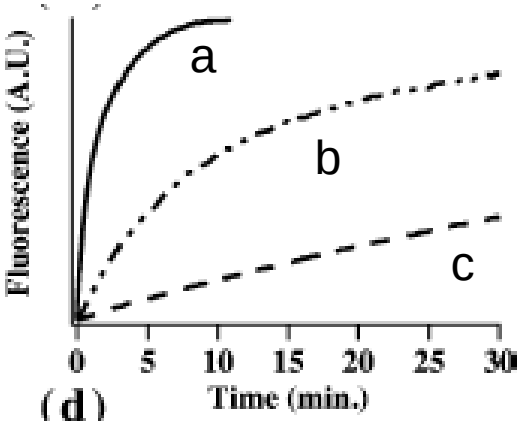

Fluorescence increase by PLA-coated mesoporous MSN nanoparticles after addition of Dopamine (a), Tyrosine (b) and Glutamic acid (c)

V. S.-Y. Lin et al., *JACS*, **2004**, 126, 1640-1641

Fluorescence chemosensors: the case of zinc

Why zinc?: Zinc is only moderately abundant in nature, ranking 23rd of the elements. Zinc is, however, following iron, the second most abundant transition metal in the body. In total, the adult human body contains 2 –3 g zinc. The pronounced Lewis acid characteristics of the Zn^{2+} ion, its single redox state, and the flexibility of its coordination sphere with respect to geometry and number of ligands associated, combined with the kinetic lability of coordinated ligands, are responsible for its broad utility within proteins. Thousands of proteins contain zinc. Zinc proteins can be divided into several groups according to the role played by zinc. In the **catalytic group** (e.g.,carbonic anhydrase and carboxypeptidase A), zinc is a direct participant in the catalytic function of the enzyme. In enzymes with **structural zinc sites** (e.g.,protein kinase C), one or more metal ions ensure appropriate folding for bioactivity. Enzymes in which zinc serves a **co-catalytic function** (e.g., superoxide dismutase), one or several zinc ions may be used for catalytic, regulatory, and structural functions. In addition, there are a large number of transcription factors that utilize zinc, the so-called **zinc fingers**.
While the total concentration of zinc in a cell is relatively high, the concentration of “free ”zinc, that is, the fraction of Zn^{2+} not strongly bound to proteins, is extremely low and tightly controlled. **Total cellular zinc can be determined by standard analytical techniques such as AAS or ICP-MS, but the determination of the “free ”or “available ” Zn^{2+} concentrations has proved difficult using classic techniques.** This is because cell fractionation can readily lead to cross-contamination of the kinetically labile metal ion between intracellular sites. Thus, the knowledge gap between the structural chemistry of zinc and zinc homeostasis and action is, at least in part, due to the lack of techniques for tracking Zn^{2+} in biological systems. This led to the emergence of zinc specific molecular sensors, which can make zinc “visible ”in tissue or even in live cells.

Spectroscopically silent zinc: The d^{10} electron configuration of the Zn^{2+} ion, the only zinc ion found in biological systems, has a number of practical implications for its detection. Zn^{2+} is colorless as it is devoid of d –d transitions. The Zn^{2+} ion is very stable and undergoes redox reactions only under extreme conditions, excluding the occurrence of ligand-to-metal charge-transfer bands in its complexes. These effects render UV-visible spectroscopy unsuitable for the detection of “free ”or complexed Zn^{2+}. Zinc is also diamagnetic in all its compounds, prohibiting, for instance, EPR spectroscopy or magnetometric measurements.The d^{10} ion is not subject to ligand field stabilization effects, making it extremely flexible with respect to the coordination geometries it can adopt in its complexes, and rendering it kinetically labile, allowing for rapid ligand exchange reactions. Finally, the major naturally occurring isotopes have zero nuclear spin, they are NMR silent.
Much of what is known about the structure and function of Zn^{2+} containing proteins has been gleaned from X-ray crystal structures, X-ray absorption data (EXAFS), and iso- morphous substitution experiments in which the Zn^{2+} was replaced by traceable metal ions. None of these techniques are suitable for the tracking of Zn^{2+} in cells and organisms. The use of the zinc radioisotope ^{65}Zn has allowed cell studies on bulk zinc uptake and egress, but this does not permit the direct observation of the temporal and spatial distribution of zinc in live cells and questions of isotope equilibration with internal pools arise. One technique to spectroscopically visualize zinc is the use of zinc-specific fluorescent molecular sensors.

Intrinsic chemosensors: the case of zinc

Desired optical properties: The **ideal chemosensor** for zinc is **nonfluorescent in the free form** and **highly fluorescent when coordinated** to zinc; possibly, the response should be ratiometric. Moreover, the **excitation wavelength** should be **as longer as possible** to avoid UV-induced cell damage and to penetrate tissue better and with less scattering (giving rise to higher resolution imagesand), and to avoid UV-grade optics in the fluorescence microscopes used to observe biological samples.

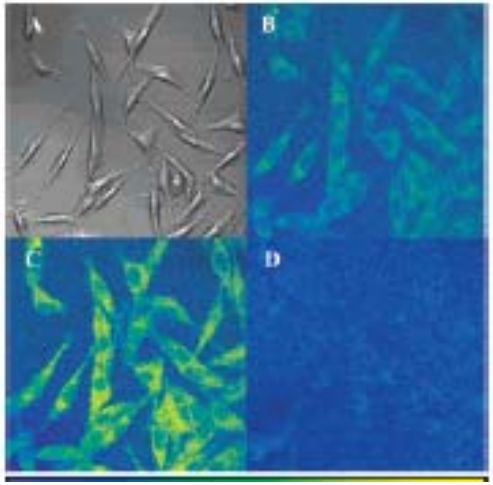

Determinazione della concentrazione di Zn(II) all'interno di cellule tumorali.

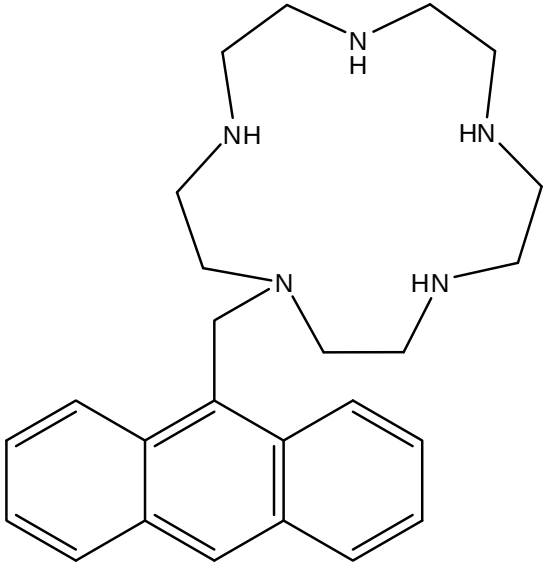

JACS 2004,126, 712-713.

Intrinsic chemosensors: the case of zinc

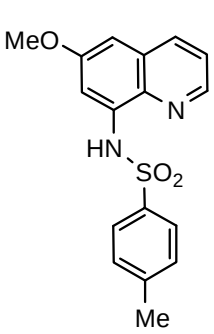

TSQ

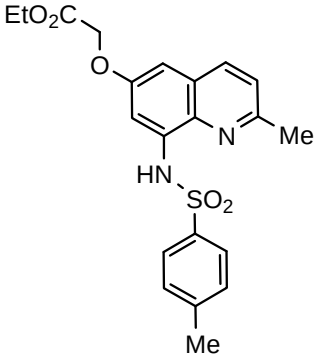

ZINQUIN

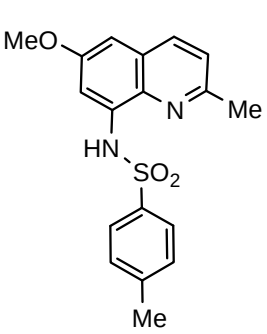

2-Me-TSQ

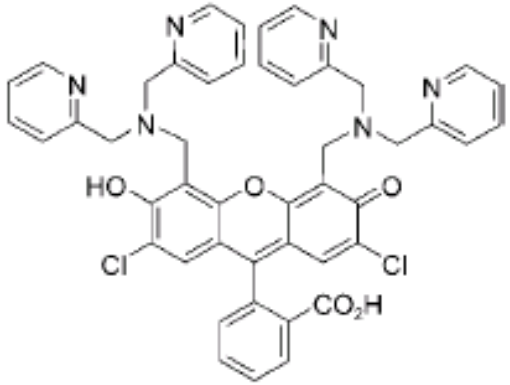

ZINPYR-1

$\Delta I > 300$; λ_{ex} 369 nm; λ_{em} 535 nm

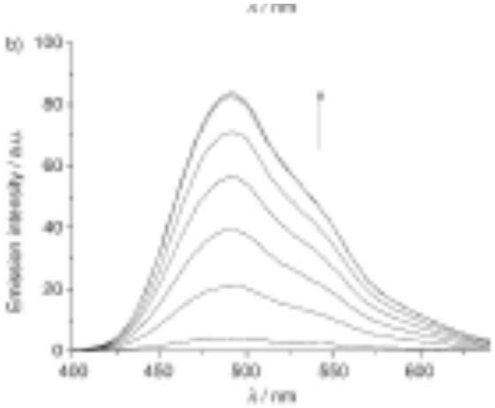

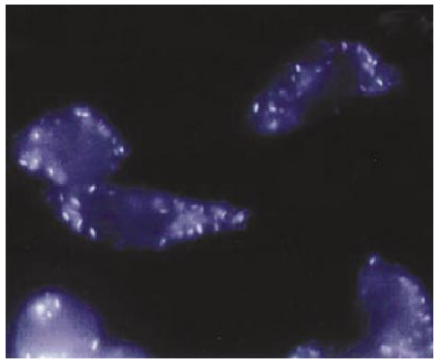

Microscopy images of mouse fibroblast cells by fluorescence in the presence of 10 mm 2-Me-TSQ. Nasir et al. *J. Biol. Inorg. Chem.* **1999**, *4*, 775.

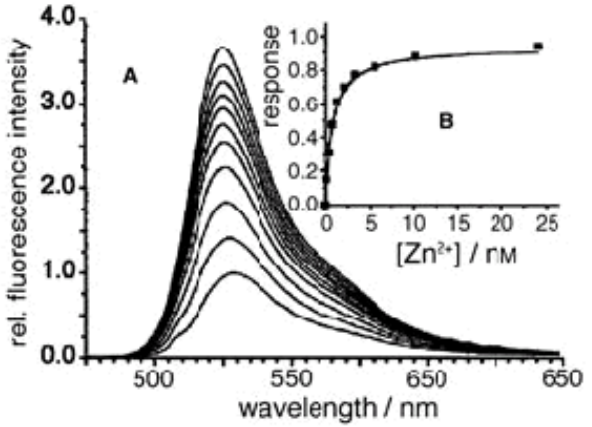

$\Delta I > 3$; λ_{ex} 509 nm; λ_{em} 525 nm

Intrinsic chemosensors: the case of zinc

Selectivity: Zinc is a borderline hard/soft metal with a variety of known coordination numbers, geometries, and donor atom sets. This makes the design of zinc-selective chelates somewhat difficult, but the number and concentration of competing metal ions in biological systems is limited, simplifying the task in practice.

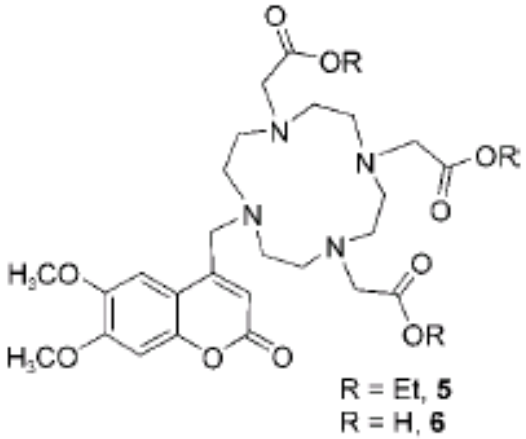

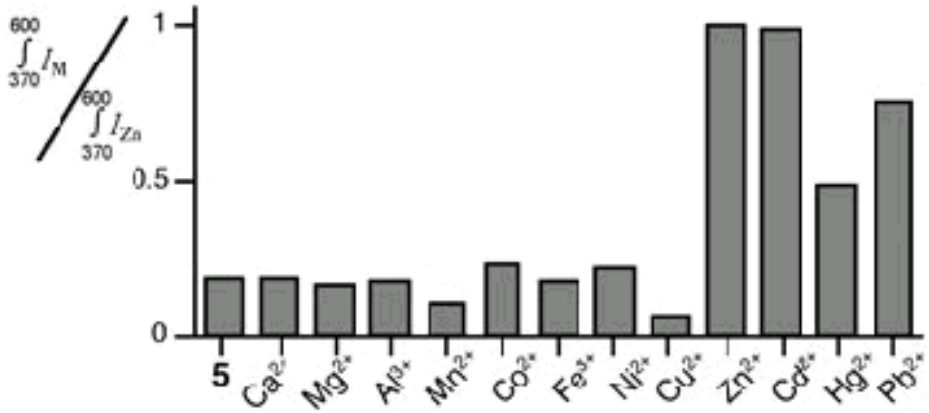

In addition to zinc, the other divalent ions of Group 12 elicit a fluorescence response. Also, the soft-ion Pb^{2+} is found to bind. However, none of these toxic ions are expected to be present in any significant amount, excluding a false positive signal for zinc.
The ions occurring in relatively large concentrations, such as Ca^{2+}, Mg^{2+} (and Na^{+}, K^{+}) do not bind to cyclen, and therefore do not induce any fluorescence, even when present in a large molar excess.

Transition metals such as Mn^{2+}, $Fe^{2/3+}$, and Cu^{2+} bind to many cyclen but they do not give a false positive fluorescence response as these paramagnetic ions quench fluorescence. In a refined and more relevant experiment, it is necessary to investigate how Zn^{2+} ions directly compete with varying concentrations of other transition-metal ions for the sensor binding site.

Intrinsic chemosensors: the case of zinc

Affinity for zinc: a fluorescence titration of a given sensor with Zn^{2+} identifies the zinc concentration range in which the sensor can be used to measure relative concentrations of zinc. If the zinc concentration is too low, no enhanced fluorescence is measured because no significant binding takes place. In the upper limit range, the sensor is saturated and cannot give any information about relative concentration changes of zinc. Thus,every sensor is characterized by a useful working range of zinc concentrations.The ideal dissociation constant K_d of the sensor for the analyte should be a value close enough to the projected concentration of the analyte to allow monitoring of changes in its concentration.

Binding kinetics: if the temporal resolution of changing zinc concentrations is desired, it is obligatory that the reversible metal binding event to the sensor is adequately fast. For instance, the binding of Zn^{2+} to the cyclen-based sensor 5 is very slow ($t_{1/2}$ =60 min). This is presumably due to the reorganization required to accommodate the metal in its convoluted binding site. Most sensors utilize non-macrocyclic polydentate chelates with fast binding kinetics. Rapidly binding sensors have been successfully used in time-resolved studies.

pH dependence: protons potentially compete with zinc for the lone pair(s) of the Lewis basic metal binding site. If the lone pair responsible for the PET process gets protonated, it becomes also less available for the quenching process, and fluorescence is switched on even in the absence of the metal ion. Hence the working pH range for any chemosensor needs to be determined to allow a judgment whether the sensor can operate within the pH range expected in the biological system studied.

Intrinsic chemosensors: the case of zinc

Biodistribution properties : Ideally, the chemosensor is taken up by the cell or tissue, thus avoiding microinjection techniques. An indication whether endocytotic mechanisms or passive diffusion through the cell membrane is responsible for the uptake of the sensor can be derived by observing the temperature-dependence of its uptake. If incubation of the cells with the sensor at 4 °C results in cell uptake, it provides a strong indication for a passive diffusion mechanism, since endocytosis at this temperature is greatly inhibited. Once in the cell, the sensor may be excreted or metabolized, leading to gradually diminishing fluorescence.

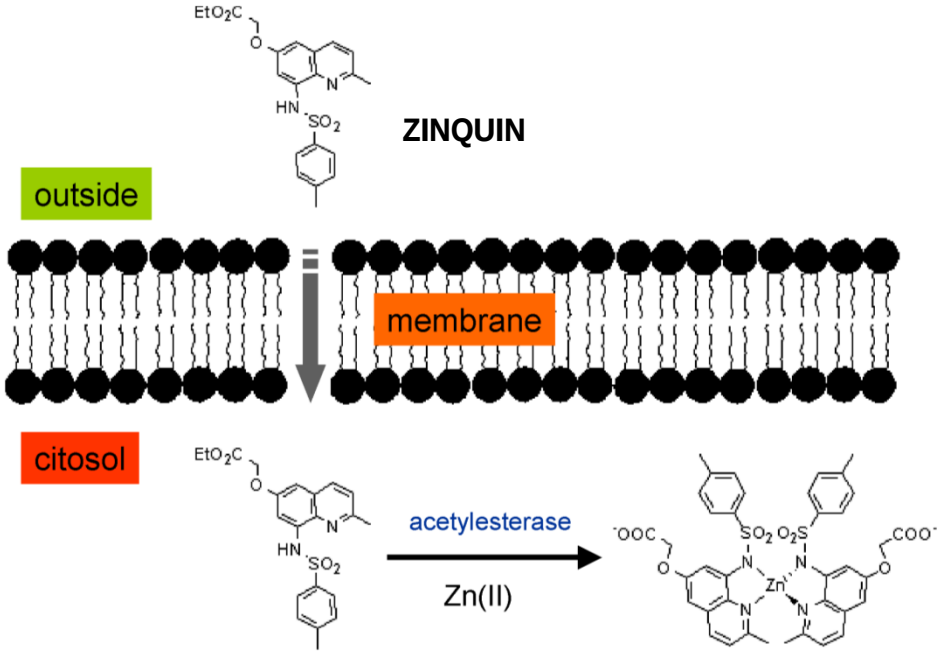

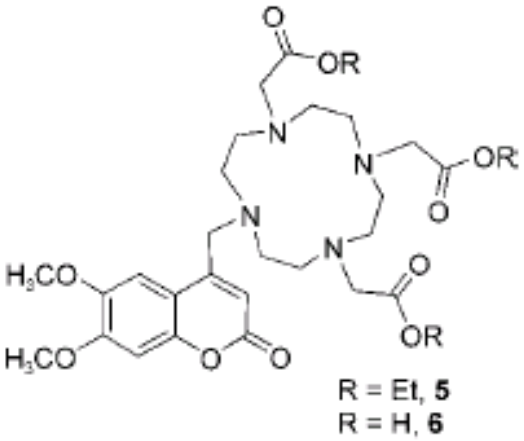

Sensor triacid **6** does not stain cells, whereas the triester **5** is taken up readily

Intrinsic chemosensors: the case of zinc

Cell-impermeable zinc chemosensors: it is known that insulin and Zn^{2+} are co-stored in pancreatic β -cells in secretory vesicles and are co-released by exocytosis.This process can be visualized by using the non-cell-permeable chemosensor FluoZin-3.
The Figure shows the burst of fluorescence following the addition of glucose to pancreatic β -cells. The time-lapse images following the burst show the fluorescence decrease due to diffusional dilution of the zinc concentration.

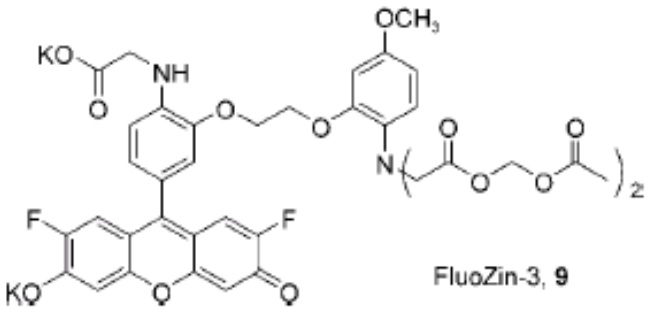

FluoZin-3, **9**

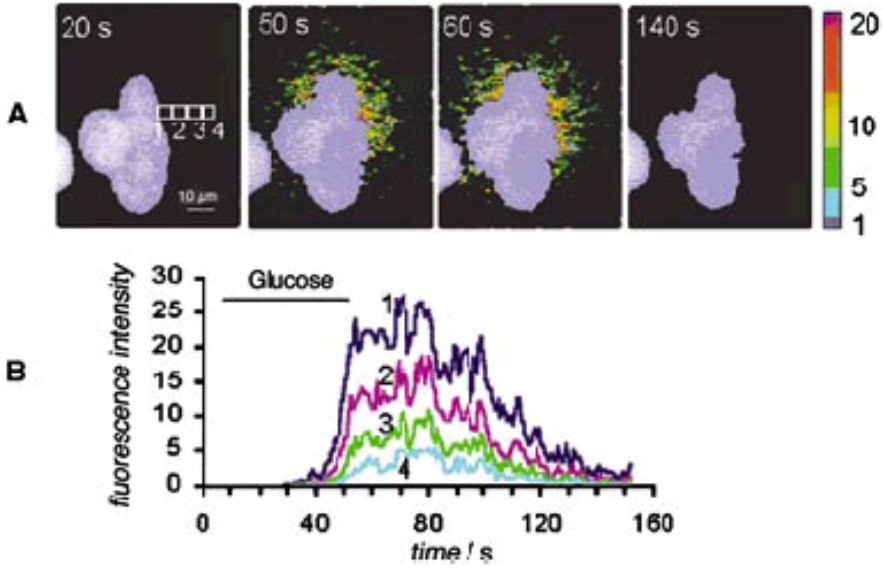

Intrinsic chemosensors: the case of zinc

Single-wavelength excitation ratiometric zinc chemosensors: The signal derived from a fluorescence microscopy image of a cell stained with a zinc-specific chemosensor allows the determination of the presence of zinc. Relative emission increases can reasonably be correlated with increases of $[Zn^{2+}]_{free}$ but the fluorescence quantum yield of the sensor is in most cases solvent-dependent. Since the solvent properties of the local environments in which the sensors accumulate are not known, the absolute I emission measured cannot be correlated directly with the concentration of zinc. However, the measurement of absolute $[Zn^{2+}]_{free}$ can be achieved by using a **ratiometric sensor**.

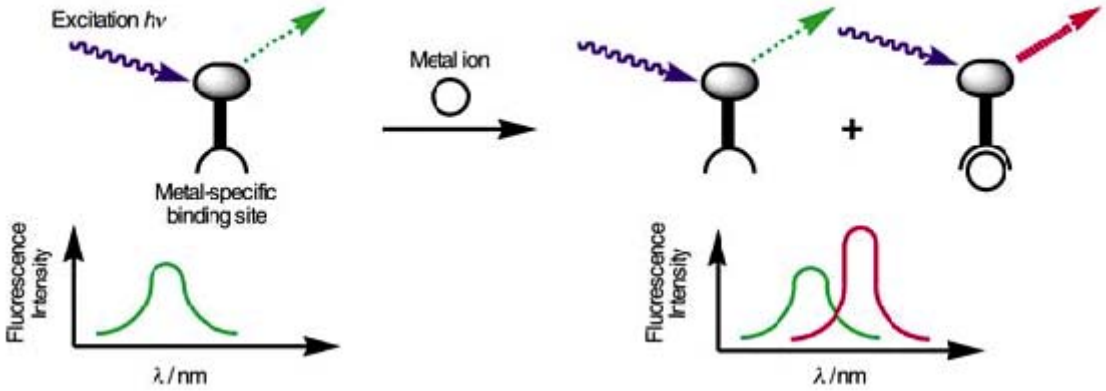

In a ratiometric sensor the binding of analyte the results in a shift of its $\lambda_{max\text{-}emission}$, which may or may not be concomitant with an increase in I emission .This $\lambda_{max\text{-}emission}$ shift should be enough to distinguish the λ max-emission of the co-existing Zn^{2+}-free and Zn^{2+} -bound species, allowing the determination of their emission ratio.

Intrinsic chemosensors: the case of zinc

Single-wavelength excitation ratiometric zinc chemosensors

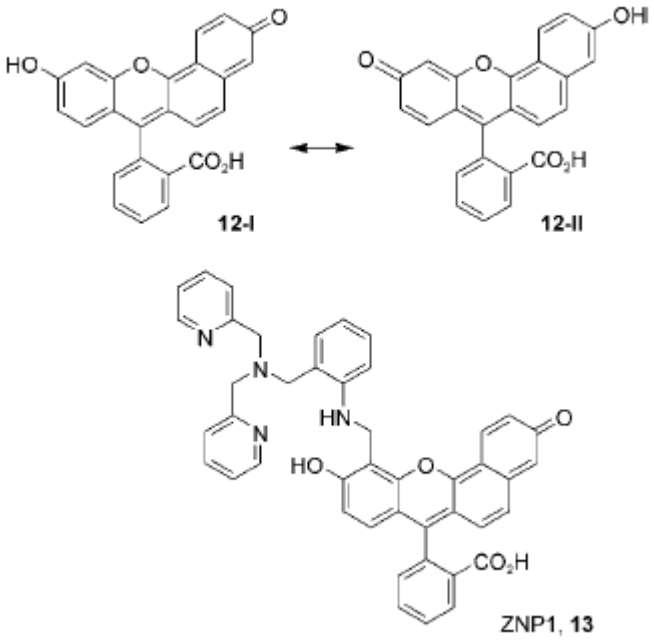

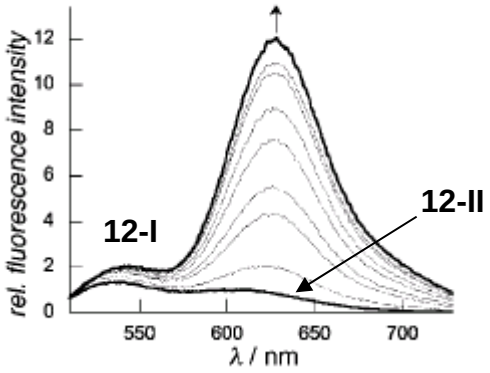

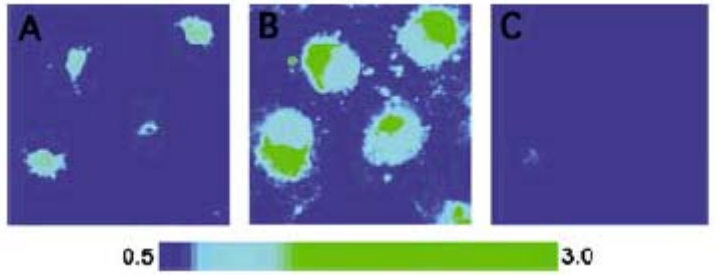

Images of live COS cells stained with ZNP1 acetate. The pseudocolors depict the ratio of the fluorescence intensities at the two emission wavelengths at 612 and 526 nm. The larger the ratio, the more zinc is present. In resting cells, little if any, “free endogenous zinc is present (A). Figure B shows the result of the addition of nitrosocyctein, an NO-delivery agent.The ratio increased, indicating the intracellular NO-triggered release of zinc.The cytosolic zinc was then chelated by TPEN, resulting in the complete loss of imageable zinc in the cells (C). TPEN = N ,N ,N ’N ’tetra(2-picolyl)ethylenediamine.

Intrinsic chemosensors: the case of zinc

Dual-wavelength excitation ratiometric zinc chemosensors

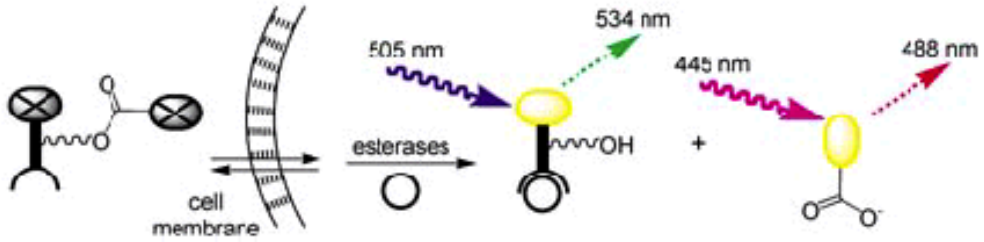

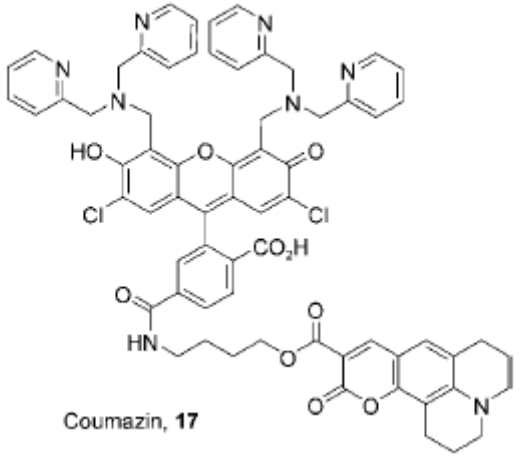

Coumazin, **17**

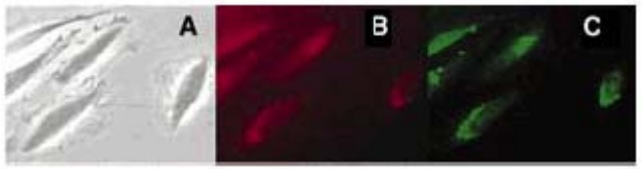

Phase contrast (A) and fluorescence (B, C) microscopy images of HeLa cells incubated with Coumazin-1 with the addition of $ZnCl_2$ and sodium pyrithione. Fluorescence images were acquired with λ excitation at 400 –440 nm, band-pass of 475 nm (B) or with λ excitation at 460 –500 nm, band-pass of 510 –560 nm (C).

PEBBLES and Zn(II)

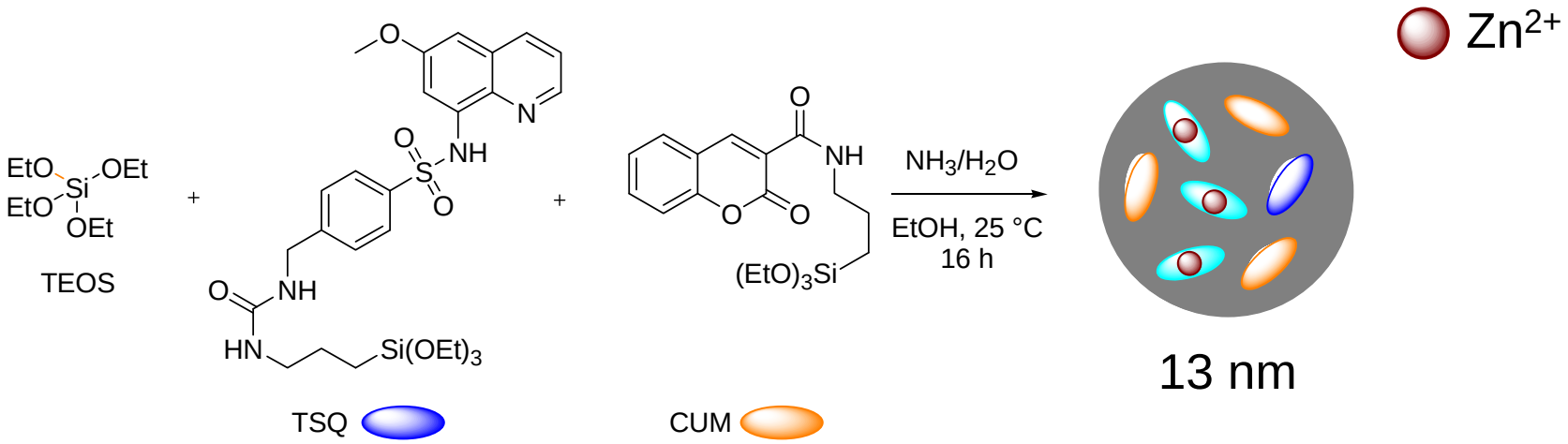

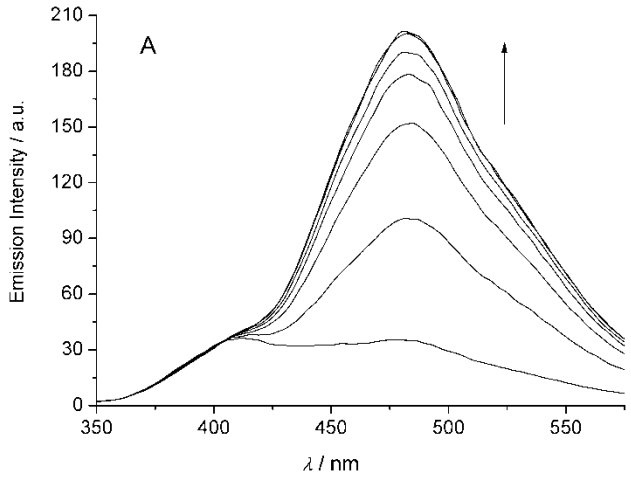

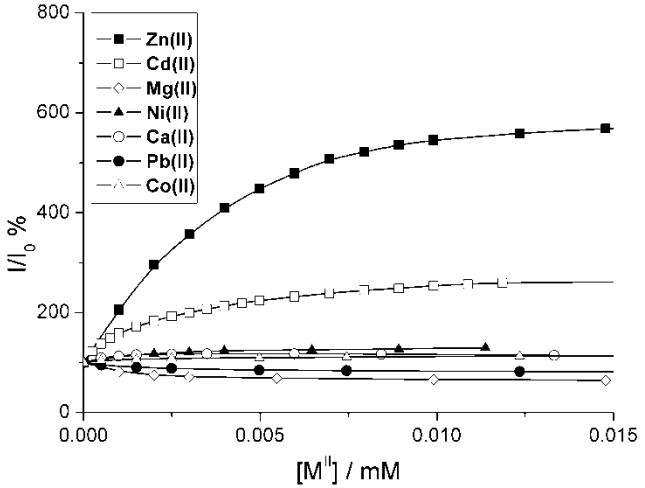

Pebbles: Kopelman et al. *Curr. Opin. Che. Biol.* ***2004***, *8*, 540-546

Chem. Eur. J **2007**, *8*, 2238-2245

PEBBLES and Zn(II)